DEVELOPMENT OF QUANTITATIVE LATERAL FLOW STRIP BIOSENSORS FOR THE DETECTION OF CANCER BIOMARKERS

A Dissertation
Submitted to the Graduate Faculty
of the
North Dakota State University
of Agriculture and Applied Science

By

Kwaku Baryeh

In Partial Fulfillment of the Requirements
for the Degree of
DOCTOR OF PHILOSOPHY

Major Department:
Chemistry and Biochemistry

April 2019

Fargo, North Dakota

North Dakota State University
Graduate School

Title

DEVELOPMENT OF QUANTITATIVE LATERAL FLOW STRIP BIOSENSORS FOR THE DETECTION OF CANCER BIOMARKERS

By

Kwaku Baryeh

The Supervisory Committee certifies that this ***disquisition*** complies with North Dakota State University's regulations and meets the accepted standards for the degree of

DOCTOR OF PHILOSOPHY

SUPERVISORY COMMITTEE:

Dr. Guodong Liu
Chair

Dr. D.K. Srivastava

Dr. Wenfang Sun

Dr. Xiwen Cai

Approved:

04-04-2019
Date

Dr. Gregory Cook
Department Chair

ABSTRACT

The detection of cancer biomarkers is of great importance in oncology. Cancer biomarkers can provide diagnostic information which can aid disease screening and early diagnosis. Further, cancer biomarkers can help predict disease prognosis and response to therapy, and also help in the monitoring of disease. Thence, the accurate and sensitive detection of cancer biomarkers which may be present at very low concentrations is of great clinical importance. Traditionally, these biomarkers have been detected predominantly by Enzyme Linked Immunosorbent Assay. The traditional biomarker detection assays generally require multiple washing steps, long assay times, and have the need for trained expertise and expensive instrumentation. In this dissertation, Lateral Flow Strip Biosensors (LFSB) that provide rapid, low-cost and user-friendly screening of cancer biomarkers are discussed. The developed biosensors have the added advantages of being portable, sensitive and highly selective, which makes them ideal for routine cancer screening. Gold nanoparticles (GNP)-based Lateral Flow Strip Immunosensors (LFSI) that colorimetrically detected carbohydrate antigen (CA 19-9) and carcinoembryonic antigen (CEA) were developed for the screening of human plasma and pancreatic cyst fluid, respectively. Further, carbon nanotube based-LFSBs that targeted CA 19-9 and CEA were developed. The CNT-based LFSBs showed improved detection limits over the conventional GNP-based LFSB. A GNP-based LFSB was also developed for the detection of exosomes using an aptamer that targeted a cell surface protein, epithelial cell adhesion molecule (EpCAM). The developed assays showed good performance and were used for the screening of pancreatic cancer patient samples. Upon further development, the assays discussed in this dissertation could find application in the clinical screening and monitoring of cancer, especially in limited resource settings.

.

ACKNOWLEDGEMENTS

I am eternally grateful to Jehovah Almighty: because I owe it all to Him.

Special gratitude to Dr. Guodong Liu for having me in his laboratory, and for his guidance and support throughout my studies. I am thankful for his financial support, research project ideas and motivation in the course of my graduate studies. Thank you, Dr. Liu.

Thank you to my Graduate Advisory Committee members (Dr. D. K. Srivastava, Dr. Wenfang Sun and Dr. Xiwen Cai) for all the constructive criticism at my committee meetings. Thank you for taking time off your busy schedules to talk to me and point me in the right direction when I needed help. A big thank you also goes to all the instructors that taught me in various courses during my doctoral studies.

I am grateful to my mate, Sunitha Takalkar, who was a wonderful study partner, lab mate and a friend. Thank you Sunitha, for all the trouble shooting and discussions that helped navigate some trying times in the laboratory. I am also grateful to the past senior students of the Liu Group (Anant Gurung, Meenu Baloda and Hui Xu) for their training and guidance when I joined the group initially. Thank you to all other students (Michelle Lund, Qiaobin Li and Xiaoguang Zhang) that worked in the lab during my stay in the Liu Group. You all made the lab a fun place to work.

Thank you to Dr. Katie Reindl, Dr. Thomas Schmittgen and Dr. Randall E. Brand who helped provide pancreatic cancer patient samples for this study.

A thousand thanks to my greatest cheerleader, my wife, Aku S. Baryeh. Thank you for your support and prayers. Thank you Aku, for proofreading this thesis and for taking care of the kids (Kwadwo, Yaw, Yaa, NanaYaa) and I all these years. Graduate school is a pain, but you made it a bit more bearable. God bless you.

Thank you to my parents Prof. Edward Baryeh and Mrs. Afua Baryeh, and to my siblings Nana Yaa Berle, Afia Yamoah, Empi Baryeh and Kofi Baryeh. I am grateful for all your prayers and support throughout my studies.

Thank you Nii-Koney Kwaku Koney, for your help troubleshooting and designing some experiments in the course of my graduate studies. Thanks for forfeiting a thousand dollars because you did not want to keep me waiting outside for hours.

I thank our funding agency NIH-COBRE (1P20GM09024) for the financial support without which none of this work would have been possible. I am thankful to the Department of Chemistry and Biochemistry for giving me the opportunity and financial support to pursue my doctoral studies. Thank you to Wendy Leach, Amy Kain and Mimi Monson for all the emails and reminders over the years.

DEDICATION

To God, for making all this possible.

To my parents, Prof. E. A. Baryeh and Mrs. Afua Baryeh, who did an awesome job raising me.

To my dear wife, Aku Selasi, who always understood.

To my kids (Kwadwo, Yaw, Yaa and NanaYaa), for being my joy.

TABLE OF CONTENTS

ABSTRACT iii

ACKNOWLEDGEMENTS iv

DEDICATION vi

LIST OF TABLES xii

LIST OF FIGURES xiii

LIST OF ABBREVIATIONS xvii

LIST OF SYMBOLS xx

1. INTRODUCTION 1

1.1. Point-of-Care Devices 2

1.1.1. Point-of-Care Device Setup 4

1.2. Lateral Flow Strip Biosensors 5

1.2.1. Biorecognition Elements for Lateral Flow Strip Biosensors 7

1.2.2. Nanomaterials for Lateral Flow Strip Biosensors 8

1.2.3. Lateral Flow Strip Biosensor Formats 9

1.3. Applications of Lateral Flow Strip Biosensors 11

1.3.1. Protein Detection on Lateral Flow Strip Biosensors 12

1.3.2. Nucleic Acid Detection on Lateral Flow Strip Biosensors 13

1.3.3. Lateral Flow Strip Biosensor Based Detection of Cells and Exosomes 13

1.3.4. Lateral Flow Strip Biosensor Based Detection of Other Small Molecules 14

1.4. Aims and Objectives of this Study 15

2. DEVELOPMENT OF QUANTITATIVE IMMUNOCHROMATOGRAPHIC ASSAY FOR RAPID AND SENSITIVE DETECTION OF CARBOHYDRATE ANTIGEN 19-9 (CA 19-9) IN HUMAN PLASMA 18

2.1. Introduction 18

2.2. Experimental Section 20

2.2.1. Apparatus 20
2.2.2. Reagents and Materials 20
2.2.3. Preparation of GNP and GNP- Anti CA 19-9 AbA Conjugates 21
2.2.4. Preparation of CA19-9 Lateral Flow Strip Biosensors 22
2.2.5. Assay Procedure 23
2.3. Results and Discussion 24
2.3.1. Principle of the Quantitative Immunochromatographic Assay (QIA) for CA 19-9 24
2.3.2. Optimization of Experimental Parameters 25
2.3.3. Analytical Performance 29
2.3.4. Detection of CA 19-9 in Healthy Human and Pancreatic Cancer Patient Plasma 31
2.4. Conclusion 32
3. QUANTITATIVE GOLD NANOPARTICLE-BASED LATERAL FLOW STRIP BIOSENSOR FOR THE DETECTION OF CARCINOEMBRYONIC ANTIGEN (CEA) IN HUMAN PANCREATIC CYST FLUID 33
3.1. Introduction 33
3.2. Experimental Section 37
3.2.1. Apparatus 37
3.2.2. Reagents and Materials 37
3.2.3. Preparation of the GNP and GNP-Anti-CEA Conjugate 38
3.2.4. Preparation of GNP-Based LFSB for CEA Detection 38
3.2.5. Assay Procedure 40
3.3. Results and Discussion 40
3.3.1. Working Principle of GNP-Based LFSB for CEA Detection 40
3.3.2. Optimization of Experimental Parameters 42
3.3.3. Analytical Performance 45

3.3.4. Detection of CEA in Human Pancreatic Cyst Fluid 47

3.4. Conclusion 48

4. MULTI-WALLED CARBON NANOTUBE-BASED LATERAL FLOW BIOSENSOR FOR ULTRASENSITIVE DETECTION OF PROTEINS IN HUMAN PLASMA 50

4.1. Introduction 50

4.2. Experimental Section 53

4.2.1. Apparatus 53

4.2.2. Reagents and Materials 53

4.2.3. Preparation of MWCNT-Antibody Conjugates 54

4.2.4. Preparation of the MWCNT-Based LFB 55

4.2.5. Assay Procedure 56

4.3. Results and Discussion 57

4.3.1. Characterization of the Shortened MWCNTs 57

4.3.2. Principle of MWCNT-Based LFB for Protein Detection 58

4.3.3. Optimization of Experimental Parameters 61

4.3.4. Analytical Performance 64

4.4. Conclusion 68

5. MULTI-WALLED CARBON NANOTUBE-BASED LATERAL FLOW STRIP BIOSENSOR FOR THE QUANTITATIVE DETECTION OF CARCINOEMBRYONIC ANTIGEN (CEA) 69

5.1. Introduction 69

5.2. Experimental Section 70

5.2.1. Apparatus 70

5.2.2. Reagents and Materials 71

5.2.3. Preparation of MWCNT-Anti-CEA Antibody Conjugate 71

5.2.4. Preparation of the MWCNT-Based LFSB for CEA Detection 72

5.2.5. Assay Procedure 73
5.3. Results and Discussion 74
5.3.1. Principle of the Developed MWCNT-Based LFSB for CEA Detection 74
5.3.2. Optimization of Experimental Parameters 75
5.3.3. Analytical Performance 79
5.4. Conclusion 81
6. MULTI-WALLED CARBON NANOTUBE-BASED LATERAL FLOW STRIP BIOSENSOR FOR THE QUANTITATIVE DETECTION OF CARBOHYDRATE ANTIGEN (CA 19-9) 82
6.1. Introduction 82
6.2. Experimental Section 83
6.2.1. Apparatus 83
6.2.2. Reagents and Materials 83
6.2.3. Preparation of MWCNT-Anti-CA 19-9 AbA Conjugate 84
6.2.4. Preparation of the MWCNT-Based LFSB for CA 19-9 Detection 85
6.2.5. Assay Procedure 86
6.3. Results and Discussion 86
6.3.1. Principle of the Developed MWCNT-Based LFSB for CA 19-9 Detection 86
6.3.2. Optimization of Experimental Parameters 88
6.3.3. Analytical Performance 92
6.4. Conclusion 94
7. GOLD NANOPARTICLE-BASED LATERAL FLOW STRIP APTASENSOR FOR THE DETECTION OF EXOSOMES FROM HUMAN PLASMA 95
7.1. Introduction 95
7.2. Experimental Section 99
7.2.1. Apparatus 99

7.2.2. Reagents and Materials 99
7.2.3. Preparation of GNPs 100
7.2.4. Preparation of GNP-Aptamer Conjugates 101
7.2.5. Preparation of GNP-Antibody Conjugates 101
7.2.6. Preparation of Streptavidin-Biotinylated DNA Probe Conjugate 101
7.2.7. Preparation of the LFSA for Exosome Detection 102
7.2.8. Preparation of Antibody-Based LFSB for Exosome Detection 103
7.2.9. Isolation of Exosomes from Human Plasma 103
7.2.10. Assay Procedure 104
7.3. Results and Discussion 104
7.3.1. Working Principle of the Developed LFSA for Exosomes Detection 104
7.3.2. Optimization of Assay Parameters 107
7.3.3. Analytical Performance 111
7.4. Conclusion 113
8. SUMMARY AND CONCLUSIONS 114
REFERENCES 117

LIST OF TABLES

Table Page

2.1. Screening of plasma samples from healthy human and pancreatic cancer patients with the developed QIA and commercial ELISA kit. 31

4.1. Comparison of developed MWCNT-LFB to previous reports of protein detection on LFBs. 67

LIST OF FIGURES

Figure — Page

1.1. Idealized concept of a POCD [8] 4

1.2. Components of a biosensor [10] 5

1.3. Setup of the lateral flow strip biosensor 6

1.4. Sandwich format lateral flow assay (image modified from reference[11]) 10

1.5. Competitive lateral flow assay (image modified from reference[11]) 11

1.6. Applications of lateral flow strip biosensors 12

2.1. Configuration of the gold nanoparticle-based lateral flow strip biosensor for the detection of CA 19-9. 22

2.2. Principle of quantitative immunochromatographic assay of CA 19-9 (a) Capture of gold nanoparticles on the test line and control line in the presence of CA 19-9 (b) Capture of gold nanoparticles on the control line in the absence of CA 19-9 (c) Measuring the intensities of test and control lines with a portable strip reader connected to a laptop computer. 25

2.3. (a) Effect of different types of nitrocellulose membranes on the S/N ratio of the assay (b) Effect of the dispensing times of Anti-CA 19-9 AbB on the S/N ratio of the assay (c) Effect of buffer components on the S/N ratio of the assay. 26

2.4. (a) Effect of the amount of Anti- CA 19-9 AbA used for conjugate preparation on the S/N ratio of the assay (b) Effect of the conjugate volume on the S/N ratio of the assay. 28

2.5. (a)Photo images of LFSBs in the presence of different concentrations of CA 19-9 (b) Calibration curve of CA 19-9 detected on developed GNP-based lateral flow strip biosensor. Each data point represents the average value obtained from three different measurements. 29

2.6. Selectivity of the developed GNP-based LFSB (concentration of CA 19-9 was 50 U mL^{-1}; Mammaglobin, Human IgG and CEA were at 100 ng mL^{-1}) 30

3.1. Scheme of the developed GNP-based Lateral Flow Strip Biosensor for the detection of CEA 39

3.2. Working Principle of the developed GNP-based LFSB for CEA detection (a) Assay in the presence of target CEA (b) assay in the absence of CEA. 41

3.3. (a) Effect of nitrocellulose membrane type on the S/N ratio of the assay (b) Effect of the dispense times of test line anti-CEA Ab F on the S/N ratio of the assay (c) Effect of buffer composition on the performance of the assay. 43

3.4. (a) Effect of the amount of anti-CEA Ab F used for conjugate preparation on the S/N ratio of the assay (b) Effect of conjugate volume on the S/N ratio of the assay. 45

3.5. (a) Photo images of assay in the presence of varying amounts (0 – 1000 ng mL^{-1}) of CEA (b) Corresponding calibration curve. Each data point corresponds to the averaged test line intensities from three replicate tests. 46

3.6. Selectivity of the developed GNP-based lateral flow strip biosensor. Assay in the presence of CEA (30 ng mL^{-1}); Mammaglobin, Trypsin, C4BP-alpha and Human IgG at concentrations of 100 ng mL^{-1}; CA 19-9 (100 U mL^{-1}); and blank (running buffer). 47

3.7. Screening of human pancreatic cyst fluid with developed GNP-based lateral flow strip biosensor. Pancreatic cancer patient cyst fluid (PC1 to PC6) and non-malignant pancreatic cyst fluid (NM). 48

4.1. Configuration of the MWCNT-based LFB for protein detection. 56

4.2. (a) TEM image of unshortened MWCNTs (b) TEM image of shortened MWCNTs; (c) FTIR spectra of MWCNT before and after acid treatment. 57

4.3. Working Principle of the developed MWCNT- based LFB. (a) Sample introduction (b) Immunoreaction between target and GaR-MWCNT conjugate (c) Capture of rabbit IgG-GaR-MWCNT complex on test line and the excess of GaR-MWCNT conjugate on the control line (d) Assay in the absence of target rabbit IgG. 59

4.4. Photo images of the GNP-based LFBs (left) and the MWCNT based LFBs (right) with varied concentration of Rabbit IgG: (a.) 5 ng mL^{-1} (b.) 1.0 ng mL^{-1} (c.) 0 ng mL^{-1}. 60

4.5. (a) Effect of membrane type on the S/N ratio of the assay (b) Effect of dispense cycles on of GaR IgG at the test line on the performance of the assay (c) Effect of running buffer composition on the S/N ratio of the assay. 62

4.6. (a) Effect of the amount of GaR IgG used for conjugate preparation on the S/N ratio of the assay. (b) Effect of the volume of conjugate per-assay-run used on the S/N ratio of the assay 64

4.7. Responses of MWCNT-based LFBs in the presence of different concentrations of rabbit IgG and corresponding photo images. 65

4.8. Calibration curves of the MWCNT-based LFB in the concentration range of (a) 5-100pg mL^{-1} (b) 0.5 to 20 ng mL^{-1}. 66

4.9. Selectivity of MWCNT-based LFB. Concentration of rabbit IgG was 100 pg mL^{-1}; CA 19-9 was at 50 U mL^{-1}; Mammaglobin, Human IgG and CEA were at 50 ng mL^{-1}. 67

4.10. Calibration curve of MWCNT-based LFB for detection of rabbit IgG in spiked human plasma (10%). 68

5.1. Setup of developed MWCNT-based LFSB for the detection of CEA. 72

5.2. Principle of the MWCNT-based lateral flow strip biosensor for CEA detection (a) Capture of MWCNT on test and control lines in the presence of CEA (b) Capture of MWCNTs on the control line in the absence of CEA (c) Reading the test and control line intensities using a portable strip reader. 75

5.3. (a) Effect of different types of nitrocellulose membranes on the S/N ratio of the assay (b) Effect of the dispensing times of Anti-CEA Ab B on the S/N ratio of the assay. (c): Effect of buffer type on the S/N ratio of the assay (d) Effect of BSA percentage in buffer on the S/N ratio of the assay. 77

5.4. (a) Effect of the amount of anti-CEA Ab A used for conjugate preparation on the S/N ratio of the assay. (b) Effect of the volume of conjugate used on the S/N ratio of the assay 78

5.5. (a) Photo images of CNT-based LFSB in the presence of varying concentrations of CEA (b) Calibration curve of CEA detected on developed MWCNT-based lateral flow strip biosensor. Each data point represents the average value obtained from three different measurements 80

5.6. Selectivity of the developed MWCNT-based LFSB (concentration of CEA was 5ng mL^{-1}, CA 19-9 was 100 U mL^{-1}, C4B-aplha, Human IgG, Mammaglobin, Thrombin were 100 ng mL^{-1}) 81

6.1. Scheme of developed MWCNT-based LFSB for the detection of CA 19-9 86

6.2. Working principle of the MWCNT-based lateral flow strip biosensor for CA 19-9 detection (a) Capture of MWCNT on test and control lines in the presence of CA 19-9 (b) Capture of MWCNTs on the control line in the absence of CA 19-9 (c) Reading the test and control line intensities using a portable strip reader 88

6.3. (a) Effect of different types of nitrocellulose membranes on the S/N ratio of the assay. (b) Effect of the dispensing times of Anti-CA 19-9 AbB on the S/N ratio of the assay. (c) Effect of buffer type on the S/N ratio of the assay. 90

6.4. (a) Effect of the amount of anti-CA 19-9 AbA used for conjugate preparation on the S/N ratio of the assay (b) Effect of the volume of conjugate used on the S/N ratio of the assay 91

6.5. (a) Photo images of MWCNT-based LFSB in the presence of varying concentrations of CA 19-9 (b) Calibration curve of CA 19-9 detected on developed MWCNT-based lateral flow strip biosensor. Each data point represents the average value obtained from three different measurements 92

6.6. Selectivity of the developed MWCNT-based LFSB (concentration of CA 19-9 was 10 U mL^{-1}; CEA, Mammaglobin, Human IgG, C4B-aplha and Thrombin were at 100 ng mL^{-1}) 93

7.1. Scheme of developed GNP-based lateral flow strip aptasensor for exosome detection 103

7.2. Working principle of the developed GNP-based LFSA (a) Capture of exosomes between test line and conjugate EpCAM aptamer and the capture of excess conjugate on the control line (b) Assay in the absence of exosomes..... 106

7.3. Photo images of the developed aptamer LFS (left) and the lateral flow immunosensor (right) with exosome concentrations 0.75 x 10^6 exosomes/µL and 20 x10^6 exosomes/µL respectively 107

7.4. Optimization of assay parameters (a) Effect of membrane type on the S/N ratio of the assay (b) Effect of dispense times of the test line aptamer on the performance of the assay (c) Effect of running buffer composition on the S/N ratio of the assay..... 108

7.5. (a) Effect of the amount of EpCAM aptamer used for conjugate preparation on the performance of the GNP-based LFSA (b) Effect of conjugate volume on the S/N ratio of the assay 110

7.6. (a) Typical images of GNP-based LFSA in the presence of varying concentration of exosomes (b) Calibration curve for developed aptasensor 112

LIST OF ABBREVIATIONS

Ab .....antibody

BSA .....Bovine Serum Albumin

CA 125.....Cancer antigen 125

CA 15-3.....Cancer antigen 15-3

CA 19-9 .....Carbohydrate antigen 19-9

CA 72-4.....Cancer antigen 72-4

Cd .....Cadmium

Cd .....Lateral

Cd^{2+} .....Cadmium ion

CEA.....Carcinoembryonic antigen

circRNA .....Circulating ribonucleic acids

CNT .....Carbon nanotubes

CTAB .....Cetyl trimethylammonium bromide

Cu^{2+} .....Copper ion

dATP .....Deoxyadenosine triphosphate

DPBS .....Dulbecco's phosphate-buffered saline

EDC .....N-Ethyl-N′-(3-dimethylaminopropyl)carbodiimide hydrochloride

ELISA .....Enzyme-linked immunosorbent assay

ELISA .....Enzyme linked immunosorbent assay

EpCAM .....Epithelial cell adhesion molecule

FTIR .....Fourier-transform infrared spectroscopy

GaM .....Goat anti mouse

GaR .....Goat anti-rabbit

GNP .....Gold nanoparticle

H_2SO_4 .....Sulfuric acid

HAuCl4 .....Chloroauric acid

HCG .....human chorionic gonadotropin

HCl .....Hydrochloric acid

Hg .....Mercury

Hg^{2+} .....Mercury

HNO_3 .....Nitric acid

hr .....hour

IA .....Immunochromatographic assay

IgG .....Immunoglobulin G

LFB .....Lateral flow biosensor

LFI .....Lateral flow immunosensor

LFSA.....Lateral flow strip aptasensor

LFSB .....Lateral flow strip biosensors

lncRNA .....Long non-coding RNA

LOD .....Limit of detection

MES .....2-(4-Morpholino) ethanesulfonic acid

$MgCl_2$ .....Magnesium chloride

min .....Minute

mins .....Minutes

miRNA .....Micro ribonucleic acid

MWCNT .....Multi-walled carbon nanotubes

$Na_3PO_4.12H_2O$ .....Sodium phosphate tribasic deodecahydrate

NaCl .....Sodium chloride

NHS .....N-hydroxysulfosuccinimide

Pb .....Lead

Pb^{2+} .....Lead ion

PBS .....Phosphate buffered saline

PBST .....Phosphate buffered saline with 1% Tween

PC .....Pancreatic cancer

pH .....Potential of hydrogen

piwi,RNA .....Piwi-interacting ribonucleic acid

POCD.....Point-of-care devices

PVP .....Polyvinylpyrrolidone

QIA .....Quantitative immunoassay

RNA.....Ribonucleic acid

RT .....Room temperature

S/N .....Signal to Noise

SDS .....Sodium dodecyl sulfate

sec .....Second

SEC .....Size exclusion chromatography

snoRNA .....Small nucleolar ribonucleic acid

SPR .....Surface plasmon resonance

TEM .....Transmission electron microscopy

Tris-HCl .....Trizma hydrochloride

USFDA .....United States Food and drugs Administration

v.....volume

wt.....weight

LIST OF SYMBOLS

° .....degrees

µg .....microgram

µL.....microliter

C.....Celsius

g.....gram

M.....molar

mg .....milligram

mL.....milliliter

mM.....millimolar

nm .....nanometer

nM.....nanomolar

pg.....picogram

U.....Unit

1. INTRODUCTION

This dissertation discusses the development of lateral flow strip biosensors (LFSB) for the sensitive and selective detection of cancer biomarkers. The LFSBs introduced in this work concentrate on the detection of biomarkers for pancreatic cancer. Biomarkers are defined as biological processes or molecules whose presence in blood or other body fluids is a sign of a normal or diseased condition.[1] Biomarkers encompass biomolecules such as nucleic acids (DNA, RNA, miRNA), proteins, carbohydrates and exosomes amongst others. DNA biomarkers can include single nucleotide polymorphism, chromosomal aberrations, alterations in copy numbers and methylation patterns of DNA.[2] With advancement in next generation sequencing various types of RNA(miRNA, circRNA, snoRNA, IncRNA, piwi,RNA) have been used as biomarkers for cancers and other diseases.[3] Cell surface receptors, secreted proteins like insulin, phosphorylation site patterns, secreted peptides are types of protein biomarkers that have been used for diagnostics and monitoring diseased conditions. Processes such as elevated cell death or proliferation may also serve as biomarkers.[4] The up or down regulation of these biomarkers can be monitored to give information for the diagnosis and prognosis of diseases, and for monitoring of response to therapy especially for cancer treatment. These biomarkers play an important role at all stages of cancerous disease progression and can give insights to treatment regiments best required.[5] The levels of cancer biomarkers can be used to stage cancers. The early detection of cancers like those of the prostate, colon, pancreas, breast etc. can meaningfully increase the survival rate of patients.

Traditionally, bulk protein detection has been done by colorimetric assays where proteins react with chemical agents to produce colored products whose intensities can be quantified by spectroscopic methods.[6] Techniques like gel electrophoresis, western blot, mass spectrometry give more specificity in detection. Immunoassays, particularly Enzyme Linked Immunosorbent Assay

(ELISA) is the most popularly used method for protein detection. ELISAs offer acceptable specificity and selectivity, however, there are major draw backs such as the need for skilled labor, batch to batch differences in antibodies, need for refrigeration, multiple wash steps and the use of expensive equipment. These shortcomings reduce ELISA applicability in settings with limited resources especially in the developing world. There has therefore been the need to development rapid, low-cost, user friendly but sensitive assays that can be used in limited resource settings.

1.1. Point-of-Care Devices

It is of immense clinical importance to be able to perform bedside testing and detection of disease biomarkers. This helps with prompt diagnosis and initiation of required therapeutic intervention. Pont-of-care devices (POCD) allow clinicians to perform diagnostic and prognostic assays in close proximity to patients without the use of costly or complicated devices.[7]

POCDs offer numerous advantages over the conventional immunoassays which are summarized below:

- Portability: With POCDs patients can self-test in the convenience of their homes. This removes the need for transporting patients to medical laboratories for routine testing. POCDs are usually miniaturized to ensure their use infield without the need to transport samples to a laboratory for testing. Results can be obtained infield and appropriate action (treatment or referral for further evaluation) taken.
- Low Cost: POCDs are developed to be inexpensive for the end users. Cost of medical testing and assay kits continues to be a hindrance to healthcare delivery globally. With POCDs, medical testing can be done at comparatively lower cost compared to conventional tests like ELISA. An ideal POCD does not require the use of expensive machinery for assay performance and assay readout. This helps

improve access to health screening for low income homes especially in the developing world where millions of people die each year from infectious diseases like malaria, AIDS etc.

- Simplicity: The hallmark of POCDs is their nonrequirement for skilled personnel. The devices are expertly designed to ensure that end users can effectively use the devices by following a simple set of defined steps. Data output for POCDs device do not require complex analysis are easy to interpret by an untrained person.
- Short Assay Times: In emergency situations being able to have quick patient test results can be the difference between life and death. POCDs can be invaluable is such settings. Assay times can be as short as 15 minutes (mins). This can also help reduce patient anxiety as they await test results.

An idealized concept of a POCD is shown in **Figure 1.1**.[8] An ideal POCD would be a disposable device that quantitatively detects multiple targets in as little as 1 μL of sample.[9] This device would detect target analyte with high sensitivity whilst eliminating cross contamination and false positive results. The device would be water proof, storable over a wide temperature range and rugged enough to resist damage from small drops.[9] The ideal POCD does not exist yet, however the forgoing provides a framework to guide research and development efforts to help achieve an ideal POCD.

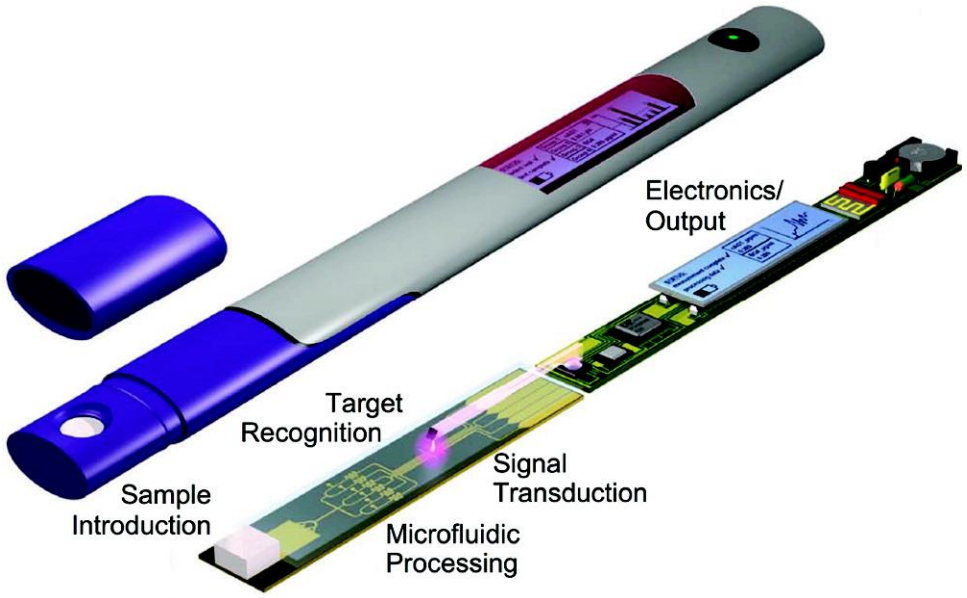

Figure 1.1. Idealized concept of a POCD [8].

1.1.1. Point-of-Care Device Setup

POCDs like all biosensors consist of three basic components (bioreceptor, transducer, signal processor) as shown in **Figure 1.2**.[10] The bioreceptor detects the presence or activity of target analyte and gives a measurable signal that can be transduced for the end user to observe. The setup can have built-in systems to help amplify the measured signal for more sensitive detection.

Various biorecognition elements like antibodies, enzymes, nucleic acids, proteins and microorganisms have been used in the development of biosensors. These serve as bioreceptors that interact with target analyte in sample. These interactions are coupled to transducers that give off measurable signal. Biosensors are very versatile and have been coupled with electrochemical, colorimetric, chemiluminescence and piezoelectric transducers over the years.

The most popular POCD that has found universal acceptance is the electrochemical glucose sensor. Since the successful commercialization of the glucose meter, lateral flow strip biosensors

have also found wide use and acceptance. The most popular of which is the home-based pregnancy test strip which tests for the presence of human chorionic gonadotropin (HCG) in urine.

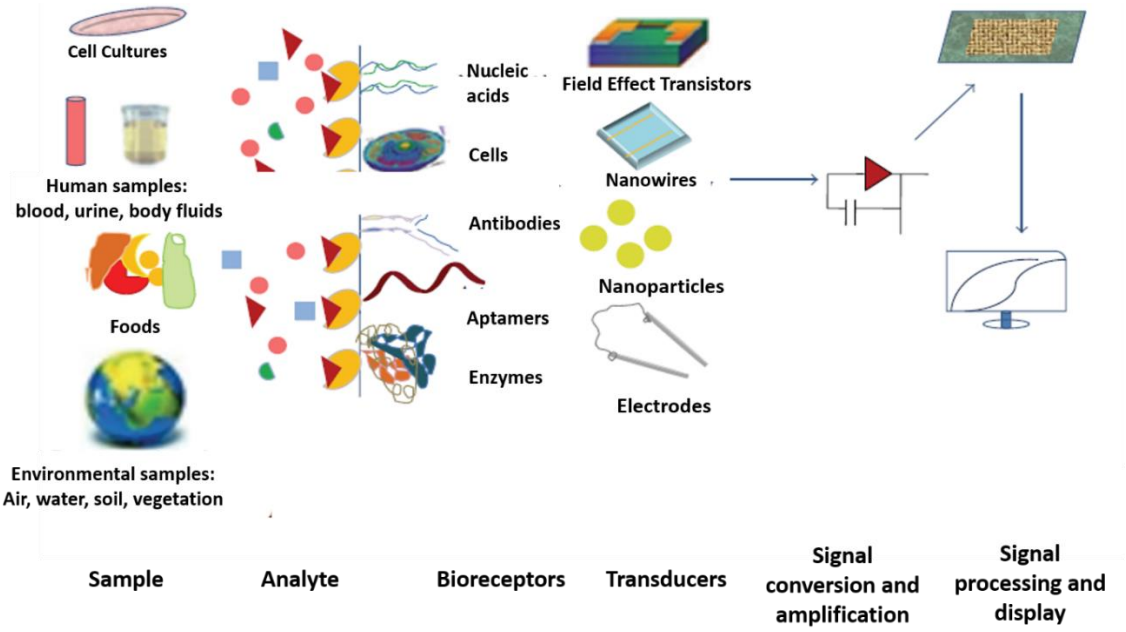

Figure 1.2. Components of a biosensor [10].

1.2. Lateral Flow Strip Biosensors

Lateral flow strip biosensors (LFSB), also referred to as dip stick biosensors are chromatographic test strips that traditionally give yes/no results for presence or absence of target analyte. The setup for the LFSB is as shown in **Figure 1.3**. The device consists of 4 main zones (i.e. sample pad, conjugate pad, nitrocellulose membrane and the absorption pad) all assembled on a sticky backing layer. The sample pad is a cellulose membrane that serves as the sample application zone. The sample pad is porous and allows the sample to travel through it. Sample pad pores must be appropriately sized to allow the movement of various targets (e.g. proteins, nucleic acids, cells and other small molecules etc.). This pad can be treated with buffers to enhance the performance of the LFSB. The treatment can serve to improve the separation of sample components, enhance continuous flow, remove interferences and also ensure optimal pH.[11] The

conjugate pad is usually made of a glassy fiber, that can soak up reasonable volume of conjugate (biorecognition elements linked to a suitable transducer). The conjugate pad should be capable of keeping the conjugate stable over the shelf life of the LFSB and release dried conjugate in the presence of buffer. The most popular transducer used for LFSB is the gold nanoparticle (GNP) because of its surface plasmon properties and ease of synthesis. The nitrocellulose membrane supports the test and control lines. Various nitrocellulose membranes exist with varying membrane pore size and thus different flow rates. The flow rates dictate the time frame for interactions between test line biorecognition elements and target analyte. The test lines and control lines are dispensed with specialized equipment to give consistent volumes per unit area of nitrocellulose membrane. The final zone is the absorption pad which is made up of cellulose fiber. The absorption pad wicks the reagents as the assay progresses to enhance capillary action across the strip. All components are assembled on the sticky backing layer such that they overlap to ensure continuous solvent flow.

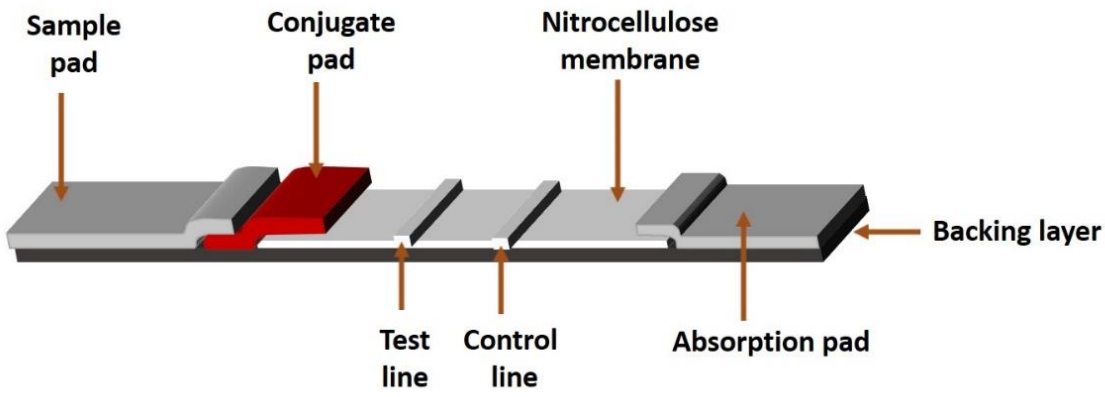

Figure 1.3. Setup of the lateral flow strip biosensor.

1.2.1. Biorecognition Elements for Lateral Flow Strip Biosensors

The sensitivity of any biosensor sterns mostly from the quality of biorecognition element used to make the sensor. Traditionally, antibodies have been used as the biorecognition elements for LFSBs. When antibodies are used as biorecognition elements for LFSBs, the biosensors are referred to as Lateral Flow Immunoassays (LFI). Antibodies have long been used in immunoassays and their sensitivity and selectivity are well reported. Two antibody classes (monoclonal and polyclonal) have been used on LFSBs. Monoclonal antibodies bind to a single epitope on the surface of the targets while polyclonal antibodies bind to multiple epitopes. Both types of antibodies have been used for the development of LFSBs. However, batch to batch variation, need for cold storage, and to a lesser extent cross-reactivity can limit the performance and applicability of antibodies for the development of POCDs.

A class of ligands called aptamers have gained increased attention in recent years and have been used in place of antibodies for the preparation of various biosensors. Aptamers are nucleic acids that can fold up into unique structures and are able to bind selectively to target molecules. Aptamers are developed through a procedure termed Systematic Evolution of Ligands by Exponential Enrichment which was first reported independently by two research groups.[12,13] Aptamers are inexpensive to synthesize, highly selective, easy to chemically modify and have the added advantage of being easy to synthesize. Aptamers have been reported for various targets including protein biomarkers. On LFSBs, aptamers have been used for the detection of proteins[14], cells[15], bacteria[16] and some small molecules[17]. Other biorecognition elements used to a lesser extent for the development of LFSBs include bacteriophages and proteins.

1.2.2. Nanomaterials for Lateral Flow Strip Biosensors

LFSBs can be developed to give colorimetric, fluorescent, chemiluminescent and electrochemical signals that can be used for qualitative and quantitative measurement of target analyte. Nanoparticles are usually employed to help give out these measurable signals. The nanoparticles also serve as carriers that support biorecognition elements that give the assays their specificities. Other substances like enzymes can also be coupled to nanoparticles as a form of signal enhancement. [18]

Gold nanoparticles (GNP) are the gold standard for lateral flow strip biosensors. GNPs are easy and inexpensive to synthesize. They are also stable for extended periods under refrigeration. GNPs are easily linked to thiol groups by thiol self-assembly. They may also be linked to antibodies by physical adsorption. GNPs, because of their surface plasmon properties have an intense size dependent red color. This makes them ideal for colorimetric LFSB applications. GNPs have been used for the detection of proteins[18], cells[15], nucleic acids[19,20] and other small molecules [21,22]. Gold nanoparticles have also been coated on silica nanorods for the detection of nucleic acids[23] and proteins [24].

Carbon nanotubes are also attractive materials for lateral flow assays development. CNTs have the advantages of having intense black color to aid colorimetric detection and have a large surface area because of their high aspect ratio which enables the attachment of numerous biorecognition elements. Acid treated CNTs have carboxyl functionalization on their surface that aids the covalent attachment of biorecognition elements. CNT's have been used for the detection of nucleic acids[25]. Magnetic carbon nanotubes based LFSBs have also been reported for the detection of proteins [26] and carbohydrate antigen (CA 19-9) [27] in whole blood.

Liposomes, which are spherical vesicles that are integrated by one or more phospholipid bilayers have also been applied on lateral flow strip biosensors. The membrane of the liposome can be modified with biorecognition elements and the interiors of the liposomes may contain colored dyes for colorimetric assays and enzymes for colorimetric enhancement and chemiluminescent assays.[28,29] Ho and Wauchup developed a liposome based LFSB for the detection of Aflatoxin B1.[30] In this assay the liposomes encapsulated a visible dye that aided colorimetric detection to target Aflatoxin B1. Liposomes have been used for detection of other targets like nucleic acids[28] and proteins[31].

Fluorescent nanoparticles and dyes have also found wide application as transducers on LFSBs. The use of quantum dots, fluorescent quenching materials, upconverting nanoparticles and lanthanide chelate labels have been reviewed. [32]

Other nanoparticles like magnetic nanoparticles, latex nanoparticles, silica nanoparticles and platinum (Pt) nanoparticles have been applied with varying degrees of sensitivity on the LFSB platform.[32]

1.2.3. Lateral Flow Strip Biosensor Formats

The most popular format of the LFSB is the sandwich type immunoassay. This format is similar to conventional sandwich immunoassays like ELISA. Here, a target molecule is captured between a primary capture antibody immobilized as test line and a secondary detection antibody. The secondary antibody is conjugated to a suitable transducer and its accumulation on the test line increases with increasing concentration of target molecule. The formation of the sandwich is dependent on the presence of the target molecule as the target serves as a bridge between the capture and detection antibodies. As shown in **Figure 1.4**, the accumulation of the conjugate on the test line results in the formation of a colored line which can be visually observed for yes/no

results. The more intense the color, the higher the concentration of target in test sample. Excess conjugates are captured by the pre-immobilized antibodies on the control line. When transducers like quantum dots, fluorescent dyes and electrochemically active species are used, the measured signal which increases with increasing amount of target can be fluorescent or electrochemical.

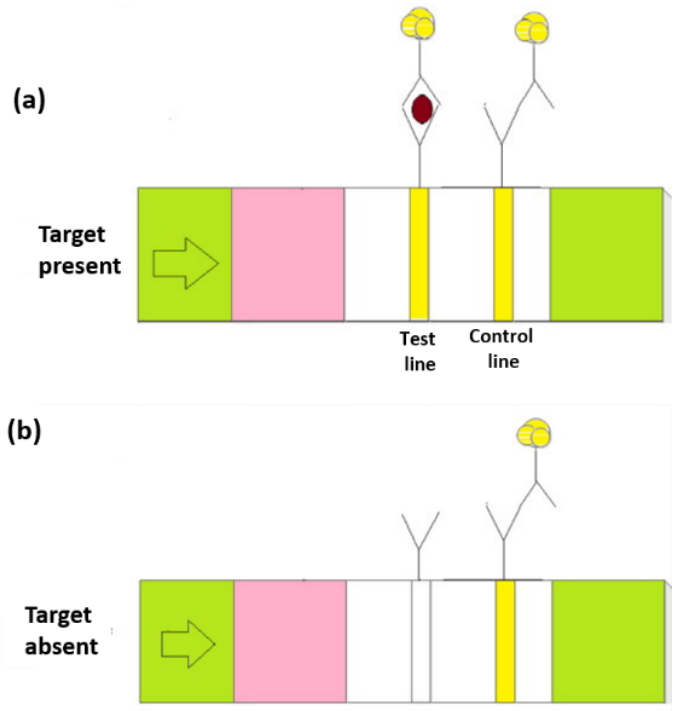

Figure 1.4. Sandwich format lateral flow assay (image modified from reference[11]).

The second format of the lateral flow assay follows the competitive format, also known as signal-off format. In this setup as shown in **Figure 1.5**, target competes with conjugates for binding to the test line biorecognition element. In the presence of target, the target preferentially binds to the test line thereby preventing conjugates immobilization on test line. Subsequently, the higher the concentration of target analyte in test sample the lesser the intensity of the signal observed on the test line. The excess conjugate is captured on the control line to validate the assay.

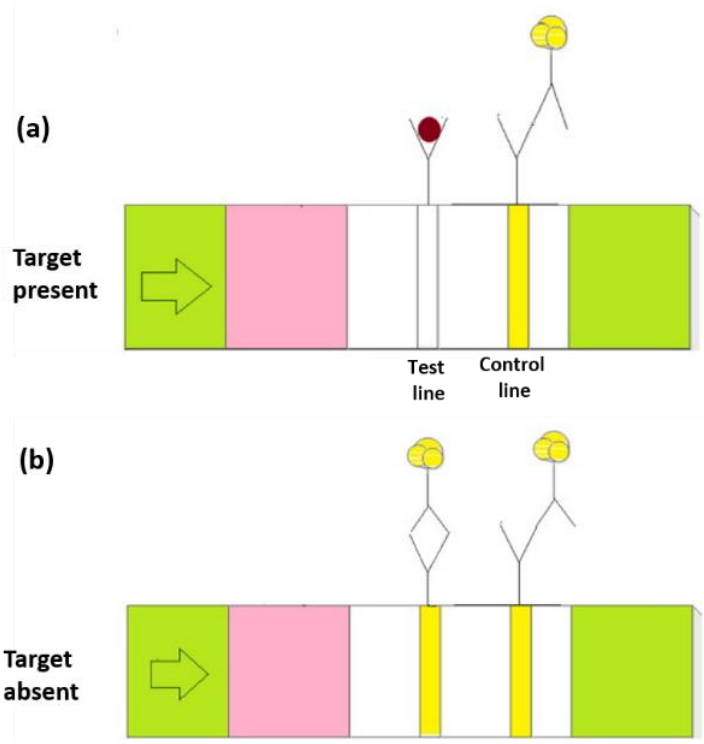

Figure 1.5. Competitive lateral flow assay (image modified from reference[11]).

A second type of competitive LFSB format has labelled analyte conjugated to a transducer and dispensed on the conjugate pad. A detection antibody is dispensed as the test line. Test solution will contain free unmodified target analyte which competes with the conjugated analyte on the conjugate pad for binding to the test line antibody.

1.3. Applications of Lateral Flow Strip Biosensors

LFSBs represent a very versatile platform and have found applicability across different industries as summarized by **Figure 1.6**. LFSBs have been applied for the detection of proteins, nucleic acids, cells and pathogens of clinical, veterinarian and food safety importance. Heavy metals, pesticides and other small molecules of agricultural and environmental safety concern have also been detected on LFSB.

Figure 1.6. Applications of lateral flow strip biosensors.

1.3.1. Protein Detection on Lateral Flow Strip Biosensors

Proteins are of importance in a variety of fields. In medical and veterinarian disciplines proteins serve as biomarkers for diseased conditions. The most widely used application of LFSB for protein detection is the home-based pregnancy test kit that detects HCG presence in urine of expectant mothers. Other proteins like fatty acid binding protein[33] and cardiac troponin[34,35] which are markers for cardiac diseases have also been detected with LFSBs. A surface-enhanced raman scattering LFSB was developed for the detection of prostate specific antigen (PSA), a marker for prostate cancer, was reported with acceptable sensitivity and selectivity.[36] Carcinoembryonic antigen (CEA) and neuron specific enolase (NSE) which can serve as markers for small cell lung cancer were simultaneously detected using magnetic nanobeads based LFSB.[37] Other proteins like albumin[38], C-reactive protein[39,40], and lipoprotein A[41] have also been detected in whole blood and plasma for the diagnosis of various metabolic disorders. LFSBs have also found application in the detection of allergenic food proteins as reviewed.[42]

1.3.2. Nucleic Acid Detection on Lateral Flow Strip Biosensors

Nucleic acids can serve as potent biomarkers for various cancers, infectious diseases and genetic disorders. Detecting nucleic acids in clinical samples is of immense importance in the medical field. There has been research over the years to develop LFSB based assays for the detection of nucleic acids. Nucleic acid hybridization dynamics is more complex and differs from that of immunoreactions. The initial nucleic acid biosensors relied on the detection of hapten modified nucleic acid amplification products using antibodies and hapten-protein complexes.[43] Other reports performed nucleic acid hybridization reactions in buffers prior to applying them on the LFSBs for detection.[29,44] Mao and coworkers[19] introduced a GNP based LFSB for the visual detection of DNA. This biosensor did not require prior incubation of DNA sequences before application on the LFSB, thus reducing the assay time significantly. Since then there has been direct detection of nucleic acids on the LFSB without the need for nucleic acid amplification.[23,25,45] Nucleic acid detection on LFSBs have been used for the detection of bacteria[29,44], viruses[46–49], plasmodium[50] and cancer related miRNA[23,51]. Additionally, LFSBs have aided the nucleic acid based identification of genetically modified organisms[52,53], chromosomal translocation[20], and genotyping of single-nucleotide polymorphisms[54].

1.3.3. Lateral Flow Strip Biosensor Based Detection of Cells and Exosomes

The detection of cells and exosomes is of importance in disease diagnosis, especially in cancer and infectious diseases. Measuring of circulating cancer cells and exosomes may help in the monitoring of patient response to therapy. Biomarkers that are displayed on the surface of cells and exosomes can be targeted using antibodies and aptamers for the detection of associated exosomes or cells on lateral flow strip assays. A lateral flow immunoassay (LFI) was reported for the detection of human pluripotent stem cells using antibodies that targeted surface proteins, stage-

specific embryonic antigens 3 and 4.[55] In other reports, whole bacteria like *Escherichia coli*[56] and *Salmonella enteritidis*[57] were detected in food including milk powder, flour, starch and eggs. Whole *Yersinia pesti* which causes bubonic plaque was also detected using an antibody aided lateral flow strip test.[58] Li and coworkers[59] also reported a multiplexed LFI for the simultaneous detection of *Pseudomonas aeruginosa* and S*taphylococcus aureus* using colloidal gold as nano-labels.

The examples cited thus far have relied on antibodies as biorecognition elements. Not much work has been done on the detection of cancer cells and exosomes using aptamer based LFSBs. Mao and coworkers[15] detected Ramos cells in a sandwich assay using a thiolated aptamer linked to a GNP and a second biotinylated capture aptamer immobilized on a solid support (nitrocellulose membrane). The GNP accumulation on the test line correlated with Ramos cell numbers. The assay was subsequently used to detect Ramos cells spiked into blood samples. Bacteria of food safety concern were also detected using aptamer based LFSBs.[16]

1.3.4. Lateral Flow Strip Biosensor Based Detection of Other Small Molecules

The LFSB platform has been used for the detection of small molecules of importance across medical, food safety and agricultural industries. Metal ions for example can play important biological functions by serving as co-factors for enzymes and as structural components of biomolecules such as hemoglobin. Other metals such as Mercury (Hg), lead (Pb), cadmium (Cd) can be toxic to living organisms. LFSBs for the detection of Pb^{2+} [60] and Cu^{2+} [61] were developed using non-cross-linked gold nanoparticle–DNAzyme conjugates. Other heavy metal such as Hg^{2+}, and Cd^{2+} have also been detected using nanogold labels.[21,62]

In the food and beverage safety industry toxins produced by various microbes and fungi are of critical heath and food safety concern. Mycotoxins like aflatoxin and ochratoxin that have

oncogenic properties have been detected on lateral flow strips.[63–65] In other work, drugs like clenbuterol [66], aminohydrantoin [67], and toxins like T2-Toxins [68] have also been detected in farm produce using LFSBs.

In the agricultural industry the use of pesticides and weedicides is important for increasing animal and crop survival and produce quality. However, if these chemicals are not regulated, they can remain in food produce and have harmful effects on the consumers. It is therefore important to measure these chemicals in foods to ensure the safety of the consumers. A reagentless LFSB was developed for the detection of acetylcholinesterase inhibitors and organophosphate pesticides[69] in beverage and food samples. Other pesticides like carbofuran and triazophos[22], carbaryl and endosulfan[70] have been detected in agricultural produce using multiplexed lateral flow assays. To assess exposure to pesticides, a lateral flow strip assay was developed for testing the presence of trichloropyridinol (a biomarker of exposure to chlorpyrifos) in human plasma.[71]

1.4. Aims and Objectives of this Study

The aim of this dissertation is to develop simple, rapid, low cost and user-friendly biosensors for the detection of cancer biomarkers to facilitate disease screening and monitoring. Clinically, the detection of biomarkers in bodily fluids can help in the early diagnosis of diseases ranging from genetic disorders, various cancers, infectious diseases and exposure to pesticides and other chemicals. Measuring of protein biomarker levels can also help monitor patient response to therapy. This can help physicians adjust drug treatment regiments to ensure higher survival rates of patients. For example, pre-surgery and post-surgery levels of a biomarker like CA 19-9 can be used to monitor the success of the surgery and confirm remission of pancreatic cancer.

For pancreatic cancer, CA 19-9 and CEA are the most popular markers used for monitoring disease and response to therapy and surgery. They have been predominantly measured by ELISA.

Though ELISAs offer acceptable sensitivity and selectivity they have the disadvantages of requiring expensive washers and readout spectrophotometers, and skilled labor. ELISA usually has multiple wash cycles and long incubation times (a few hours to overnight incubation) that can result in long assay times. On the contrary, lateral flow assays offer a quick, inexpensive and simple alternative to the traditional ELISA tests. Lateral flow assays require low sample volumes but achieve good sensitivity and selectivity. This dissertation seeks to discuss the development of LFSBs for the detection of cancer biomarkers directly and indirectly from pancreatic cancer patient samples.

- A rapid and sensitive GNP-based LFSB was developed for the quantitative detection of CA 19-9 in human plasma. The visual detection limit of the assay was 5ng mL^{-1} which was below the reference value (37 U mL^{-1}). The assay was successfully used to detect CA 19-9 in human plasma and assay results were validated with commercial ELISA test kits.
- A quantitative and rapid GNP-based LFSB was developed for the detection of CEA in human pancreatic cyst fluid. The developed assay had good sensitivity with detection limit of 2 ng mL^{-1}. The assay was successfully used to distinguish mucinous from non-malignant pancreatic cyst.
- A MWCNT-based LFSB for ultrasensitive detection of proteins in human plasma was developed. Combining the advantages of lateral flow assays with the unique physical properties of CNT (color, high aspect ratio and ease of surface modification), the optimized LFB had a detection limit 1.32 pg mL^{-1} of rabbit IgG. This detection limit was 3 orders lower than the detection limit of the GNP-based

LFSB for rabbit IgG detection. The assay was successfully used for the detection of rabbit IgG spiked in human plasma.

- Based on the improved sensitivity of the MWCNT-based LFSB developed for protein detection in human plasma, a MWCNT-based LFSB was developed for the screening of CEA. The assay showed improved detection limits of 0.1 ng mL^{-1} relative to CEA detection on GNP-based LFSB with detection limit of 2 ng mL^{-1}.
- A MWCNT- based LFSB was developed for the detection of CA-19-9. The developed biosensor showed good sensitivity with a visual detection limit of 0.14 U mL^{-1} CA 19-9 in buffered solution, which was an about 35-fold improvement over the GNP-based LFSB for CA 19-9 detection. Further, it showed a linear dynamic range of 5 to 100 U mL^{-1} CA 19-9.
- A lateral flow strip aptasensor (LFSA) was developed for the quantitative detection of pancreatic cancer exosomes using GNP as colorimetric labels. The assay targeted an exosome surface protein (EpCAM), whose expression changes in pancreatic cancer patients. The developed assay had a low detection limit of 1.3 x 10^3 exosomes μL^{-1} which was over 60-folds lower than a previously reported antibody based LFSB for exosome detection.[72]

2. DEVELOPMENT OF QUANTITATIVE IMMUNOCHROMATOGRAPHIC ASSAY FOR RAPID AND SENSITIVE DETECTION OF CARBOHYDRATE ANTIGEN 19-9 (CA 19-9) IN HUMAN PLASMA[†]

2.1. Introduction

Changes in the levels of various biochemical molecules have been known to be associated with diseased conditions for years. These molecules are termed biomarkers and represent a very diverse group of molecules including proteins (enzyme, antibodies, cell surface receptors, secreted proteins), nucleic acids (DNA, microRNAs), carbohydrates, peptides and other molecules.[5] In cancer research, biomarkers are used for disease diagnosis, monitoring patient response to therapy, post-operative monitoring, progression of disease condition and disease recurrence.[5,73] Carbohydrate antigen sialyl Lewis commonly denoted as CA 19-9, is a cancer biomarker that was first isolated in 1979 by Koprowski and coworkers from colorectal carcinoma and later from pancreatic carcinoma.[74,75] CA 19-9 is the main tumor biomarker for digestive tract associated cancers.[76–78] The highest CA 19-9 expression has been reported to occur in pancreatic cancer. [79] CA 19-9 is also associated with other digestive tract cancers, including stomach and bile cancer. Others like breast, lung, and ovarian cancers have also been reported to be associated with elevated CA 19-9. [80,81] Elevated CA 19-9 has also been linked with non-cancerous conditions such as pancreatitis, bile inflammation, cirrhosis and obstructive jaundice disease.[80,81] Despite its low specificity, CA 19-9 remains the only United States Food and Drug Administration (USFDA)

[†] The work discussed in this chapter was co-authored by Kwaku Baryeh, Sunitha Takalkar, Michelle Lund and Guodong Liu. The work was previously published in the Journal of Pharmaceutical and Biomedical Analysis.[119] Kwaku Baryeh was the primary developer of the conclusions that are advanced here. Kwaku Baryeh drafted and revised all versions of this chapter. Sunitha Takalkar, Michelle Lund and Guodong Liu proofread the manuscript and helped trouble shoot experimental conditions.

approved biomarker for pancreatic cancer and is the most accurate single biomarker for pancreatic cancer.[82]

Pancreatic cancer is one of the deadliest cancers with a yearly diagnosis rate close to its annual mortality rate.[83] Hence, sensitive and specific determination of low levels of CA 19-9 in biological fluids would be advantageous in clinical diagnosis, prognosis and monitoring of pancreatic cancer patient response to therapy.

A variety of strategies and techniques have been developed to detect CA 19-9. Most of these assays utilize CA 19-9 monoclonal antibody 1116-NS-19-9 clone as a specific probe to recognize CA 19-9.[80] One of the first CA 19-9 assays developed was a radioimmunoassay reported in 1983.[84] Since then there have been reports of enzyme linked immunosorbent, photoelectrochemical, fluorescent and electrochemical assays for detection of CA 19-9.[85–87] There are also reports of CA 19-9 detection using Surface Plasmon Resonance (SPR) and Raman Spectroscopy.[88,89] Though most of these methods have provided acceptable detection limits and specificities to CA 19-9, there remains drawbacks such as the use of radioactive materials, extensive sample preparations and wash steps, enzyme reactions, long assay times and the requirement for technical expertise, as well as expensive and specialized instrumentation.

Immunochromatographic assay (IA), also named lateral flow immunoassay (LFI), is a point-of-care approach, which overcomes the drawbacks of traditional immunoassays. Lateral flow assays have been used for the detection of various targets ranging from proteins and nucleic acids to other small molecules.[24,25,45,90–96] Various nanoparticles (e.g. GNPs, quantum dots, silver nanoparticles among others) have been used in lateral flow assays with varying degrees of sensitivity. GNPs are however the gold standard for lateral flow assays due to their stability, ease of preparation and low cost. The surface plasmon property of GNPs gives them intense size

dependent coloration, which makes them highly desirable for LFSB applications. The color of GNPs enables naked eye detection of analyte on LFSBs. GNPs have shown great versatility for use in the analysis of complex matrixes including food, water and clinical samples (e.g. plasma, serum). [24,25,90–96] Traditional LFIs are qualitative (Yes/No) or semi-quantitative assays. Recently, our group and others have developed quantitative LFSBs for rapid and sensitive detection of various analytes.[24,25,45,91,94–96] In this work, a quantitative immunochromatographic assay (QIA) was developed using a GNP-based LFSB and a portable strip reader for the rapid and sensitive detection of CA 19-9 in human plasma. This has the advantages of being rapid, sensitive and low cost as compared to the conventional CA19-9 immunoassays and immunosensors.

2.2. Experimental Section

2.2.1. Apparatus

Biojet BJQ 3000 dispenser, Clamshell Laminator, and the Guillotine cutting module CM 4000 manufactured by Biodot LTD (Irvine, CA, USA) were used to prepare lateral flow strip biosensors. Portable test strip reader (DT2032) was purchased from Shanghai Goldbio Tech. Co., LTD (Shanghai, China).

2.2.2. Reagents and Materials

Gold chloride trihydrate ($HAuCl_4$), trisodium citrate, sodium deodocylsulfate (SDS), sodium chloride (NaCl), Tween 20, sucrose, trisodium phosphate (Na_3PO_4), hexadecyltrimethylammonium bromide (CTAB), trizma hydrochloride (Tris-HCl, pH=8.0), phosphate buffered saline (PBS, pH=7.4, 0.01M), PBS with 0.05% Tween-20 (PBST, pH=7.4), bovine serum antigen (BSA) and immunoglobulin (IgG) from human plasma were obtained from Sigma Aldrich (St. Louis, MO, USA). Nitrocellulose membranes (HFC090MC100,

HFC180MC100, HFC240MC100), glass fiber (GFCP000800) and fiber pads were (CFSP001700) obtained from Millipore (Billerica, MA, USA).

Native CA 19-9 protein (30-AC14) and mouse anti-CA19-9 antibodies with catalogue numbers of 10-CA19A and 10-CA19B were purchased from Fitzgerald Industries International (Acton, MA, USA). The anti-CA 19-9 antibodies were designated as anti-CA 19-9 AbA and anti-CA 19-9 AbB, respectively. Human mammaglobin was purchased from Creative BioMart (Shirley, NY, USA). CA 19-9 ELISA kit (EHCA 19-9) and goat anti-mouse IgG (A16092) was purchased from Thermofisher Scientific (Waltham, MA, USA). Healthy human plasma samples were purchased from Golden West Biologicals, Inc. (Temecula, CA, USA). Blood samples from pancreatic cancer patients were provided by Sanford Clinic (Fargo, ND, USA, IRB#: SM17227). All reagents used were analytical grade chemicals. All solutions used in the study were prepared in ultrapure (>18 MΩ) water made from Milli-Q water purification system by Millipore (Billerica, MA, USA).

2.2.3. Preparation of GNP and GNP- Anti CA 19-9 AbA Conjugates

GNPs with typical diameters averaging 13 nm ± 3.5 nm were prepared as previously reported.[97] Briefly, glassware used for the preparation of the GNPs were soaked with *aqua regia* (3:1; HCl:HNO_3) followed by thorough washing with distilled water. Fifty microliters of 50% w/v $HAuCl_4$ was added to 250 mL ultrapure water in glassware. The mixture was heated and brought to boil under vigorous stirring. Sodium citrate solution was added, and the mixture was allowed to boil until the characteristic red color of GNPs was observed. The solution was boiled for an additional 10 mins. Prepared GNP solution was cooled down to room temperature (RT) and stored at 4°C until further used.

GNP-Anti CA 19-9 AbA conjugates were prepared by incubating anti-CA19-9A AbA at a concentration of 75 µg in 1 mL of 5-fold concentrated GNPs at pH=9. The mixture was incubated at RT for 1 hour on a shaker at low speed. After which 10% BSA solution was added to a final concentration of 1%. The mixture was further incubated for 1 hour with gentle mixing. The mixture was then centrifuged at 12,000 rpm for 15 mins at 4°C. The supernatant containing excess antibodies was discarded and pelleted GNP-Anti CA19-9 AbA conjugate was resuspended in PBS containing 1% BSA to wash it. The washing was repeated twice, and conjugate was finally suspended in a buffer containing 20 mM sodium phosphate, 0.25 % Tween-20, 10 % sucrose and 5 % BSA. Prepared conjugates were stored at 4°C until used.

2.2.4. Preparation of CA19-9 Lateral Flow Strip Biosensors

The setup for the developed GNP-based LFSB is as pictured in **Figure 2.1.** The biosensor was composed of a sample pad, conjugate pad, nitrocellulose membrane and an absorption pad all immobilized on a sticky backing layer.

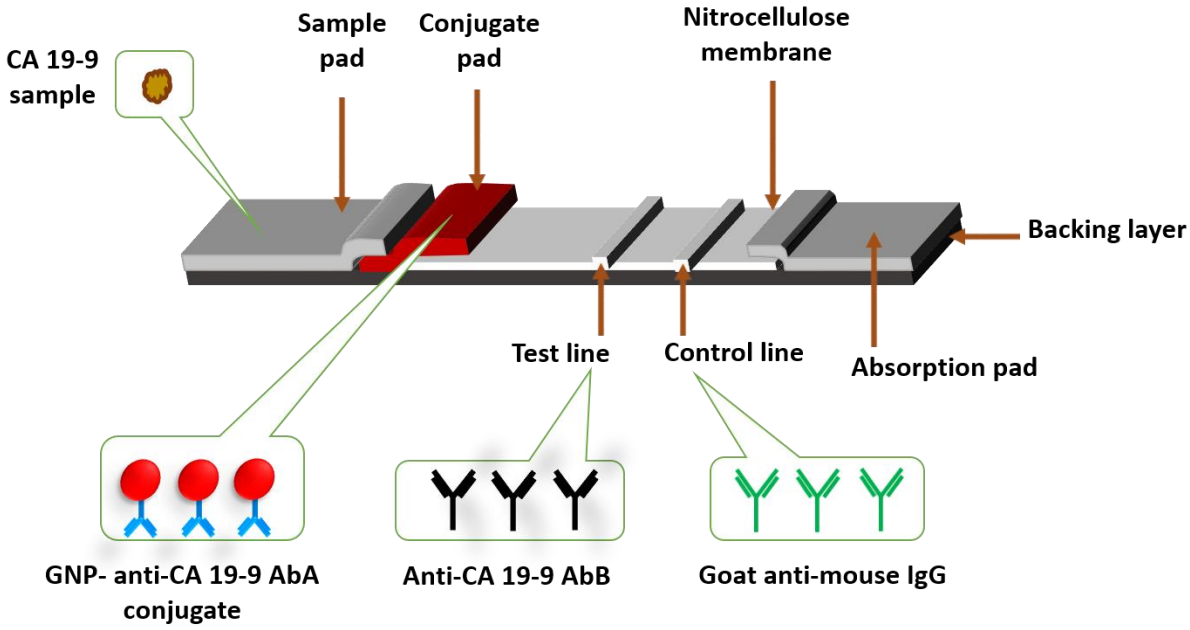

Figure 2.1. Configuration of the gold nanoparticle-based lateral flow strip biosensor for the detection of CA 19-9.

The sample pad was a cellulose fiber pad (17 mm x 300 mm) and pretreated with a buffer (0.05 M Tris-HCl + 0.25% Triton X-100 + 0.15 mM NaCl, pH 8.0) for 1 hr after which it was dried at 37°C and stored in a desiccator at RT until used. The conjugate pad was a glassy fiber membrane on which the GNP-Anti-CA19-9 AbA conjugate was dispensed on before an assay. The test and control lines of LFSB, which were 3 mm apart, were prepared by dispensing anti-CA19-9 AbB (0.5 mg mL^{-1}) and goat anti-mouse IgG (1 mg mL^{-1}) respectively onto the nitrocellulose membrane (25 mm ×x 300 mm). The nitrocellulose membrane was dried at 37°C for 1 hr and subsequently kept at 4°C until used. The absorption pad was a cellulose pad with dimensions 17mm x 300mm. All components were assembled onto a 60 mm × 300 mm adhesive plastic layer with a clamshell laminator. To ensure the continuous migration of solution along the LFSB, the components were overlapped by 2 mm. The assembly was then cut down to strips with 3 mm width using a Guillotine cutting module CM 4000. Prepared strips were kept at 4°C until used.

2.2.5. Assay Procedure

One hundred microliters of CA 19-9 sample solution prepared in running buffer (PBS + 1% BSA + 0.5 mM CTAB) was applied to the sample pad of the developed LFSB. The solution could travel through the membranes in 15 mins. An extra 100 µL of running buffer was added to wash the test strip. The washing step removes any nonspecifically adsorbed conjugates and thus reduces background signal. The test results could be read visually with the naked eye after 5 mins. To get quantitative data, the intensities of the test and control lines were read with a portable test strip reader. Human plasma samples were tested with a similar procedure as above. Prior to testing, plasma samples were diluted 2-fold with PBS buffer containing 2% BSA and 1% CTAB. Pancreatic cancer plasma samples were prepared by centrifuging blood samples at 3000 x g and collecting the supernatant.

2.3. Results and Discussion

2.3.1. Principle of the Quantitative Immunochromatographic Assay (QIA) for CA 19-9

Figure 2.2 illustrates the principle of the QIA for the detection of CA 19-9. Anti-CA 19-9 Ab B and goat anti-mouse IgG antibody were pre-immobilized on the nitrocellulose membrane to form the test line and control lines respectively. Anti-CA 19-9 Ab A was used as detection antibody and was immobilized on the GNP surface. The GNP-anti-CA 19-9 Ab A conjugate was dispensed on the conjugate pad.

Sample solution containing CA 19-9 was applied on the sample application pad. The solution migrated by capillary action, and upon reaching the conjugate pad, rehydrated the GNP-anti-CA 19-9 Ab A conjugates. An immune-complex (GNP-anti-CA 19-9 Ab A-CA 19-9) was formed between the CA 19-9 and anti-CA 19-9 Ab A of the GNP-anti-CA 19-9-AbA conjugates and continued to migrate along the strip. The complex was captured on the test zone through a second immunoreaction between the CA 19-9 and the immobilized anti-CA 19-9 Ab B. The accumulation of GNPs in the test zone was visualized as a characteristic red band (**Figure 2.2. a**). The excess GNP-anti CA 19-9 Ab A conjugates continued to migrate and were captured on the control zone by the immune-events between goat anti-mouse IgG and anti-CA 19-9 Ab A. This resulted in the formation of a second red band (**Figure 2.2. a**). In the absence of CA 19-9, no red band was observed in the test zone. In this case, a single red band (control line) showed that the LFSB was working well (**Figure 2.2. b**). The strips were observed with the naked eye for qualitative analysis. Quantitative analysis is performed by reading the optical intensity of the test and control lines with a portable strip reader (**Figure 2.2. c**). The strip reader connected with a laptop which had an installed software that transduced the line intensities into characteristic peaks.

The peak area on the computer monitor was proportional to the number of GNPs captured on the test line, which was in-turn proportional to the concentration of CA 19-9 in the sample solution.

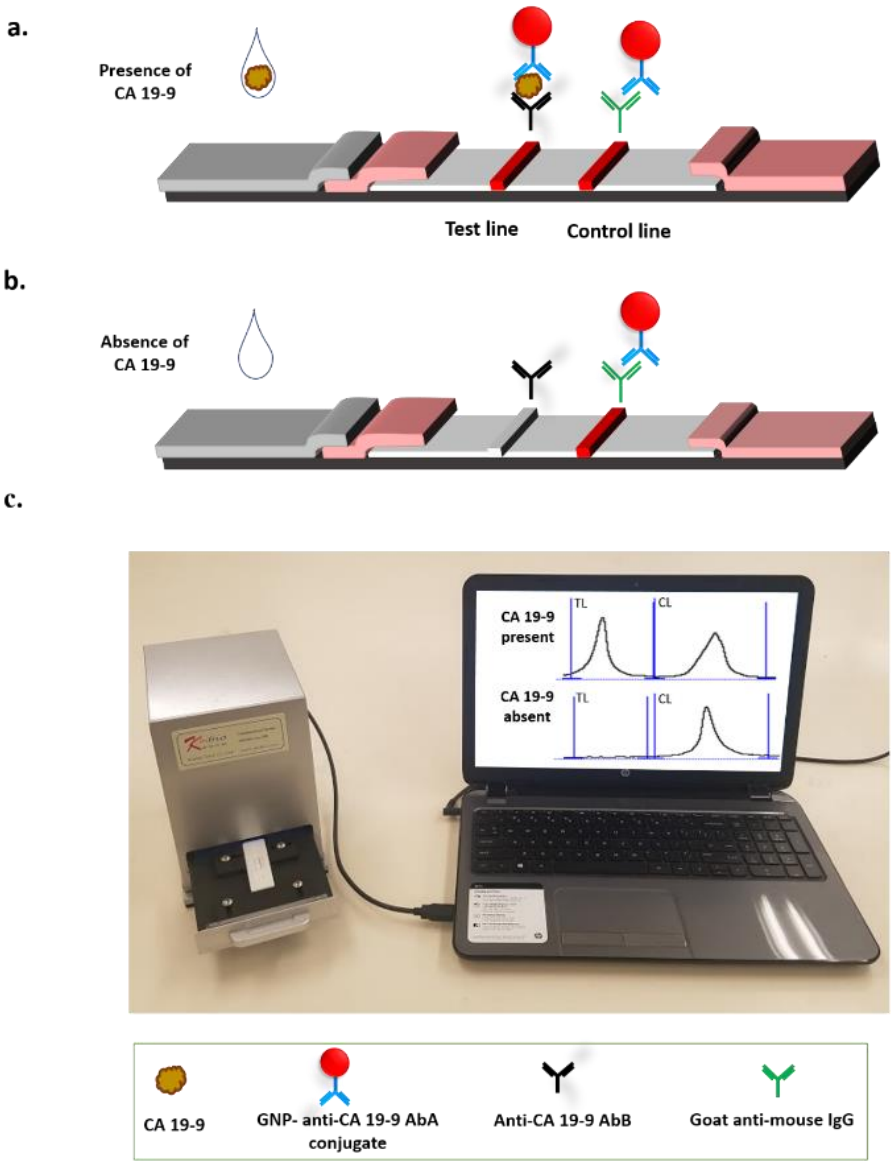

Figure 2.2. Principle of quantitative immunochromatographic assay of CA 19-9 (a) Capture of gold nanoparticles on the test line and control line in the presence of CA 19-9 (b) Capture of gold nanoparticles on the control line in the absence of CA 19-9 (c) Measuring the intensities of test and control lines with a portable strip reader connected to a laptop computer.

2.3.2. Optimization of Experimental Parameters

Assay parameters including the membrane type, antibody concentration, amount of GNP-anti-CA 19-9 conjugates and the components of the running buffer were optimized to obtain the

best sensitivity and reproducibility of the assay. The flow rate of sample solution on the nitrocellulose membrane dictated the time frame within which CA 19-9 interacted with the antibodies on the GNP surface, test line and control line. Three membranes HF090MC100, HF180MC100 and HF240MC100 with flow time of 90, 180 and 240 seconds (sec) as reported by the manufacturer were evaluated for their performance in the LFSB. From **Figure 2.3. a**, it is observed that the 90sec membrane had the highest signal to noise (S/N) ratio. Although the 180 sec and 240 sec membranes increased the immunoreaction time, it led to high background signal and hence lowered the S/N ratios. Therefore, the 90sec membrane was chosen to prepare the LFSBs.

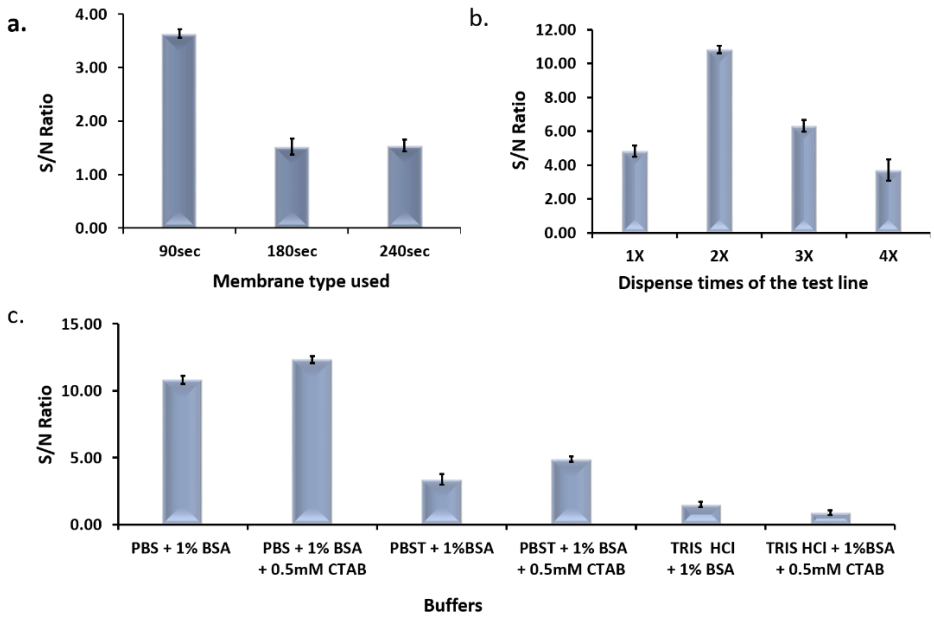

Figure 2.3. (a) Effect of different types of nitrocellulose membranes on the S/N ratio of the assay (b) Effect of the dispensing times of Anti-CA 19-9 AbB on the S/N ratio of the assay (c) Effect of buffer components on the S/N ratio of the assay.

The signal of the LFSB was affected by the amount of anti-CA 19-9-AbB immobilized on the test zone, which needed to be enough to generate the test band with minimum nonspecific adsorption. The anti-CA 19-9 AbB solution was dispensed on the test zone with different dispensing times and the S/N ratios of the LFSBs were compared. As shown in **Figure 2.3 b,** the

highest S/N ratio of the LFSB was obtained when the dispensing times was 2. At dispense times of 3 and 4, the S/N ratio reduced. This is most likely the result of increased non-specific interaction at high concentration of antibody as well as steric hindrance. Therefore, 2 times dispense cycles of the test line was used for further development of the LFSB.

The composition of running buffer has a substantial influence on the performance of the LFSB. Various buffers including PBS + 1% BSA, PBS + 1% BSA + 0.5 mM CTAB, PBST + 1% BSA, PBST + 1% BSA + 0.5 mM CTAB, Tris-HCl + 1% BSA and Tris-HCl + 1% BSA + 0.5 mM CTAB were tested. It was observed that the highest S/N ratio was obtained with PBS+1% BSA+0.5 mM CTAB (**Figure 2.3. c**), which was therefore used as running buffer for subsequent experiments.

The amount of anti-CA 19-9 AbA used to prepare GNP-anti-CA 19-9 AbA conjugates played a key role in the sensitivity of the assay. Various concentrations of anti-CA 19-9 AbA were used to prepare the conjugates and the S/N ratios of LFSBs were compared (**Figure 2.4 a**). From the graph, low S/N ratios of LFSBs were obtained with low concentrations of antibody. The reason could be low coating density of antibody on the GNP surface, which reduced the efficiency of immunoreactions during the assay. Beyond 75 µg of antibodies for conjugate preparation, there was a reduction in the S/N ratio of the assay. The low S/N ratio at higher concentrations could be attributed to overcrowding of the antibodies on the surface of the GNP thus reducing accessibility to bind target CA 19-9. As shown in **Figure 2.4. a**, 75 µg of anti-CA 19-9 AbA gave the highest S/N ratio and was thus chosen for subsequent assays.

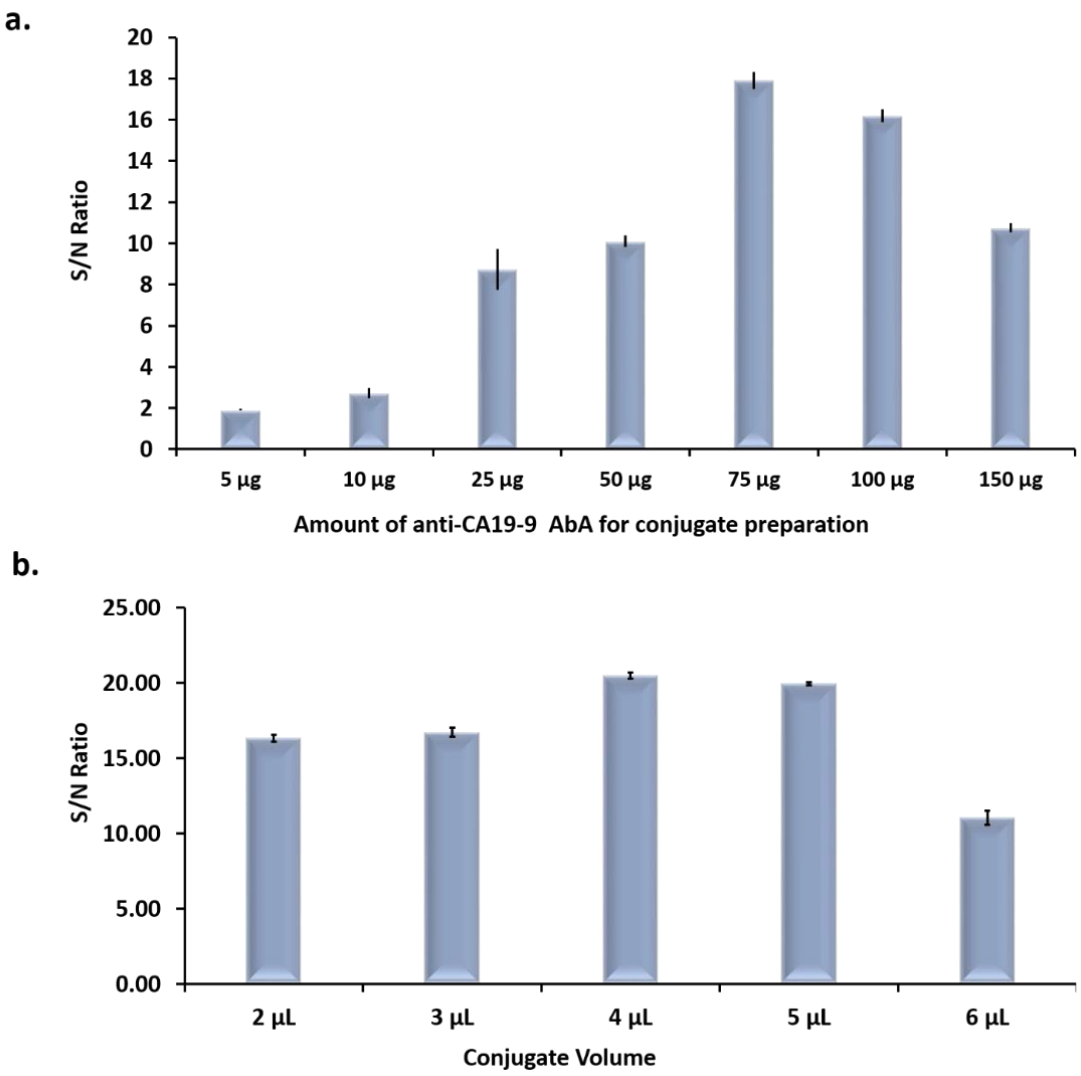

Figure 2.4. (a) Effect of the amount of Anti- CA 19-9 AbA used for conjugate preparation on the S/N ratio of the assay (b) Effect of the conjugate volume on the S/N ratio of the assay.

The amount of GNP-anti-CA 19-9 AbA conjugate dispensed on the conjugate pad was also optimized to obtain the best sensitivity of the assay. Different volumes of GNP-anti CA 19-9 AbA were loaded on the conjugate pad and the S/N ratios of the assay were compared. As presented in **Figure 2.4 b**, the S/N ratio peaked at 4 µL, after which the S/N ratio reduced. Beyond 4 µL of conjugate, there was increased background signal due to increased nonspecific adsorption thus reducing the S/N ratios. A conjugate volume of 4 µL was adopted for further assay development.

2.3.3. Analytical Performance

Under the optimized experimental conditions, the GNP-based LFSBs were used to detect different concentrations of CA 19-9. Sample solutions were prepared by diluting the CA 19-9 stock solution in running buffer. All tests were run in triplicates.

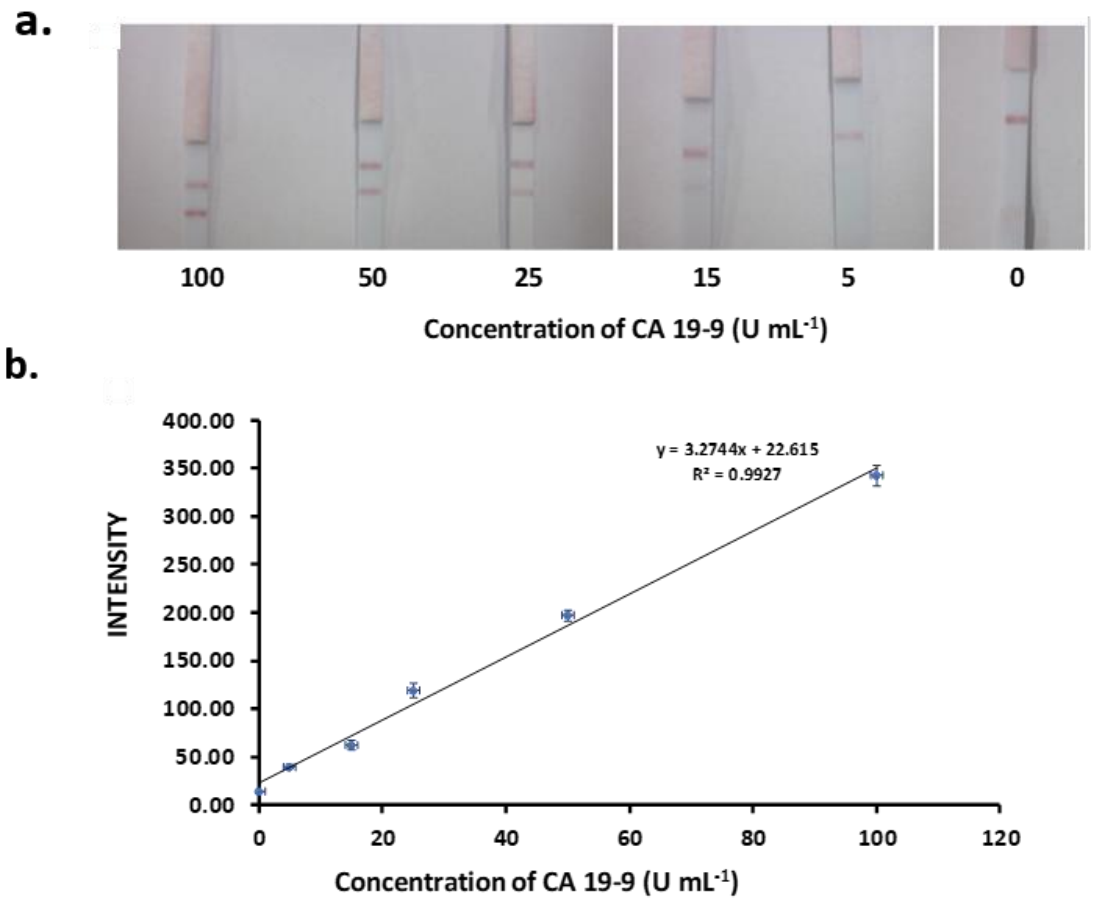

Figure 2.5. (a)Photo images of LFSBs in the presence of different concentrations of CA 19-9 (b) Calibration curve of CA 19-9 detected on developed GNP-based lateral flow strip biosensor. Each data point represents the average value obtained from three different measurements.

Figure 2.5. a presents the typical photo images of the LFSBs with increasing concentrations (0 to 100 U mL^{-1}). As expected, the intensities of the test-lines increased with increasing concentrations of CA 19-9. No test line was observed on the test zone of LFSB in the absence of CA 19-9 (control), indicating negligible nonspecific adsorption. The test line was still

observed at 5 U mL^{-1} of CA 19-9, which was the visual detection limit of CA 19-9 without instrumentation. All LFSBs showed the red control-line, which was a validation of the proper performance of the developed LFSBs. Quantitative detection was obtained by reading the intensity of the test line with the aid of a portable strip reader. The peak areas increased with the increasing intensity of the test lines, and thus correlated with increasing CA 19-9 concentrations. The resulting calibration curve (**Figure 2.5. b**) was plotted using the peak areas versus CA 19-9 concentration to yield a linear dynamic range between 5 and 100 U mL^{-1} (R^2=0.9927, y= 3.274x + 22.615). The limit of detection (LOD) of the assay (S/N =3) was determined to be 5 U mL^{-1}. Aside the low detection limit achieved, the developed LFSB showed good reproducibility. Six replicate tests were performed in the absence and presence of 30 U mL^{-1} of CA 19-9. The relative standard deviation of testing 0 U mL^{-1} and 30 U mL^{-1} were 2.1% and 3.2%, respectively (data not shown). The selectivity of the assay was studied by testing a series of probable interferences including CEA, human IgG and mammaglobin. As shown in **Figure 2.6.**, a high response was observed when 30 U mL^{-1} CA 19-9 was tested, whereas negligible signals were obtained from other proteins with concentrations of 100 ng mL^{-1}, indicating the excellent specificity of the assay.

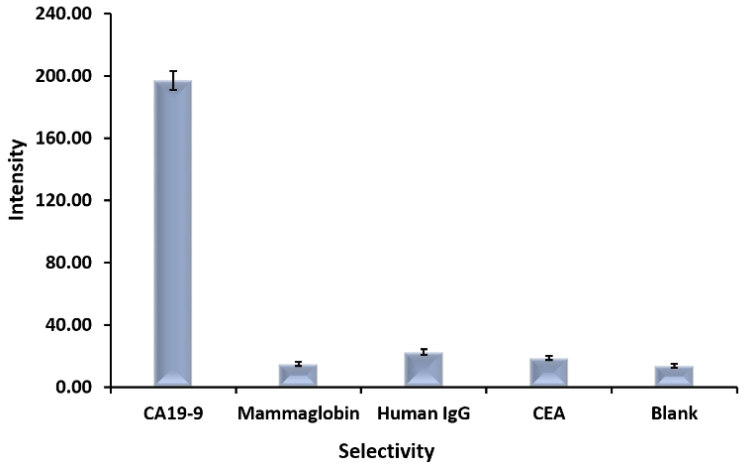

Figure 2.6. Selectivity of the developed GNP-based LFSB (concentration of CA 19-9 was 50 U mL^{-1}; Mammaglobin, Human IgG and CEA were at 100 ng mL^{-1}).

2.3.4. Detection of CA 19-9 in Healthy Human and Pancreatic Cancer Patient Plasma

The developed assay was used to detect the concentrations of CA 19-9 in healthy human plasma and pancreatic cancer patient plasma samples. Six plasma samples each from healthy humans and pancreatic cancer patients were tested, and the results were validated with commercially available ELISA kit. Plasma samples from healthy humans were purchased from Golden West Biologicals, Inc. (Temecula, CA). Blood samples from pancreatic cancer patients were provided by Sanford Clinic. Plasma of pancreatic cancer patients were prepared by spinning the blood samples in an EP tube at 3000 g for 10 min and collecting the supernatant. Plasma (50 µL) was diluted two-fold in a buffer containing PBS+2% BSA+1% CTAB before the test. **Table 2.1** shows the results from the developed QIA and ELISA. One can see that the analytical results of the QIA are in good agreement with the results obtained from ELISA, indicating that the QIA had good reliability for quantifying CA 19-9 concentrations in clinical samples.

Table 2.1. Screening of plasma samples from healthy human and pancreatic cancer patients with the developed QIA and commercial ELISA kit.

Plasma sample	This assay (QIA)	Commercial ELISA
Healthy human plasma sample 1	12.67 ± 0.38	11.88 ± 0.75
Healthy human plasma sample 2	30.76 ± 1.21	32.13 ± 1.62
Healthy human plasma sample 3	0	0
Healthy human plasma sample 4	24.56 ± 1.48	25.72 ± 2.11
Healthy human plasma sample 5	10.51 ±	11.87 ± 0.92
Healthy human plasma sample 6	21.92 ± 1.23	20.56 ± 1.01
Pancreatic cancer patient sample 1	97.03 ± 0.67	95.72 ± 1.01
Pancreatic cancer patient sample 2	113.49 ± 4.3	116.49 ± 3.45
Pancreatic cancer patient sample 3	40.56 ± 2.12	42.26 ± 1.25
Pancreatic cancer patient sample 4	0	0
Pancreatic cancer patient sample 5	84.61 ± 2.56	86.45 ± 2.88
Pancreatic cancer patient sample 6	97.03 ± 0.67	95.72 ± 1.01

2.4. Conclusion

A quantitative immunochromatographic assay was developed by using GNP-based lateral flow strip biosensor and a portable reader for the rapid and sensitive detection of CA 19-9. The assay was successfully applied to quantitate CA 19-9 concentrations in healthy human plasma and pancreatic cancer patient plasma samples. The detection limit of 5 U mL^{-1} achieved is sufficiently sensitive for clinical screening of CA 19-9 in plasma as the reported reference value of CA 19-9 in healthy human plasma is 37 U mL^{-1}.[89] The developed assay provides a simple, rapid and inexpensive method to detect CA 19-9 in human plasma. The GNP-based lateral flow strip biosensor shows great promise for clinical application and biomedical screening, particularly in limited resource settings.

3. QUANTITATIVE GOLD NANOPARTICLE-BASED LATERAL FLOW STRIP BIOSENSOR FOR THE DETECTION OF CARCINOEMBRYONIC ANTIGEN (CEA) IN HUMAN PANCREATIC CYST FLUID

3.1. Introduction

Pancreatic cancer (PC), though the fourteenth most prevalent cancer, is the fourth leading cause of cancer related deaths in the United States.[98] Much of the mortality from PC is the result of ineffective early diagnostic tests for PC screening. Traditionally PC has been diagnosed using imaging techniques like computed tomography, magnetic resonance imaging and angiography.[99] Other methods such as endoscopic ultrasound have also been used. The endoscopic ultrasound has the added advantage of being able to obtain tissue biopsies during examination, however, endoscopy is invasive and presents discomfort for patients. These diagnostic methods require the use of expensive equipment, skilled labor and expertise, and are therefore not feasible for routine screening.

Biosensors present an alternative to the above-mentioned techniques. Biosensors are self-contained devices that can screen biological samples and provide quantitative and semiquantitative analytical information using biorecognition elements linked to transducers.[100,101] Biosensors for disease screening rely on biomarkers which are molecules whose upregulation or downregulation can be an indication of a diseased or abnormal medical condition. For pancreatic cancer, the two most common biomarkers used for screening are carcinoembryonic antigen (CEA) and carbohydrate antigen (CA 19-9). CEA was initially developed solely for pancreatic cancer and has become the most commonly used diagnostic marker for gastrointestinal cancers. Elevated CEA levels in pancreatic cancer patients prior to therapy has been linked to poor prognosis.[98]

Of interest, CEA levels in pancreatic cyst fluid has been useful in the differentiation of benign and malignant pancreatic lesions. CEA remains the most effective protein biomarker linked to malignant pancreatic cysts. In 2004, a study showed that cyst fluid CEA levels was superior to endoscopic ultrasound, cytology and other biomarkers such as CA 72-4, CA 125, CA 19-9, and CA 15-3 at differentiating between mucinous and non-mucinous pancreatic lesions.[102] The diagnostic information obtained from cyst fluid analysis can determine whether patients are discharged, undergo further testing or scheduled for surgery.[98,103] Cancerous pancreatic cysts are rare compared to the much more common benign pancreatic cyst.[104] Pancreatic cancer once symptomatic, is invariably fatal. It is important that pancreatic cyst fluids are properly screened to give definitive diagnosis to avoid unnecessary surgery because the corrective surgery (pancreatic resection) is a major surgery that can result in complications and sometimes death.[104] Cyst fluid samples are usually collected by either needle or endoscopic ultrasound biopsies. Cyst fluid biopsies generally result in samples a few microliters in volume depending on the size of the cyst. It is therefore of import to develop diagnostic assays that have very small sample volume requirements.

CEA has been predominantly detected using enzyme-linked immunosorbent assays (ELISA).[105] In ELISA, CEA is captured between capture antibodies pre-immobilized in a well plate, and detection antibodies labelled with enzymes such as horse radish peroxidase or alkaline phosphatase. Upon introduction of enzyme substrate, the substrate is converted to a colored complex whose absorbance can be measured for quantitative data. ELISA has seen wide application for detecting proteins and is the most popular protein detection assay used for medical and diagnostic purposes. However, ELISA suffers setbacks such as the need for expensive plate readers, washers and requirement for trained expertise. Also, ELISA involves many washing steps

and long incubation hours. The assay time for ELISAs can vary from a few hours to as long as 2 days which makes them unsuitable for point-of-care applications.[105] Other methods like electrochemical assays that make use of nanoparticles for signal enhancement have also been reported for the detection of CEA.[106,107] There has also been a label free electrochemical assay utilizing silver-molybdenum disulfide-graphene oxide nanocomposite scaffold as a means of signal amplification for highly sensitive CEA detection.[108] CEA has also been detected using label-free surface plasmon resonance (SPR) [109] as well as gold nanoparticle enhanced SPR[110,111]. Other immunoassays utilizing platforms like quartz crystal microbalance [112,113] and Raman spectroscopy [114,115] have also been reported for CEA detection. These immunosensors offer low to acceptable sensitivity but suffer disadvantages of being expensive, requiring skilled expertise and having complex data processing requirements.

Lateral flow strip biosensors (LFSB) offer a simple, rapid and inexpensive alternative to the traditional immunoassays. The simplicity of the LFSBs means their operation do not require expensive equipment nor trained technical personnel. In its simplest form, qualitative test results can be read with the naked eye for colorimetric LFSBs. Additionally, LFSBs have high specificity and good sensitivity, exhibit less or no interference due to inherent chromatographic separation, and have long term stability under non-refrigerated conditions.[11] Their portability makes them prime candidates for point-of-care applications. The LFSB is a very versatile platform and has been applied widely in the medical, food and beverage, environmental monitoring industries for the detection of proteins [18,24,38,116], nucleic acids [23,25,28], cells [15], toxins [63,117], bacteria [117,118], and other small molecules [11,17]. For the transduction of target molecules capture into measurable signals, various nanoparticles like GNP [15,72,119], carbon nanotubes [25], fluorescent nanoparticles [23,120,121], magnetized carbon nanotubes [26,27], GNP-coated silica nanorods [24,45] and liposomes [28,116]

have been used with varying degrees of sensitivity. However, GNPs are the gold standard for lateral flow strip biosensors. GNPs have intense red color because of their surface plasmon property that makes them ideal for colorimetric LFSB applications. In addition, GNPs are stable, simple and inexpensive to prepare, and easy to conjugate to biorecognition elements. GNPs have been used for the detection of various targets with good sensitivity.[11,19,72] We previously reported a GNP-based lateral flow strip biosensor for the detection of CA 19-9 in human plasma samples that showed good performance and was able to distinguish between of healthy and pancreatic cancer patient samples.[119]

This work reports a simple, rapid and sensitive GNP-based lateral flow strip biosensor for the detection of CEA protein in pancreatic cyst fluid. The developed biosensor detected CEA in a sandwich type immunoassay by capturing target CEA in-between a capture antibody immobilized on a solid support (nitrocellulose membrane) and a GNP-linked detection antibody. The CEA dependent accumulation of GNPs on the test zone gave a red colored band that gave qualitative data via visual observation or quantitative data by reading test line intensities with a portable strip reader. The developed assay had the added advantage of requiring low sample volumes which makes it ideal for the screening of pancreatic cyst fluid biopsies. The developed GNP-based LFSB was sufficiently sensitive with a detection limit of 2 ng mL^{-1} without any form of signal amplification. The assay was successfully applied for the detection of CEA in pancreatic cyst fluid, and positively distinguished between mucinous and non-malignant pancreatic cysts. The developed assay shows great potential for the clinical screening of CEA in limited resource settings.

3.2. Experimental Section

3.2.1. Apparatus

The Biojet BJQ 3000 dispenser, Clamshell Laminator and Guillotine cutting module CM 4000 used for the assembling of the LFSB were bought from Biodot LTD (Irvine, CA, USA). Strips were quantitatively read with a portable strip reader (DT2032) acquired from Shanghai Goldbio Tech. Co., LTD (Shanghai, China). Strip images were captured with a S7 smart phone by Samsung Electronics (Seoul, South Korea).

3.2.2. Reagents and Materials

Gold (III) chloride ($HAuCl_2$), phosphate buffered saline (0.01 M PBS, pH 7.4), trizma hydrochloride buffer solution (Tris-HCl, 1.0 M, pH 8.0), tween 20, triton X-100, bovine serum albumin (BSA), sucrose, sodium chloride (NaCl), magnesium chloride ($MgCl_2$) and sodium phosphate tribasic deodecahydrate ($Na_3PO_4.12H_2O$) were purchased from Sigma–Aldrich (St. Louis, MO, USA) and were used without further purification. Native CA 19-9 (30-AC14), native CEA protein (30-1819) and anti-CEA antibodies (10-C10F and 10-C10G) were purchased from Fitzgerald Inc. Goat anti-mouse immunoglobulin G (IgG), trypsin and human IgG were purchased from Thermofisher Scientific (Waltham, MA, USA). Recombinant C4b-binding protein alpha chain (C4BP- α) was purchased from MyBioSource Inc. (San Diego, CA, USA). Human mammaglobin was bought from Creative BioMart (Shirley, NY, USA). Glass fibers (GFCP000800), cellulose fiber (CFSP001700), and nitrocellulose membranes (HFC090MC100, HFC135MC100, HFC180MC100) were purchased from Sigma–Aldrich (St. Louis, MO, USA) for biosensor fabrication. Human pancreatic cyst fluid samples were obtained from the University of Pittsburg Medical Center. All reagents were analytical grade. All solutions used in the study were

prepared in ultrapure (≥18M Ω) water from Millipore Milli-Q water purification system (Billerica, MA, USA).

3.2.3. Preparation of the GNP and GNP-Anti-CEA Conjugate

GNPs with diameters 13nm ± 3.5 were prepared by the citrate reduction method as previously described.[97] Glassware was washed with detergent and thoroughly rinsed with water. The glass vessels were then soaked in *aqua regia* (3:1; $HCl:HNO_3$) overnight and rinsed with copious amounts of water. Fifty microliters (50uL) of 50% w/v $HAuCl_4$ was mixed with ultrapure water in a glass vessel. The mixture was brought to boil with constant stirring. Sodium citrate was added, and the mixture was boiled with constant stirring until the color of the solution changed to the characteristic red color of GNPs. The solution was boiled for 10 additional minutes. The prepared GNPs were then cooled to room temperature and stored at 4°C until used.

One milliliter (1mL) of 5-fold concentrated GNPs were prepared by spinning prepared GNPs at 12,400 rpm for 15 mins. GNP pellets were collected and resuspended in water at pH=9. Forty micrograms (40ug) of anti-CEA Ab G (10-C10G) was added and incubated at room temperature for 2 hours with gentle shaking. BSA solution (10% w/v) was subsequently added to a final concentration of 1% and mixture was further incubated for 1hour. Prepared GNP anti-CEA conjugates were washed with 1% BSA solution by spinning at 12,400 rpm for 15 mins. The washing step was repeated two more times. The conjugates were then suspended in 1.0 mL eluent buffer (20 mM $Na_3PO_4 \cdot 12H_2O$, 5% BSA, 10% sucrose, and 0.25% Tween-20). The conjugates were stored at 4°C until used.

3.2.4. Preparation of GNP-Based LFSB for CEA Detection

The setup for the GNP-based LFSB for CEA detection was as shown in **Figure 3.1.** The biosensor consisted of three major components (conjugate pad, nitrocellulose membrane and

absorption pad) all assembled on a sticky nonporous plastic backing card. The conjugate pad was a glassy fiber onto which the conjugate was dispensed prior to assay runs. The glassy material was porous to enable the holding of adequate amounts of conjugates. The conjugate pad was also capable of releasing the conjugates when assay was run. The nitrocellulose membrane supported the test and control line biorecognition elements. Anti-CEA Ab F (10-C10F) and goat anti-mouse IgG at concentrations of 1 mg mL^{-1} were dispensed as test and control lines respectively. After dispensing, the membrane was dried at 37°C for 1hour. Membranes were stored at 4°C until used. The absorption pad was a cellulose pad that wicked the assay fluids and provided capillary force as assay was run. All three components were assembled on the sticky backing layer and secured using the Clamshell Laminator. The components overlapped by at least 2mm to ensure continuous fluid flow. The assembled biosensor was cut into 3mm width strips with the guillotine cutter. Prepared biosensors were kept at 4°C until used.

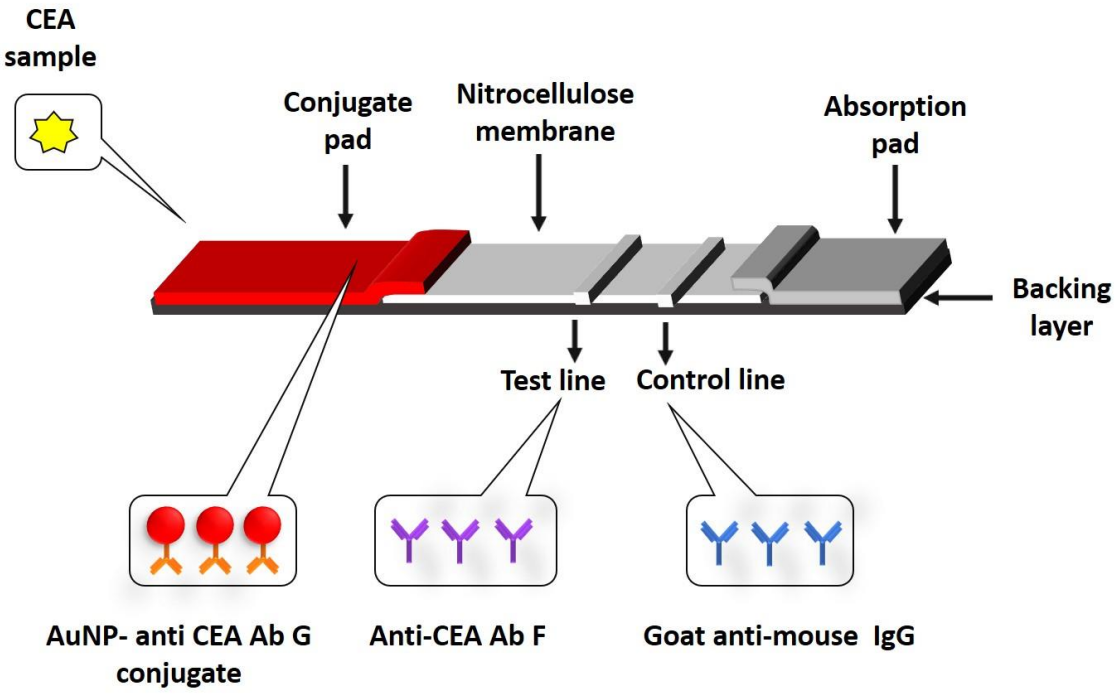

Figure 3.1. Scheme of the developed GNP-based Lateral Flow Strip Biosensor for the detection of CEA.

3.2.5. Assay Procedure

GNP-anti CEA Ab G conjugate was dispensed on the conjugate pad and allowed to air dry for 5 mins prior to running the assay. 100 µL of native CEA protein dissolved in running buffer (PBS + 1%Tween + 1% BSA + 1% PVP) was applied to the conjugate pad. The solution run through the strip for 20 mins. The GNP-based LFSB was then washed with 100 µL of running buffer. The washing step helped remove any nonspecifically adsorbed GNP-anti CEA conjugates on the test zone. The biosensor could be visually observed for qualitative data within 30 mins. The test and control line intensities were read with the portable strip reader to obtain quantitative data. To test the GNP-based LFSB's performance on real samples, pancreatic cyst fluid samples were diluted down to 10% v/v in running buffer with final buffer composition (PBST + 1% BSA + 1% PVP). Assay procedure and acquisition of test and control line intensities were the same as described earlier.

3.3. Results and Discussion

3.3.1. Working Principle of GNP-Based LFSB for CEA Detection

The GNP-based LFSB detected target CEA following a sandwich type immunoassay format as depicted in **Figure 3.2**. Anti-CEA Ab F and goat anti-mouse IgG were pre-immobilized on the nitrocellulose membrane as test and control lines. Anti- CEA Ab G served as the detection antibody and thus used for the preparation of the GNP-conjugate. The GNP-anti-CEA Ab G conjugate was dispensed onto the conjugate pad. When target was applied to the conjugate pad, the CEA moved by capillary action and underwent an immunoreaction with the anti-CEA Ab G of the GNP-conjugate to form an immunocomplex (GNP-anti-CEA Ab G-CEA). The immunocomplex moved further onto the nitrocellulose membrane and the CEA component underwent a second immunoreaction with the test line anti-CEA Ab F. The immunocomplex was

thus immobilized on the test line in presence of CEA resulting in a characteristic red colored line due to the GNP component. Excess GNP-anti-CEA Ab G conjugate moved further to the control line and were captured by the goat-anti mouse IgG resulting in a red second band on the control line. Thus, in the presence of target, two red bands were observable on the GNP-based LFSB (**Figure 3.2. a**). No immunoreaction occurred on test line in the absence of target CEA, however, the GNP-anti-CEA conjugates were captured on the control line resulting in a single red band (**Figure 3.2. b**). The test strips were examined with the naked eye for qualitative information. For quantitative data, test and control line intensities were read with the portable strip reader connected to a computer. The strip reader captured images of the test and control lines and converted their pixel intensities into gaussian peaks. The area under the curves gave indication of the number of GNPs immobilized on the test line which was directly proportional to the CEA levels present in test samples.

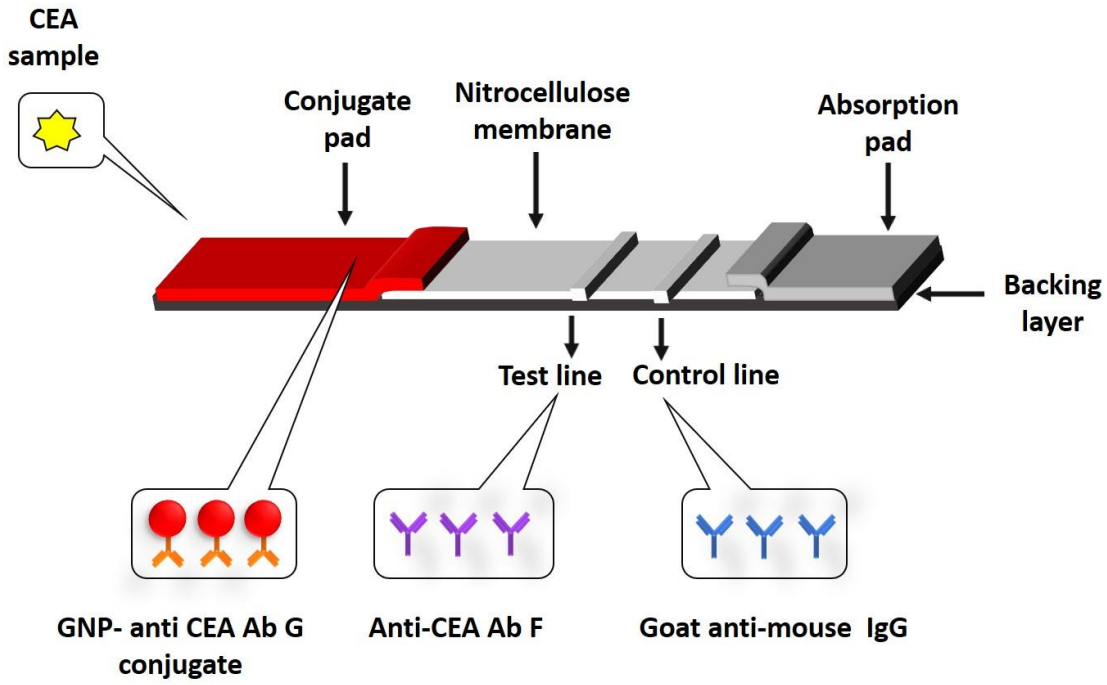

Figure 3.2. Working Principle of the developed GNP-based LFSB for CEA detection (a) Assay in the presence of target CEA (b) assay in the absence of CEA.

3.3.2. Optimization of Experimental Parameters

The performance of the GNP-based LFSB relied on the interplay of several assay parameters (type of nitrocellulose membrane, dispense times of test line, running buffer composition, antibody concentration for conjugate preparation and the volume of conjugate used per test run). It was necessary to optimize these experimental conditions to attain the best sensitivity and specificity of the developed assay.

The first line of optimization was selecting the type of nitrocellulose membrane on which the test and control line antibodies were dispensed. Three membranes (HF090MC100, HF135MC100, HF180MC100) with flow rates of 90, 135 and 180 sec $4cm^{-1}$ membrane were tested for their performance on the GNP-based LFSB and their signal-to-noise (S/N) ratios compared (**Figure 3.3. a**). The membrane flow rate determined the time frame of exposure for the test and control line immunoreactions. As seen from **Figure 3.3. a**, the 90sec membrane showed lowered S/N ratio. This was ascribed to the faster flow rate of the 90 sec membrane which reduced the exposure time for the test and control line immunoreactions. This resulted in lowered test line intensities which lowered the S/N ratio. The 180sec membrane which had the slowest flow rate showed the lowest S/N ratio. The slow flow rate increased the exposure time for the test zone immunoreaction. This resulted in increased nonspecific interactions which increased background signals and resulted in the observed low S/N ratio. The best S/N ratio was observed with the 135sec membrane which had the optimal flow rate to maximize the S/N ratios.

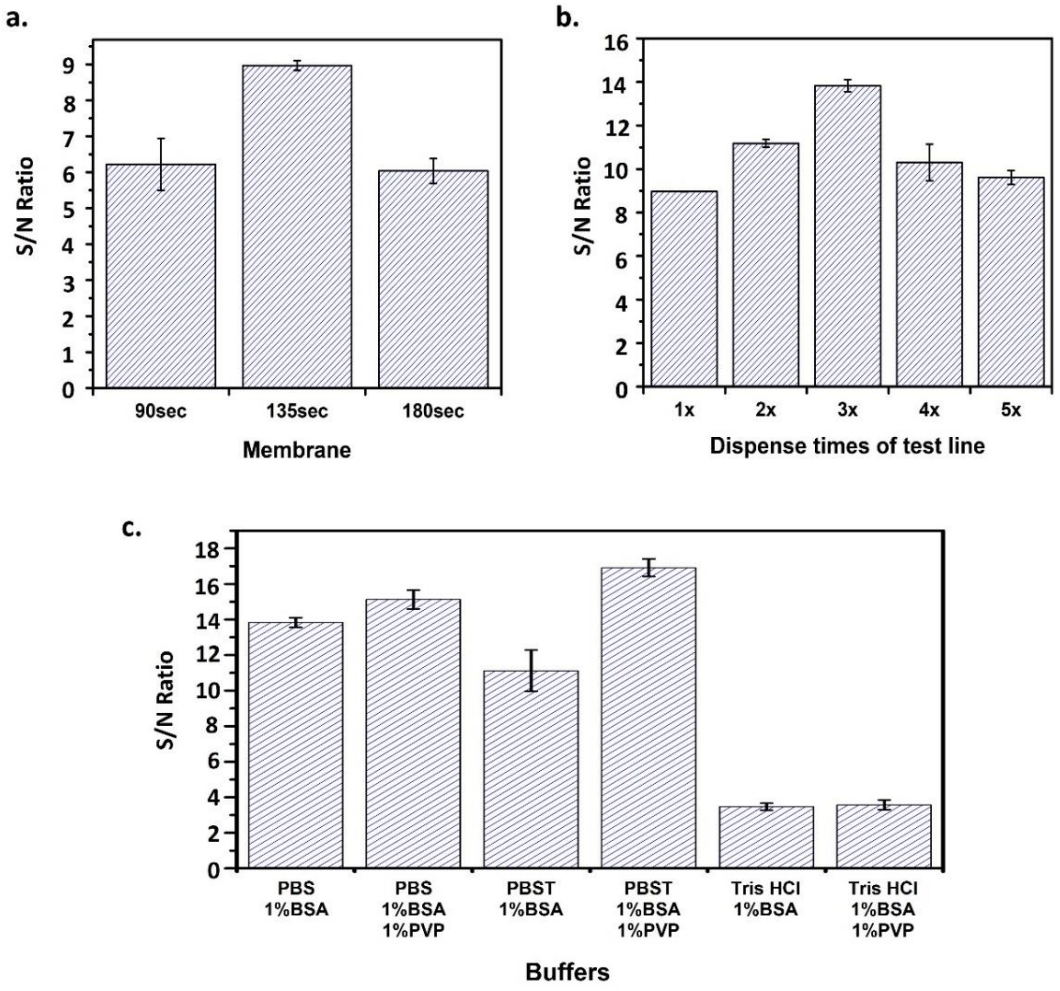

Figure 3.3. (a) Effect of nitrocellulose membrane type on the S/N ratio of the assay (b) Effect of the dispense times of test line anti-CEA Ab F on the S/N ratio of the assay (c) Effect of buffer composition on the performance of the assay.

The dispense times of the test line antibody was the next parameter to be optimized. The antibody concentration on the test line significantly affected the performance of the developed assay. The anti-CEA Ab F was dispensed varying number of times (1, 2, 3, 4 and 5) on the nitrocellulose membrane and their S/N ratios compared (**Figure 3.3. b**). Lower concentrations of antibodies at 1 and 2 times dispense cycles resulted in lowered test line intensities and thence lower S/N ratios. At higher dispensed cycles (4 and 5x) there was lowering of S/N ratios as increased antibody concentration on test line led to increased nonspecific interaction. The highest S/N ratio

was observed at 3x dispense cycles which had the ideal antibody coverage. 3x dispensing of the test line antibody and was chosen for further development of the biosensor.

The immunoreactions in the assay occurred in buffer solutions and the strength of these interactions were affected by the buffer compositions. Different buffered solutions including PBS + 1% BSA, PBS + 1%BSA + 1%PVP, PBST + 1% BSA, PBST + 1%BSA + 1%PVP, Tris-HCl + 1% BSA and Tris-HCl + 1% BSA + 1%PVP were tested for their performance on the GNP-based LFSB and their S/N ratios compared (**Figure 3.3. c**). The highest S/N ratio was measured in PBST + 1%BSA + 1%PVP, which was then chosen for further development of the LFSB.

The amount of anti-CEA Ab G coated on the surface of the GNPs was the next parameter to be optimized. To 1mL of 5-fold concentrated GNPs, varying amounts (10, 20, 30, 40, and 50 µg) of anti-CEA Ab G was added for the preparation of the conjugate. The prepared GNP- anti-CEA Ab G conjugates were tested for their performance on the LFSB and their S/N ratios compared (**Figure 3.4. a**). At 10 µg of anti-CEA Ab G, the lowest S/N ratio was observed. This was attributed to insufficient coverage of the GNP surface and lowered sandwich formation efficiency in the assay, which resulted in low test line intensities. The highest S/N ratios were observed when 20 µg of anti-CEA Ab was used for conjugate preparation. Beyond 20 µg there was a steady reduction in S/N ratios. The lowered performance was ascribed to steric hindrance due to antibody over-crowding on the surface of the GNPs. The over-crowding hindered the accessibility of the target CEA for binding to the of anti-CEA Ab G on the GNPs. 20 µg anti-CEA Ab G was therefore chosen for further preparation of conjugates for development of the GNP-based LFSB.

The final parameter optimized was the amount of GNP-anti-CEA Ab G conjugate dispensed on the conjugate pad. Varying volumes (2, 4, 6 and 8 µL) of conjugate were dispensed

on the conjugate pad and their performance on the LFSB compared as shown in **Figure 3.4. b**. Having low volumes of conjugates (2 and 4µL) dispensed resulted in lowered test line intensities and thus lowered S/N ratios. The S/N ratio peaked at 6 µL of conjugate, beyond which there was lowered S/N ratios. At higher volume beyond 6 µL conjugate, there was increased nonspecific interactions which led to high background signals and thus the observed lower S/N ratios. 6 µL of GNP- anti-CEA Ab G conjugate was therefore used for further testing.

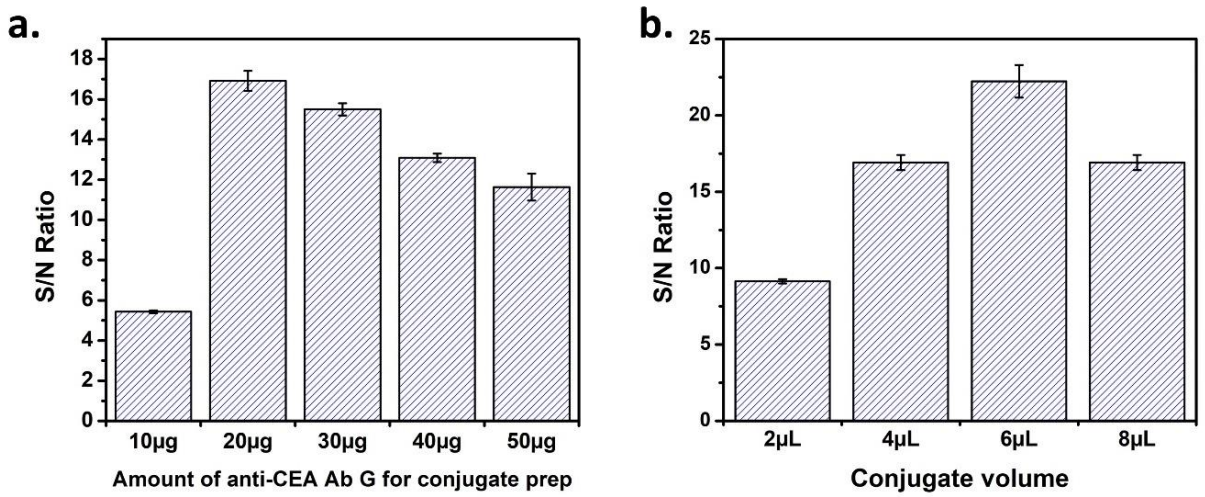

Figure 3.4. (a) Effect of the amount of anti-CEA Ab F used for conjugate preparation on the S/N ratio of the assay (b) Effect of conjugate volume on the S/N ratio of the assay.

3.3.3. Analytical Performance

Under optimized conditions (135sec membrane, 3x dispense cycles of the test line, PBST + 1%BSA + 1%PVP running buffer, 20 µg anti-CEA Ab G for conjugate preparation, and 6 µL conjugate per test) CEA with concentrations ranging from 0 to100 ng mL^{-1} was tested on the developed GNP-based LFSB. Photo images of the strips were taken as displayed in **Figure 3.5. a**. The intensity of the test line increased with increasing concentration of target CEA. In the absence of CEA, no visible test line band was observable. This proved that after the optimization process there was negligible nonspecific interactions. For quantitative data the test line intensities were

measured with the portable strip reader and peak intensities were plotted against corresponding CEA concentrations to obtain a calibration curve (**Figure 3.5. b**). The calibration curve had good linearity with $R^2 = 0.9937$. The equation of the curve was $y = 7.3807x + 22.079$, where y was peak intensity and x was the concentration of CEA (ng mL^{-1}). The assay showed good performance with linear dynamic range from 3 to 100 ng mL^{-1}. The detection limit of the assay was determined to be 2 ng mL^{-1} (S/N=3).

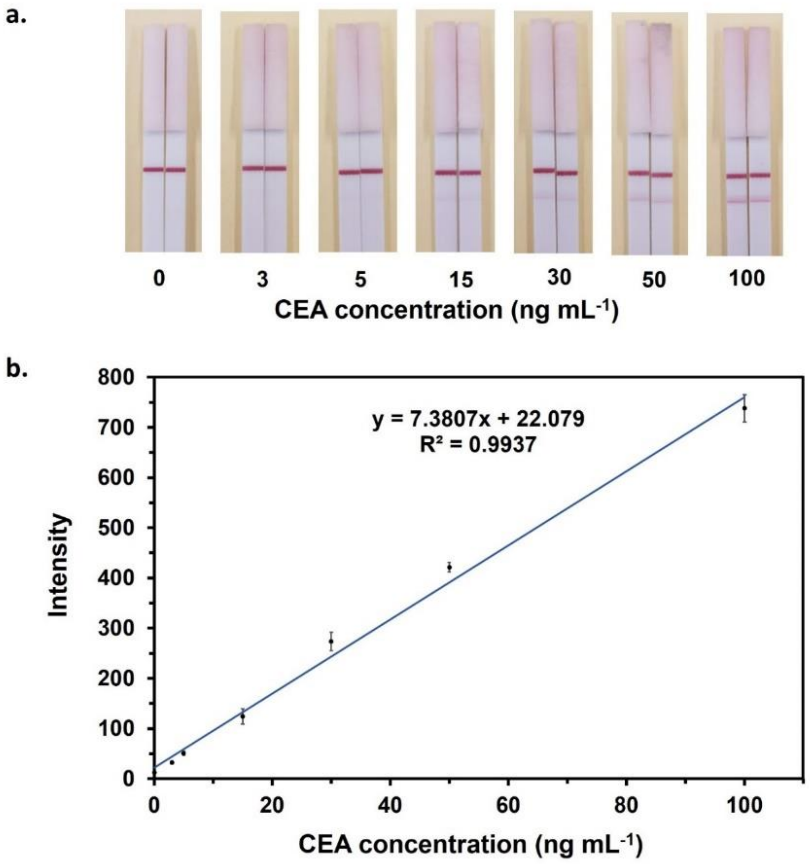

Figure 3.5. (a) Photo images of assay in the presence of varying amounts (0 – 100 ng mL^{-1}) of CEA (b) Corresponding calibration curve. Each data point corresponds to the averaged test line intensities from three replicate tests.

The developed assay also showed good reproducibility. Six replicates of CEA at concentrations of 5 and 50ng mL^{-1} were tested with the GNP-based LFSB and the relative standard deviations were 5.23% and 7.15% respectively (data not shown). To assess the selectivity of the

developed assay, CA-19-9 at concentration of 100U mL^{-1} and various proteins like mammaglobin, trypsin, Human IgG and C4BP-alpha at concentrations of 100ng mL^{-1} were tested and their signals compared to CEA protein at 30ng mL^{-1} (**Figure 3.6.**). As observed, CEA at 30ng mL^{-1} showed a much higher test line peak intensity compared to the other targets. The test line intensities from the other proteins and CA19-9 were akin to the signal of the blank, indicating excellent selectivity of the developed biosensor.

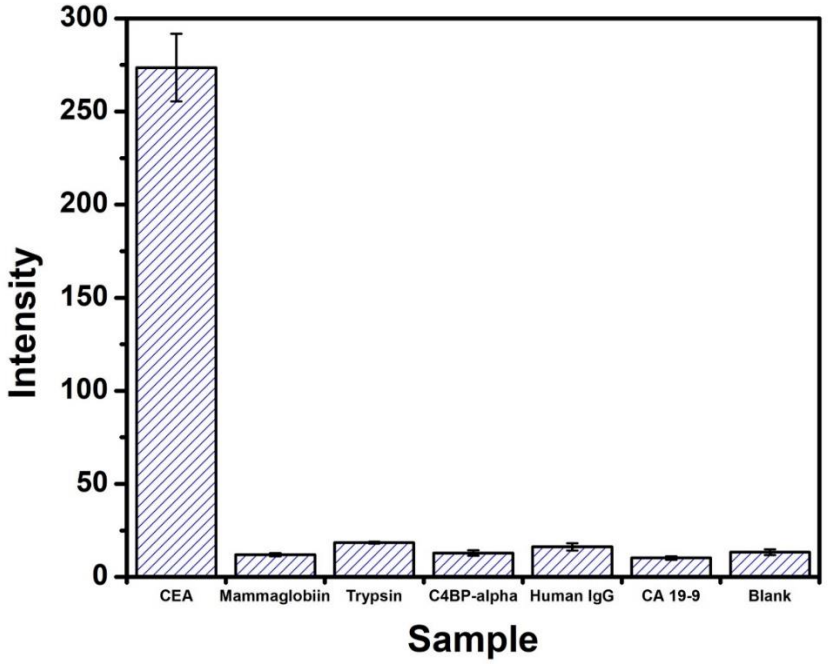

Figure 3.6. Selectivity of the developed GNP-based lateral flow strip biosensor. Assay in the presence of CEA (30 ng mL^{-1}); Mammaglobin, Trypsin, C4BP-alpha and Human IgG at concentrations of 100 ng mL^{-1}; CA 19-9 (100 U mL^{-1}); and blank (running buffer).

3.3.4. Detection of CEA in Human Pancreatic Cyst Fluid

To access the feasibility of the developed GNP-based LFSB for clinical diagnostics, CEA concentrations in pancreatic cyst fluid samples were measured using the developed sensor. The pancreatic cyst fluid samples were obtained from the University of Pittsburg Medical Center. There were 7 samples in total; six pancreatic cancer patient cyst fluid samples (PC 1 to PC 6) and one non-malignant pancreatic cyst sample (NM).

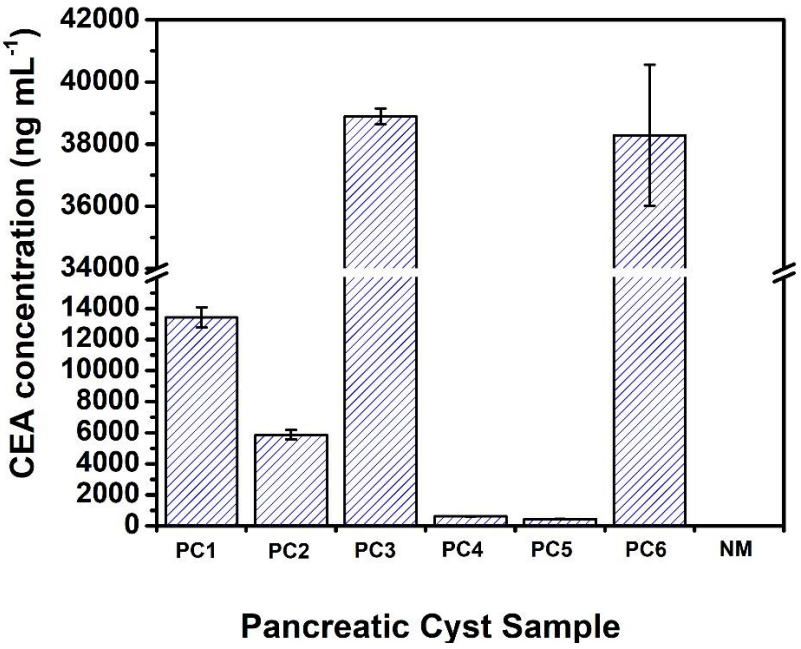

Figure 3.7. Screening of human pancreatic cyst fluid with developed GNP-based lateral flow strip biosensor. Pancreatic cancer patient cyst fluid (PC1 to PC6) and non-malignant pancreatic cyst fluid (NM).

From **Figure 3.7** it is observed that the pancreatic cancer cyst fluid samples showed significantly higher CEA levels compared to the non-malignant cyst fluid sample. The reference CEA value employed was 192 ng mL^{-1} as previously reported.[102] All six pancreatic cancer patient cyst fluid samples showed levels above the reference value. The developed biosensor showed good performance in the pancreatic cyst fluid and was able to distinguish mucinous cyst from non-malignant pancreatic cysts. The developed GNP-based LFSB exhibits great potential for the clinical screening of CEA levels in pancreatic cyst fluid samples.

3.4. Conclusion

A GNP-based lateral flow strip biosensor was developed for the rapid and sensitive detection of CEA. Quantitative data was collected by reading test line intensities with a portable strip reader. The developed assay was successfully used to measure CEA levels in pancreatic cancer cyst fluids, and to distinguish mucinous pancreatic cyst from non-malignant pancreatic cyst.

The detection limit if the assay was determined to be 2 ng mL^{-1} (S/N ratio=3) which was well below the CEA reference value of 192 ng mL^{-1} in pancreatic cyst fluid. The developed GNP-based LFSB presents a simple, rapid and low-cost assay for the quantitative measurement of CEA levels in pancreatic cyst fluids. The developed assay has the potential to be applied clinically for diagnostics particularly in limited resource settings.

4. MULTI-WALLED CARBON NANOTUBE-BASED LATERAL FLOW BIOSENSOR FOR ULTRASENSITIVE DETECTION OF PROTEINS IN HUMAN PLASMA

4.1. Introduction

The detection of proteins is an area of interest in various fields of study. Protein levels have served as indicators of quality and safety in the food and beverage industries. In the medical and veterinarian fields various ailments can be diagnosed by detecting protein biomarkers associated with the diseased conditions. Traditional protein assays which involve reaction of proteins with various chemicals to give colored complexes only afford information about bulk protein content and amino acid composition.[6,122–125] Based on their sequences, proteins with aromatic ringed amino acids have characteristic absorbance at 280 nm which have been utilized for protein quantitation. Methods like agarose and polyacrylamide electrophoresis which separate out proteins have also been used for protein detection.[125,126] These methods generally involve multiple steps and lack sufficient selectivity and sensitivity. There is therefore the need for assays that provide more selective and sensitive protein detection.

Immunoassays utilize antibodies to capture target analytes and provide a selective method for detecting proteins. Immunoassays have gained a lot of attention for protein detection in medical diagnosis, quality control in the food industry as well as in environmental analysis.[127–129] The most commonly used immunoassay approach for the detection of proteins is the Enzyme-Linked Immunosorbent Assay (ELISA). ELISAs have gained increased use in medical laboratories as well as external quality control and proficiency testing organizations.[130] Traditional ELISA assays utilize antibodies labelled with enzymes such as horse-radish peroxidase which catalyzes substrate conversion to colored complexes. The intensities of the enzymatic product which is target protein dependent can be measured by spectroscopic techniques to obtain quantitative data. ELISAs offer

acceptable selectivity and sensitivity, however, tedious test procedures, prolonged assay time and requirement of highly trained personnel which limit its applications for point-of-care and in-field detection.[131] Although the introduction of automated ELISA instrument has overcome some of the disadvantages of the traditional ELISA, the cost is still of significant concern.[18]

Immunosensors are highly versatile and can be linked with various transducers based on electrochemical, optical and piezoelectric technologies.[125,132] Electrochemical immunosensors that utilize enzyme labels such as horse-radish peroxidase, glucose oxidase, acetylcholinesterase, tyrosine etc. have been reviewed .[133] The enzymatic products with electrochemical activities give measurable electrical signals. Other electrochemical assays measuring change in electrical conductivity upon protein capture have also been reported.[134] Nanoparticles like gold and platinum nanoparticles, and quantum dots (QDs) have been used as labels to improve the sensitivity of electrochemical assays.[135–137] In spite of their high sensitivity, electrochemical assays can suffer drawbacks of having low reproducibility, and fragility of enzyme based systems which can limit their application for biomarker screening.

Lateral flow biosensors (LFB) which are paper-based sensors circumvent the shortcomings of the aforementioned immunoassays. In recent years, LFBs have attracted considerable interest because they offer simple, rapid, portable and low-cost detection of analyte.[11,18,119,138,139] Lateral flow assays are therefore ideal for POC applications. LFBs are highly versatile and have been used in a variety of sample matrices across different industries.[18,24,25,45,90,96,119,140] Various nanoparticles have been utilized as labels for the detection of analyte on lateral flow strips.[25,27,45,141–143] Gold nanoparticles are the gold standard for the preparation of LFBs and have been developed for the detection of various targets.[18,19,119,144] GNPs are usually used as labels for the generation of visible signal because of their surface plasmon property that gives them a size dependent red color.[21,145]

However, because of the limited surface area of the GNPs, the assays often suffer from low sensitivity. Innovative signal amplification protocols have been reported using enzymes[18], catalytic nanoparticles[146] and dual conjugates[147]. These amplification strategies improve the sensitivity of the LFBs, however, because of the low concentration of certain protein biomarkers in physiological fluids, there is the need for more sensitive LFBs.

Since their discovery in 1991[148], carbon nanotubes (CNTs) have attracted significant attention because of their unique properties.[149–151] CNTs provide a large surface area for biomolecular conjugation (Zhang et. al., 2011).[152] They therefore have the potential to be used in place of GNPs as labels in LFBs. Based on this premise, our group previously published a CNT-based lateral flow assay for the detection of DNA which showed improvement over the conventional GNP-based LFB for DNA detection.[25] Abera and Choi reported an electrochemical detection of human IgG based on changes in resistance of the test zone of LFB upon CNT accumulation. This electrochemical assay suffered low sensitivity with a detection limit of 20 µg mL^{-1}.[153] Meng and colleagues reported a cotton string assay that utilized CNTs for the visual detection of ferroprotein. The cotton strip assay achieved an improved LOD of 50 ng mL^{-1}.[154] Subsequently, there has been a report of a GNP-decorated carbon nanotube nanocomposite-based cotton string assay for the detection of Squamous cell carcinoma antigen with detection limit 3ng mL^{-1}.[155] The cotton string assay was unable to improve on the detection limits of the GNP-based LFBs. There is still the need for more sensitive LFBs for clinical diagnosis as some medically important proteins are present at very low concentrations.

In this study, a MWCNT-based LFB is introduced for the ultrasensitive detection of proteins in human plasma. The assay utilized the unique properties (color, high aspect ratio and ease of surface modification) of MWCNTs to aid the highly sensitive detection of proteins. Rabbit

IgG was adopted as a model target to demonstrate the proof-of-concept. Rabbit IgG was captured in a sandwich assay between capture antibody immobilized on the test zone and detection antibody conjugated to the shortened multi-walled CNTs. Accumulation of CNTs on the test line gave a black colored line which was detectable with the naked eye at 5 pg mL^{-1}. A detection limit of 1.32 pg mL^{-1} was achieved after optimization of experimental parameters. The detection limit of the developed assay was over 3 orders lower than that of previous GNP-based LFB. The clinical diagnostic utility of the developed MWCNT-based LFB was successfully demonstrated by detecting rabbit IgG spiked into human plasma samples. The promising properties of the approach are reported in the following sections.

4.2. Experimental Section

4.2.1. Apparatus

The Airjet AJQ 3000 dispenser, Biojet BJQ 3000 dispenser, Clamshell Laminator, and Guillotine Cutting module CM 4000 were purchased from Biodot LTD (Irvine, CA, USA), Quantitative data was collected using a portable test strip reader (DT2032) purchased from Shanghai Goldbio Tech. Co., LTD (Shanghai, China). Fourier-transformation infrared (FTIR) spectral readings were performed on Nicolet iS10 FTIR spectrometer manufactured by Thermo Fisher Scientific, Inc. (Rockford, IL, USA). Absorbance measurements were performed on the Nanodrop purchased from Thermo Fisher Scientific, Inc. (Rockford, IL, USA).

4.2.2. Reagents and Materials

Carboxylated multi-walled carbon nanotubes (carboxyl-MWCNT) (purity > 95 wt%) was purchased from Sun NanoTech (Nanchang, Jiangxi Province, China). Rabbit immunoglobulin (IgG), Goat anti-rabbit IgG (GaR IgG), donkey anti-goat IgG, human-IgG and thrombin were obtained from Thermo Fisher Scientific, Inc. (Rockford, IL, USA). Carcinoembryonic antigen

(CEA) and carbohydrate antigen (CA 19-9) were obtained from Fitzgerald Industries International (Acton, MA, USA). Human mammaglobin was purchased from Creative BioMart (Shirley, NY, USA).

N-(3-Dimethylaminopropyl)-N'-ethylcarbodiimide hydrochloride (EDC) , N-hydroxysulfosuccinimide (sulfo-NHS), 2-(4-Morpholino) ethanesulfonic acid (MES), tween 20, triton X-100, bovine serum albumin (BSA), sucrose, polyvinylpyrrolidone (PVP), phosphate buffer saline (0.01 M PBS, pH 7.4) and trizma hydrochloride buffer solution (Tris-HCl, 1.0 M, pH 8.0) were purchased from Sigma–Aldrich (St. Louis, MO, USA) and were used without further purification. Glass fibers (GFCP000800), cellulose fiber sample pads (CFSP001700), nitrocellulose membranes (HFC090MC100, HFC180MC100, HFC240MC100) were purchased from Millipore (Billerica, MA). Human plasma were purchased from Golden West Bio (Temecula, CA, USA). All the chemicals used in this study were analytical reagent grade. Solutions used were prepared with ultrapure (≥18M Ω) water from Millipore Milli-Q water purification system (Billerica, MA, USA).

4.2.3. Preparation of MWCNT-Antibody Conjugates

The carboxyl-MWCNTs were treated with mixed acid solution (HNO_3:H_2SO_4, 1:3) under ultrasonication for 3 hours to shorten them. The acid treatment has been reported to shorten the lengths and introduce carboxyl groups onto the surface of CNTs.[156] The shortened carboxyl-MWCNTs was washed by centrifugation with ultrapure water until the pH of supernatant was neutral. Shortened carboxyl-MWCNT (0.5 mg) was mixed with EDC (9.6 mg) and sulfo-NHS (5.43 mg) in 1mL MES buffer (0.1 M, pH 6.0) to activate the carboxyl groups. The mixture was incubated at room temperature (RT) for 15 min followed by washing by centrifugation (10,000 rpm for 5min). The supernatant was removed, and the pellet was resuspended in PBS buffer. The

washing step was repeated 3 times. The resulting pellet was resuspended in PBS and GaR IgG was added to a final volume of 1.0 mL. The mixture was then incubated overnight at 4°C with gentle shaking. This mixture was then centrifuged at 5,000 rpm for 5 min. The supernatant was removed, and pellet was resuspended in PBS. The supernatant was monitored at each wash step using the nanodrop to determine concentration of excess GaR IgG. The conjugate was washed till no protein absorbance was measurable in the supernatant. Based on the amount unbound GaR in the supernatant relative to initial GaR concentration it was calculated that 1.0 mg of CNTs binds 18.83 ± 0.5 µg GaR IgG. After the final wash the GaR IgG-CNT conjugate was resuspended in 1.0 mL eluent buffer (20 mM $Na_3PO_4 \cdot 12H_2O$, 5% BSA, 10% sucrose, and 0.25% Tween-20). The conjugate was stored at 4°C until used.

4.2.4. Preparation of the MWCNT-Based LFB

The CNT-based LFB consisted of a conjugate pad, nitrocellulose membrane and absorbent pad as shown in **Figure 4.1**. The conjugate pad (21 mm ×30 cm) was a porous glassy fiber membrane on which the conjugate was dropped. Desired volumes of GaR IgG and Donkey anti-goat IgG solutions were dispensed on the nitrocellulose membrane (25 mm×30 cm) as test and control zones respectively, using the Biojet BJQ 3000 dispenser. The distance between the test and control lines was about 3 mm. After dispensing, the membrane was dried at 37°C for 1 hr and stored at 4°C. All three components were assembled on an adhesive plastic backing layer (60 mm×30 cm) using the clamshell laminator. Each component was overlapped by at least 2 mm to ensure that the test solution could migrate through the strip during the assay. The assembly was cut with the Guillotine cutting module CM 4000 into 3 mm width strips. The prepared strips were stored at 4°C until used.

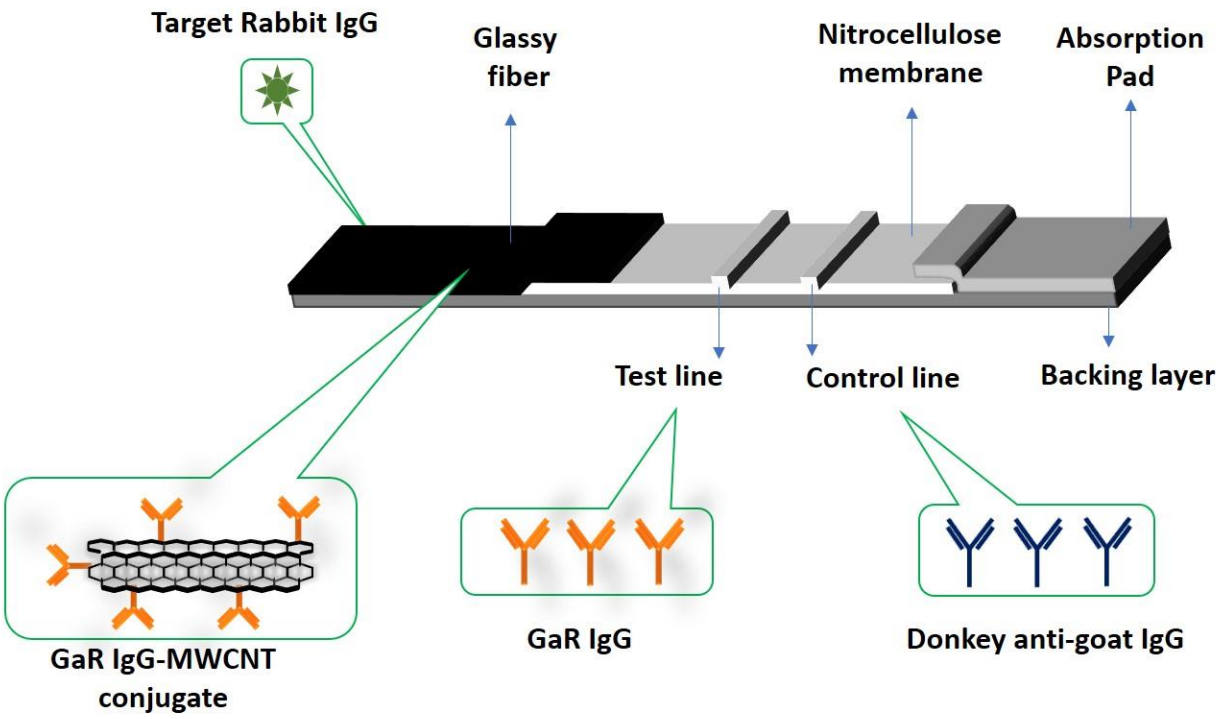

Figure 4.1. Configuration of the MWCNT-based LFB for protein detection.

4.2.5. Assay Procedure

GaR IgG-MWCNT (4 µL) was dropped on the conjugate pad and allowed to air dry for 5mins. One hundred microliters (100 µL) of sample Rabbit IgG solution prepared in running buffer (PBS 1% BSA, 1% PVP) was applied to the MWCNT-LFB. The solution travelled along the biosensor from the conjugate pad towards the absorption pad. After 20 mins, 100 µL of running buffer was added to wash the strip. The washing step was to clear up any nonspecifically adsorbed conjugates on the nitrocellulose membrane to reduce background signals. The test and control lines could be visually evaluated within 20 mins. For quantitative measurements, the optical intensity of the test and control lines were read with a portable strip reader. To test the strip performance in plasma, 10% human plasma spiked with different concentrations of Rabbit IgG were prepared in PBS containing 1% BSA and 1% PVP. The test procedure and quantitative data acquisition were the same as described above.

4.3. Results and Discussion

4.3.1. Characterization of the Shortened MWCNTs

Figure 4.2. a and b show the typical transmission electron microscopy images of the MWCNTs before and after acid treatment. One can see the average length of the unshortened MWCNT is around 1 to 3 µm (**Figure 4.2. a**), and the length of the shortened MWCNT is around 200 to 600 nm (**Figure 4.2. b**). The length of MWCNT was reduced significantly after acid treatment.

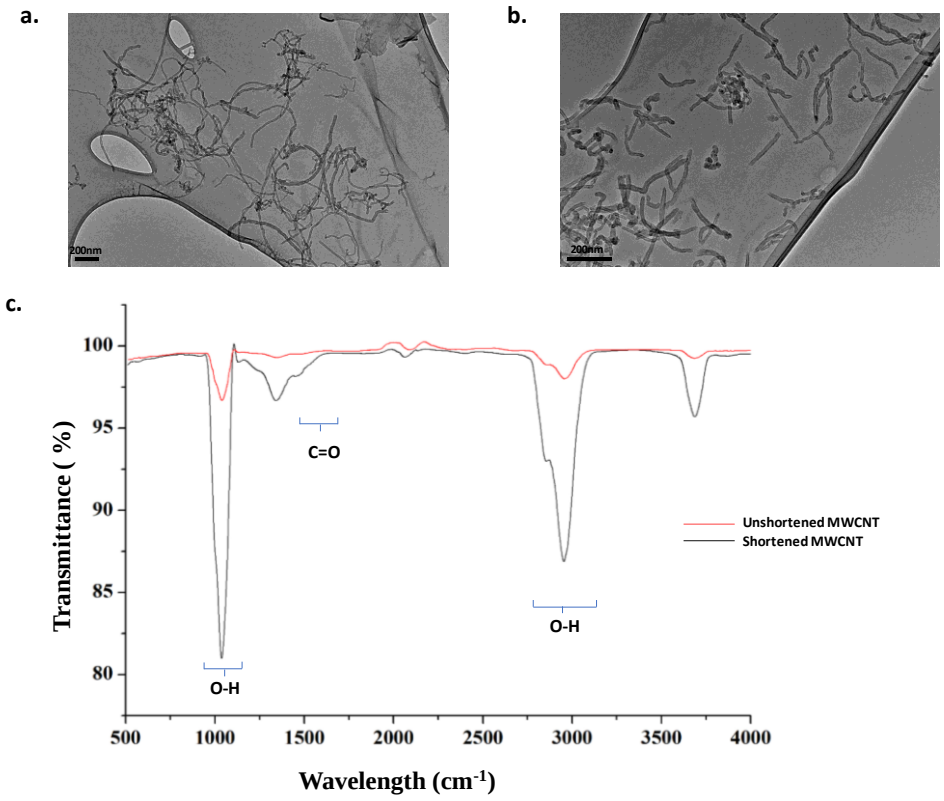

Figure 4.2. (a) TEM image of unshortened MWCNTs (b) TEM image of shortened MWCNTs; (c) FTIR spectra of MWCNT before and after acid treatment.

The shortened MWCNTs were analyzed by FTIR to assess the surface functionality before and after acid treatment. Using equal mass (0.2 mg) of shortened and unshortened MWCNTs, the FTIR spectra showed increased band intensities for O-H stretch, and C=O after acid treatment as

shown in **Figure 4.2. c**. This was an indication of increased carboxylation of the MWCNT after the acid treatment.

4.3.2. Principle of MWCNT-Based LFB for Protein Detection

The working principle of the MWCNT-based LFB is illustrated in **Figure 4.3**. Rabbit IgG and polyclonal GaR IgG were used as a model to demonstrate the proof-of-concept. Polyclonal GaR IgG interacted with the rabbit IgG in more than one site and was used as both capture and detection antibody to prepare the LFB. Typically, GaR IgG-MWCNT conjugate solution with a desired volume was dropped on the conjugate pad and allowed to air-dry. Sample solution containing rabbit IgG was applied to the conjugate pad (**Figure 4.3. a**). The solution migrated by capillary action through the strip. Target first interacted with the GaR IgG-MWCNT conjugate and an immunoreaction occurred between the rabbit IgG and the GaR IgG on the MWCNT surface (**Figure 4.3. b**). This formed a rabbit IgG-GaR IgG-MWCNT complex which continued to migrate along the test strip. Upon reaching the test zone, pre-immobilized GaR IgG reacted with the rabbit IgG of the complex in a second immunoreaction event. A characteristic black band was observed on the test zone because of the accumulation of MWCNTs (**Figure 4.3. c**). The intensity of the black band on test zone was dependent on the concentration of target rabbit IgG. Once the solution reached the control zone, the excess GaR IgG-MWCNT conjugates were captured on the control zone by the secondary antibody (Donkey anti-goat IgG). Thus, in the presence of target two black bands were visually observed for qualitative data (**Figure 4.3. c).**

In the absence of the target IgG, one black band was observed due to the capture of the GaR IgG-MWCNT conjugate on the control zone by the pre-immobilized donkey anti-goat IgG (**Figure 4.3. d**). In this case, the black band of the control zone showed that the LFB was in good working condition. There was no black band on the test zone in this case because the rabbit IgG

(which was absent) was required for the formation of sandwich structure on the test zone. Quantitative data was obtained by reading the test band intensities using the portable strip reader.

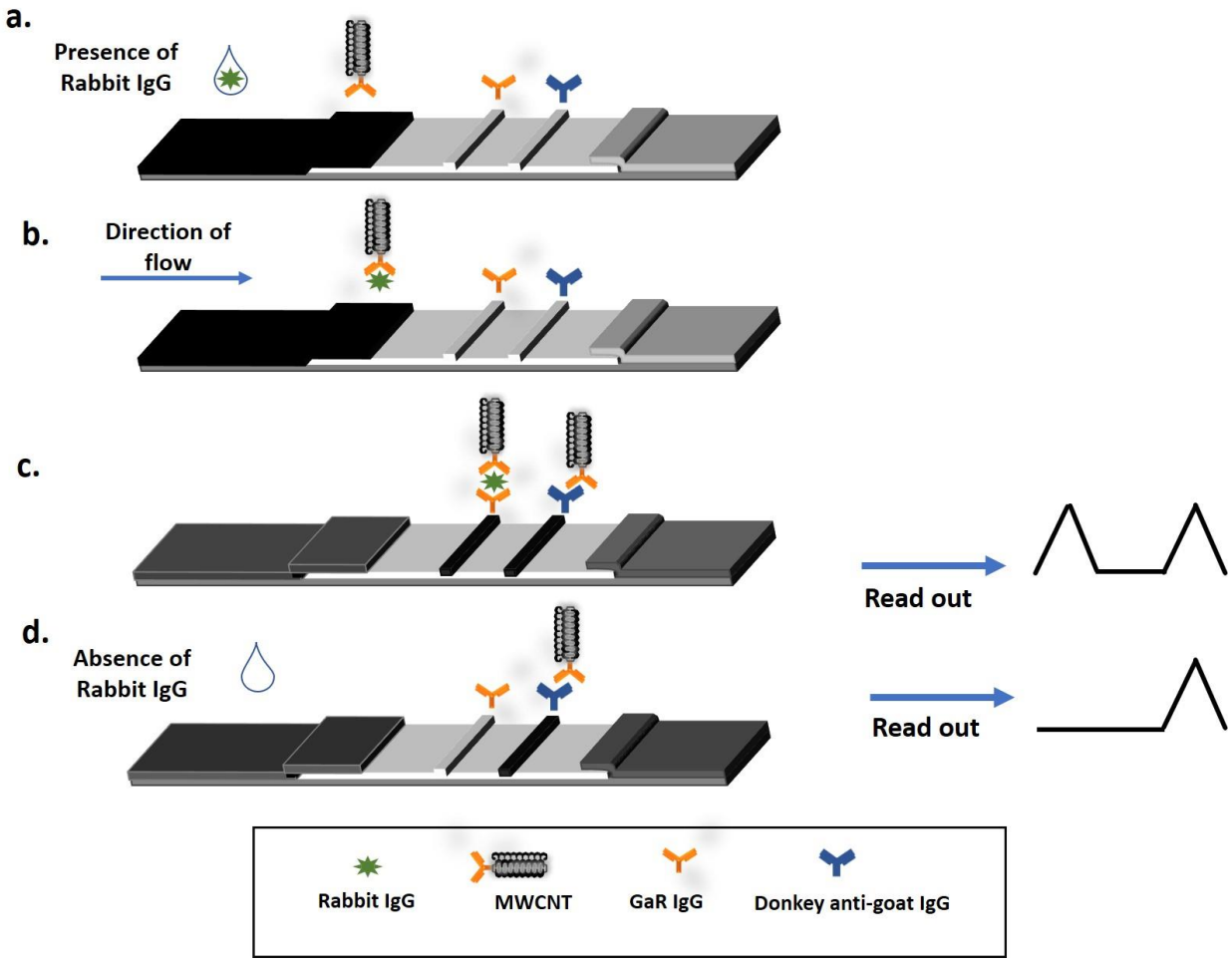

Figure 4.3. Working Principle of the developed MWCNT- based LFB. (a) Sample introduction (b) Immunoreaction between target and GaR-MWCNT conjugate (c) Capture of rabbit IgG-GaR-MWCNT complex on test line and the excess of GaR-MWCNT conjugate on the control line (d) Assay in the absence of target rabbit IgG.

To confirm the proposed signal improvement obtainable by replacing GNPs with MWCNTs as labels for protein detection on the LFB, sample solutions with three different concentrations of rabbit IgG were tested on the MWCNT-based LFB and the traditional GNP-based LFB. **Figure 4.4** shows the photo images of LFBs after testing 5, 1 and 0 ng mL^{-1} rabbit IgG in sample solutions.

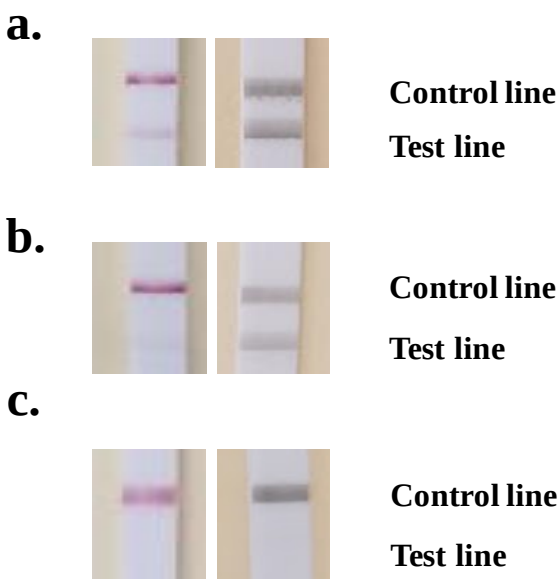

Figure 4.4. Photo images of the GNP-based LFBs (left) and the MWCNT based LFBs (right) with varied concentration of Rabbit IgG: (a.) 5 ng mL^{-1} (b.) 1.0 ng mL^{-1} (c.) 0 ng mL^{-1}.

In the presence of 5 ng mL^{-1} target, the MWCNT-based LFB shows a very intense black band while the GNP-based LFB shows a significantly less intense test band (**Figure 4.4. a**). For the 1 ng mL^{-1} rabbit IgG test, again, the MWCNT-based LFB showed a prominent black band on the test zone and a barely visible red band was observed on the GNP-based LFB (**Figure 4.4. b**). In the absence of target there was no visible test zone band on either LFBs (**Figure 4.4. c**). The above results indicate that the use of MWCNT label significantly increased the signal of the test band on the LFB. The improved sensitivity achieved by the CNTs is mainly due to their large aspect ratio which enabled immobilization of increased amounts of antibodies that improved the capture efficiency of target rabbit IgG. Also, the intense black color of the MWCNTs increased their contrast against the white nitrocellulose membrane which supported the test and control zones.

4.3.3. Optimization of Experimental Parameters

To attain the highest sensitivity of detection various assay parameters including type of nitrocellulose membrane, dispense times of test line, buffer conditions, conjugates were optimized. Firstly, the nitrocellulose membrane on which the test line and control lines were dispensed was optimization. The performance of three membranes (HF090MC100, HF180MC100 and HF240MC100 with flow rates of 90secs, 180secs and 240secs per 4 cm respectively as reported by the manufacturer) were assessed for their performance on the MWCNT-LFB. The flow rate on the nitrocellulose membrane dictated the time frame for the immunoreactions at the test and control lines. As shown in **Figure 4.5. a**, the 180sec membrane showed the best signal to noise (S/N) ratio. With the 90sec membrane, the flow rate was rapid, and this reduced the time frame for interaction between the target and test line antibodies thus reducing the observed signal. For 240sec membrane, due to the slower flow rate, there was longer exposure time for the test line immuno-reaction which led to increased background. The 180sec membrane had an optimal flow rate that maximized the S/N ratio and was therefore chosen for further development of the LFB.

The amount of antibodies on the test line was integral to the sensitivity of the developed MWCNT-LFB. The GaR IgG of then test line was dispensed different number of times and their S/N ratios compared. From **Figure. 4.5. a**, it is seen that S/N ratio gradually increased with cumulative number of dispense cycles. Five times (5x) dispensing gave the highest S/N ratio. From 1 to 4 times dispensing, there was increase in the measured signal, however, the concentration of antibodies on the test line was not enough to give optimal test line intensities. Beyond 5x dispensing of the test line antibodies, there was increased background signal due to increased nonspecific interactions. For further development of the MWCNT-LFB, 5x dispense times of the test line was chosen.

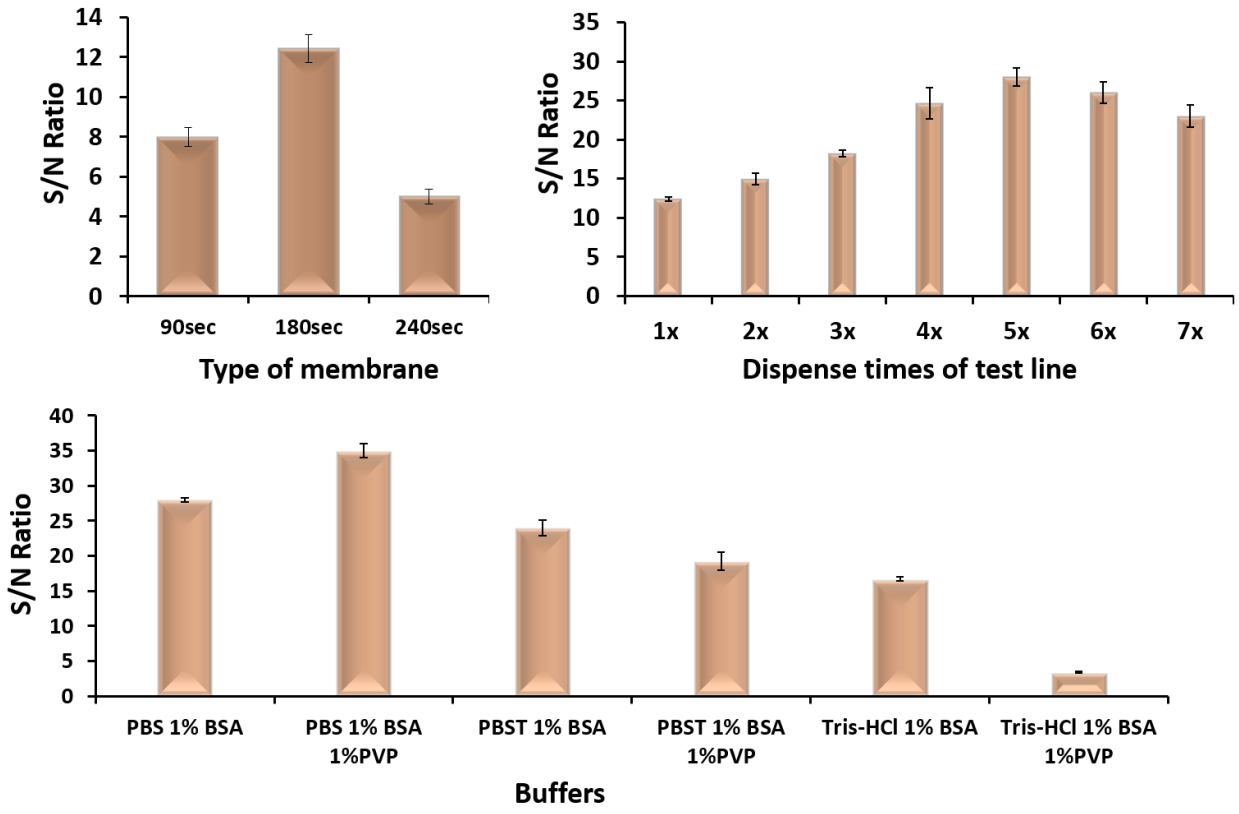

Figure 4.5. (a) Effect of membrane type on the S/N ratio of the assay (b) Effect of dispense cycles on of GaR IgG at the test line on the performance of the assay (c) Effect of running buffer composition on the S/N ratio of the assay.

The immunoreactions in the sensor occurred in buffer solution. The composition of these buffers affected the extent of these interactions. From **Figure 4.5. c**, it is seen that the PBS 1%BSA had better performance than PBST 1%BSA and Tris-HCl 1% BSA buffers. Addition of PVP, a surfactant, further increased the S/N ratio in the PBS 1%BSA Buffer. Thence, PBS 1%BSA 1%PVP was used as running buffer for subsequent testing.

The quantity of antibodies immobilized on the MWCNT-antibody conjugates was also considered. A variation of the amount of GaR IgG used for conjugate preparation showed that 50 µg of GaR IgG gave the best S/N ratio (**Figure 4.6. a**). At lower amounts of GaR IgG for conjugate preparation the lower S/N ratio observed was attributed to insufficient coverage of the MWCNT

which resulted in lower signals. The accessibility of the immobilized GaR IgG on the MWCNT was essential for the attainment of optimal sensitivity of the developed assay. Beyond 50 µg of GaR IgG there was a decrease in the S/N ratio. This decrease in S/N ratio was ascribed to overcrowding of conjugate IgG which introduced stearic hindrance. This reduced the efficiency of the immunoreactions at the test and control lines. Subsequent conjugates for the assay were prepared using 50 µg of GaR IgG.

The intensities of test and control zones were greatly influenced by the amount of conjugate used for the assay. S/N ratio dependence on changing amount of conjugate per assay is shown in **Figure 4.6. b**. The highest S/N ratio was observed at 2 µL conjugate per assay. Under 2 µL conjugate, volume, the observed reduction in S/N ratio was attributed to inadequate amount of conjugate resulting in reduced test line intensities. Beyond 2 µL conjugate, there was reduced S/N ratio due to excess conjugate. The excess conjugate resulted in increased nonspecific interactions that led to high background signals. A volume of 2 µL conjugate was used for further testing of the developed CNT-LFSB.

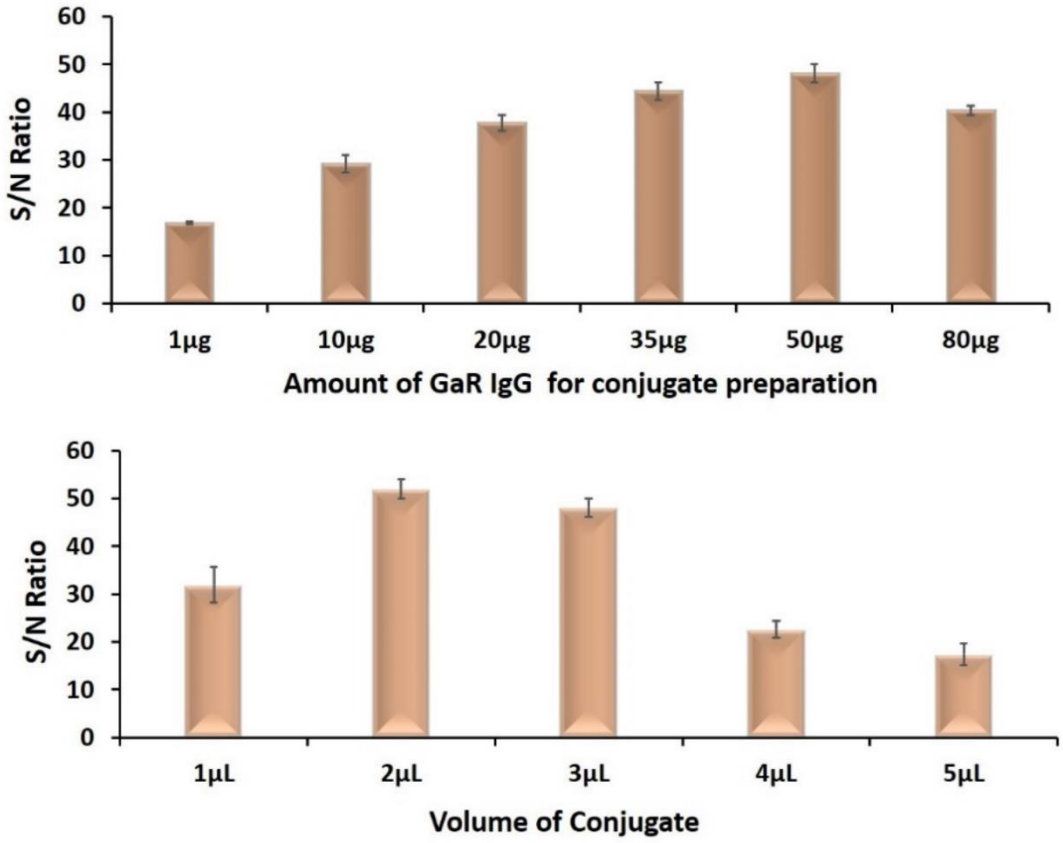

Figure 4.6. (a) Effect of the amount of GaR IgG used for conjugate preparation on the S/N ratio of the assay. (b) Effect of the volume of conjugate per-assay-run used on the S/N ratio of the assay.

In summary, the following experimental conditions gave the sensitivity while keeping background signals to a minimum: (a) using HF180MC100 to prepare the LFB; (b) dispensing test zone two times; (c) using PBS+1% BSA+1% PVP buffer as running buffer; (d) using 50 µg mL^{-1} of GaR IgG to prepare the GaR IgG-MWCNT conjugates; (e) loading 2 µL of GaR IgG-MWCNT conjugates on conjugate pads.

4.3.4. Analytical Performance

Based on the optimized experimental conditions, sample solutions with different concentrations of rabbit IgG were tested on the CNT-based LFB. Each test was run three times. The captured MWCNTs on the test zone could be observed visually for qualitative data. Quantitative data was obtained by measuring the intensity of the test and control lines with a

portable strip reader. **Figure 4.7** shows the typical photo images of the LFBs and corresponding responses from the strip reader. It is observed that the test line intensities increased with the rising concentrations of Rabbit IgG. The test line was quite visible even in the presence of 0.005 ng mL^{-1} (5 pg mL^{-1}) IgG, which could be estimated as a threshold for the qualitative detection of the target IgG. This threshold is 1000 times lower than previous report using GNP label.[24]

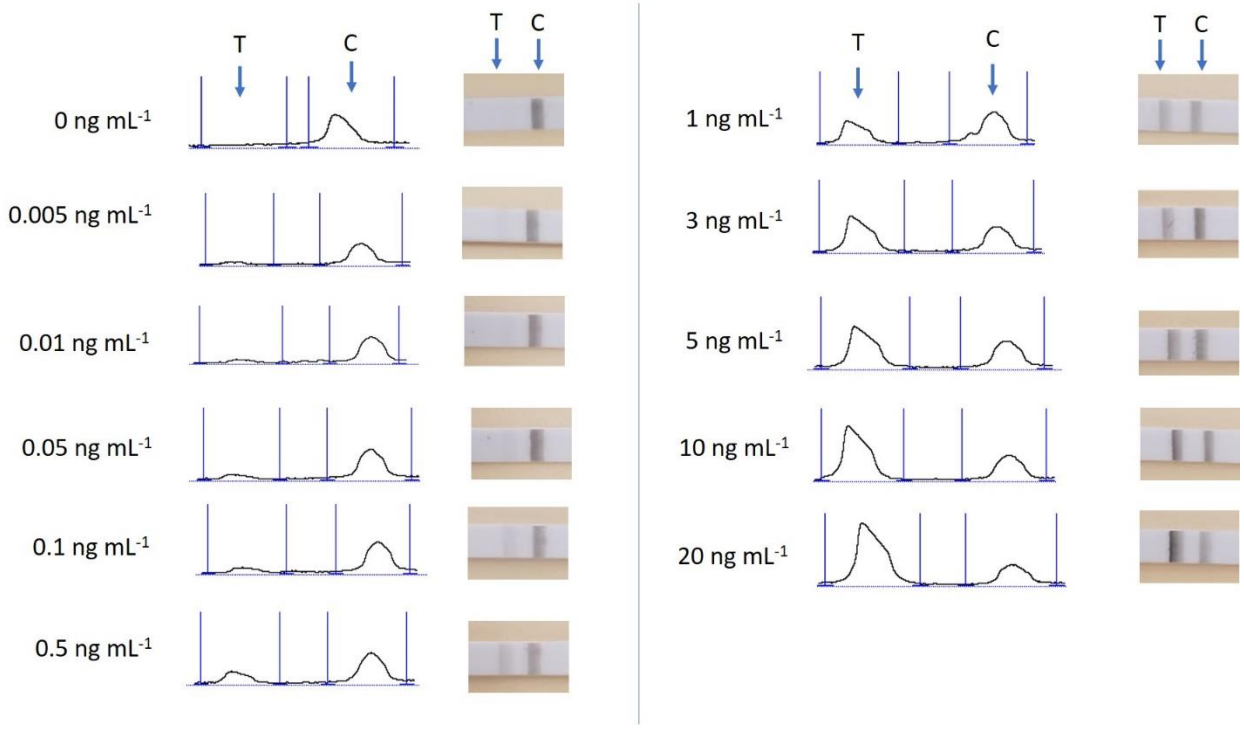

Figure 4.7. Responses of MWCNT-based LFBs in the presence of different concentrations of rabbit IgG and corresponding photo images.

In the blank test which had running buffer devoid of target rabbit IgG, there was no observable band on the test line. All tests showed a black control line which served as validation that the LFBs were working properly. From **Figure 4.7**, a series of well-defined peaks were observed, and the peak areas increased with increasing rabbit IgG concentration. The resulting calibration curve of the peak area(intensity) against the logarithm of Rabbit IgG concentration had two dynamic ranges of 5 pg - 100 pg mL^{-1} and 0.5 - 25 ng mL^{-1} (**Figure 4.8.**).

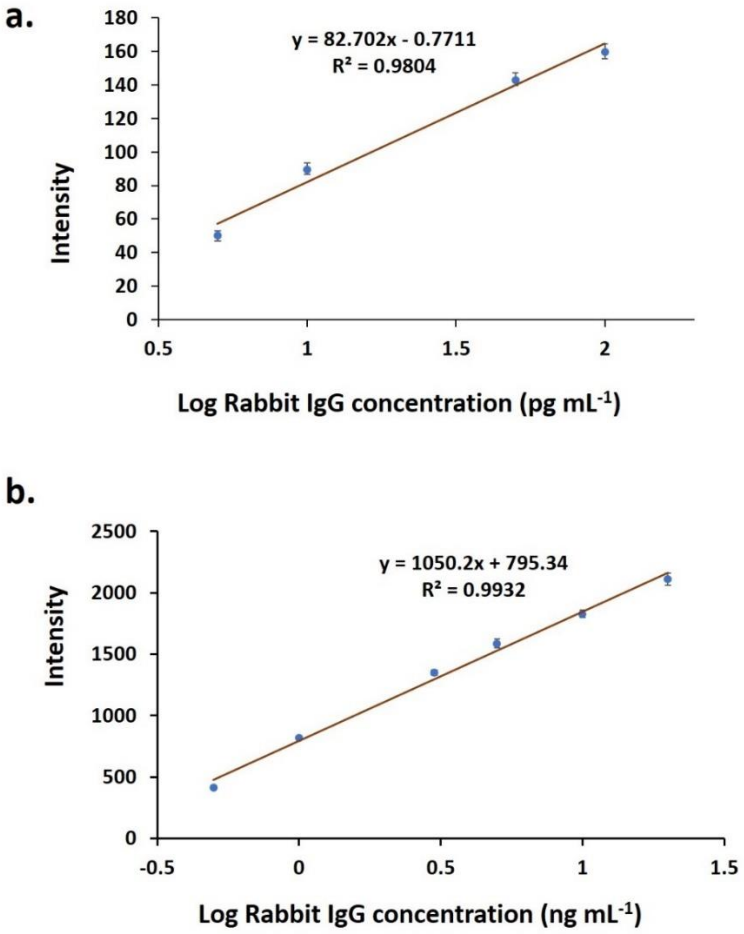

Figure 4.8. Calibration curves of the MWCNT-based LFB in the concentration range of (a) 5-100pg mL^{-1} (b) 0.5 to 20 ng mL^{-1}.

The LOD (based on S/N ratio=3) was determined to be 1.32 pg mL^{-1}, which is three orders lower than that of GNP-based LFB.[18] **Table 4.1.** shows a comparison of the developed MWCNT-LFB to some previously reported lateral flow assays. The MWCNT-LFB shows significant improvement in the LOD over the previous reports. To the best of our knowledge, this is the most sensitive protein detection on LFB which does not involve any form of signal amplification. The reproducibility of the MWCNT-based LFB was assessed by running six replicate tests in the absence and presence of 5 ng mL^{-1} rabbit IgG. The intensities of the test lines were all within a

standard deviation from the mean. Relative standard deviation of 3.8% and 4.3% respectively were calculated (data not shown).

Table 4.1. Comparison of developed MWCNT-LFB to previous reports of protein detection on LFBs.

Label	Readout System	Target	Membrane material	Detection Limit	Reference
GNP	Colorimetric	Rabbit IgG	Nitrocellulose	0.5 ng mL^{-1}	18
GNP/silica nanorods	Colorimetric	Rabbit IgG	Nitrocellulose	0.01 ng mL^{-1}	24
CNT	Electrochemical	Human IgG	Nitrocellulose	25 µg mL^{-1}	153
CNT	Colorimetric	Human Ferritin	Cotton string	50 ng mL^{-1}	154
GNP-coated CNT	Colorimetric	Squamous cell carcinoma antigen	Cotton string	2.32 ng mL^{-1}	155
CNT	Colorimetric	methamphetamine	Nitrocellulose	62.5 ng mL^{-1}	157
CNT	Colorimetric	Rabbit IgG	Nitrocellulose	1.32 pg mL^{-1}	This work

To confirm the specificity of the detection antibodies for the target rabbit IgG, 50 ng mL^{-1} of three different proteins (mammaglobin, human IgG and CEA) and 50 U mL^{-1} of carbohydrate antigen 19-9(CA 19-9) were tested and compared to the signal from 5 ng mL^{-1} rabbit IgG. (**Figure 4.9.**) There was no cross-reaction observed, indicating the GaR IgG was highly specific for the rabbit IgG target.

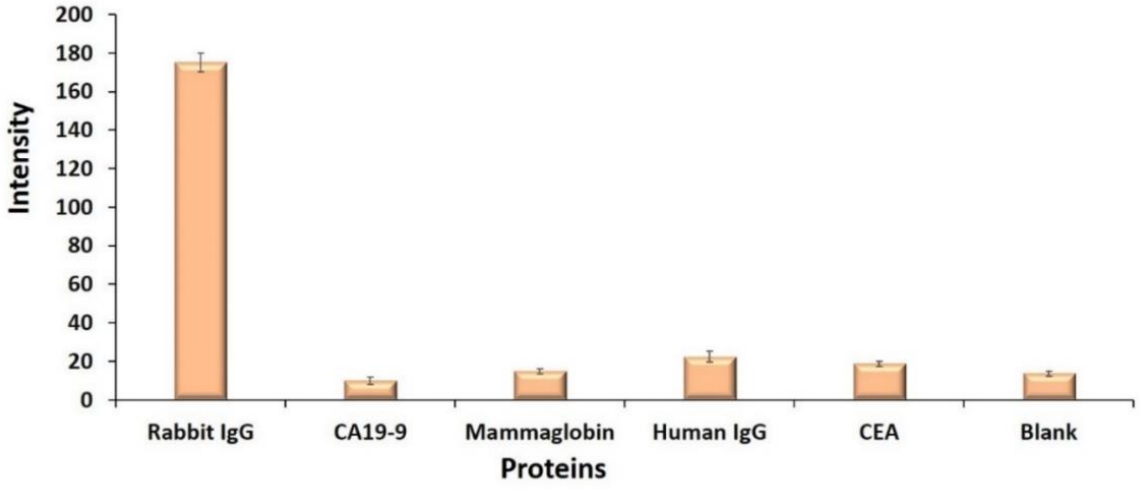

Figure 4.9. Selectivity of MWCNT-based LFB. Concentration of rabbit IgG was 100 pg mL^{-1}; CA 19-9 was at 50 U mL^{-1}; Mammaglobin, Human IgG and CEA were at 50 ng mL^{-1}.

To assess the feasibility of applying the developed MWCNT-based LFB for protein detection under clinical settings, human plasma spiked with different concentrations of rabbit IgG was tested. The assay showed satisfactory performance in 10% human plasma with dynamic range of 1 ng mL^{-1} to 50 ng mL^{-1} as displayed in the calibration curve (**Figure 4.10.**).

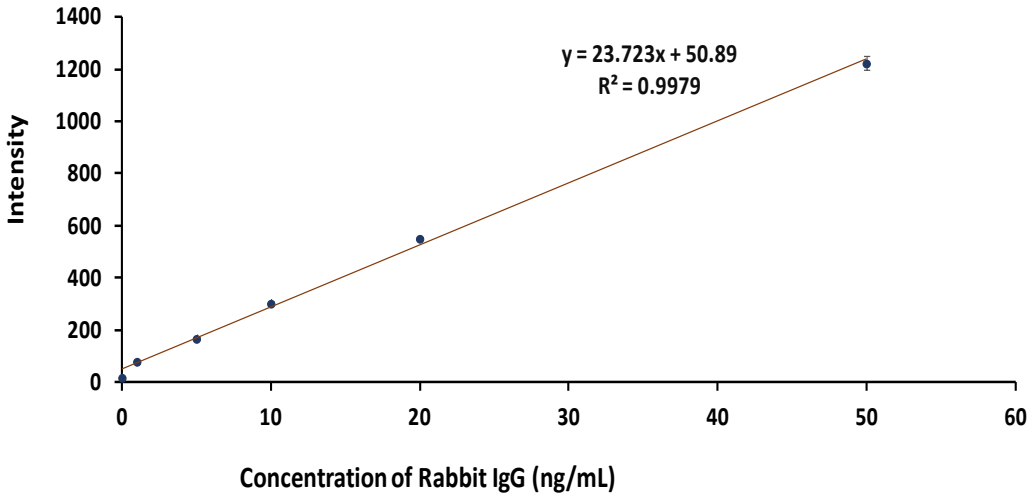

Figure 4.10. Calibration curve of MWCNT-based LFB for detection of rabbit IgG in spiked human plasma (10%).

4.4. Conclusion

A carbon nanotube-based lateral flow biosensor was successfully developed for quantitative detection of rabbit IgG. Under optimized conditions, 5 pg mL^{-1} of the target could be visually detected with the naked eye without any instrumentation. The LOD was 1.32 pg mL^{-1} (S/N= 3), which is over 3 orders lower than previous report using gold nanoparticle as label.[18] The MWCNT-based LFB showed high reproducibility and specificity which are essential for clinical applications. The biosensor was successfully able to detect rabbit IgG spiked into human plasma within 20 mins. The developed MWCNT-LFBS holds enormous potential for the simple, fast and inexpensive point-of care detection of various clinically important proteins.

5. MULTI-WALLED CARBON NANOTUBE-BASED LATERAL FLOW STRIP BIOSENSOR FOR THE QUANTITATIVE DETECTION OF CARCINOEMBRYONIC ANTIGEN (CEA)

5.1. Introduction

Pancreatic cancer, though it accounts for about 3% of cancer cases annually is the third leading cause of cancer related deaths in the United States after lung and breast cancers.[158] Surgical resection of tumors is the primary treatment for pancreatic cancer, however at diagnosis most patients are beyond surgical intervention.[98] There is the lack of reliable routine assay for the screening of pancreatic cancer to enable increased rate of early diagnosis.

CEA was first discovered in fetal gut, liver, and pancreas. CEA levels are elevated in newborns, but the levels rapidly drop after birth. CEA is found elevated in various cancers of the gastrointestinal system as well as others like breast [159], lung [160] and ovarian [161] cancers. CEA levels in human serum can give information about recrudescence and metastatic state of a tumor.[90] CEA is the most extensively used protein biomarker for cancer diagnosis and its levels are elevated in 30-60% of pancreatic cancer patients.[162] CEA has been detected mainly by ELISA. Though, ELISAs provides low to acceptable detection limits for CEA detection, they have the drawbacks of requiring long sample preparation and wash times, skilled labor for its operation and expensive plate readers. These drawbacks limit ELISA application for routine screening.

Lateral flow Strip Biosensors are portable point-of-care devices that can rapidly detect cancer biomarkers with sensitivity and selectivity. Lateral flow assays have been used for the detection of various targets ranging from nucleic acids, proteins, carbohydrates and other smaller molecules. Various nanoparticles including gold nanoparticles (GNP) [15,18,119], fluorescent nanoparticles [23,120,121], GNP-coated silica nanorods [24,45] amongst others [26,28,116] have been used on

LFSBs. These nanoparticles have provided low to acceptable sensitivities; however, GNPs are the most widely used transducers for lateral flow biosensor applications. GNP lateral flow biosensors have gained patronage because of their red color that facilitates visual detection, and their ease of synthesis and conjugation to biorecognition elements. Also, GNP based LFSBs have limited sensitivity for detecting very low concentrations of biomarkers.

In previous work (Chapter 4), protein biomarker detection was demonstrated using MWCNTs as transducers. The MWCNT-based biosensor enabled an over 400-fold reduction in detection limit for immunoglobulin detection as compared to the GNP-based LFSB system. CNTs have the advantage of having intense black color that gives sharp contrast and facilitates the visual detection of analyte. Further, CNTs have large aspect ratio that allows the immobilization of increased amounts of biorecognition elements.

Here, a MWCNT-based LFSB is developed for the ultrasensitive detection of CEA. The assay depended on the capture of CEA between a pre-immobilized capture antibody and a MWNCT-antibody conjugate. The accumulation of MWCNTs on the test zone enabled the visual detection of CEA. Quantitative data was collected using a portable strip reader.

5.2. Experimental Section

5.2.1. Apparatus

The Airjet AJQ 3000 dispenser, Biojet BJQ 3000 dispenser, Clamshell Laminator, and Guillotine Cutting Module CM 4000 were purchased from Biodot LTD (Irvine, CA, USA). Quantitative data was collected using a portable test strip reader (DT2032) purchased from Shanghai Goldbio Tech. Co., LTD (Shanghai, China).

5.2.2. Reagents and Materials

Carboxylated multi-walled carbon nanotubes (carboxyl-MWCNT) (purity > 95 wt%) was purchased from Sun NanoTech (Nanchang, Jiangxi Province, China). Native CA 19-9 (30-AC14) and native CEA protein (30-1819) was purchased from Fitzgerald Industries International (Acton, MA, USA). CEA antibodies with catalogue numbers PIMIC0101 and PIMIC0102 were purchased from Fisher Scientific (Hampton, NH, USA). The CEA antibodies, PIMIC0101 and PIMIC0102, were designated CEA Ab B and CEA Ab A respectively. Human mammaglobin was purchased from Creative BioMart (Shirley, NY, USA). Goat anti-Mouse IgG (GaM IgG) and thrombin were obtained from Thermo Fisher Scientific, Inc. (Rockford, IL, USA).

N-(3-Dimethylaminopropyl)-N'-ethylcarbodiimide hydrochloride (EDC) , N-hydroxysulfosuccinimide (sulfo-NHS), 2-(4-Morpholino) ethanesulfonic acid (MES), tween 20, triton X-100, bovine serum albumin (BSA), sucrose, polyvinylpyrrolidone (PVP), phosphate buffer saline (0.01 M PBS, pH 7.4) and trizma hydrochloride buffer solution (Tris-HCl, 1.0 M, pH 8.0) were purchased from Sigma–Aldrich (St. Louis, MO, USA) and were used without further purification. Glass fibers (GFCP000800), cellulose fiber sample pads (CFSP001700), nitrocellulose membranes (HFC090MC100, HFC180MC100, HFC240MC100) were purchased from Millipore (Billerica, MA, USA). All the chemicals used in this study were analytical reagent grade. Solutions used were prepared with ultrapure (≥18M Ω) water from Millipore Milli-Q water purification system (Billerica, MA, USA).

5.2.3. Preparation of MWCNT-Anti-CEA Antibody Conjugate

Multi-wall carboxylated MWCNTs was suspended in acidic solution (HNO_3:H_2SO_4, 1:3). The suspension was then kept under ultrasonication for 3hours. The acid treatment served to shorten and further add carboxyl groups onto the surface of the MWCNTs. The shortened CNTs

were then washed by centrifugation until the pH of the supernatant was neutral. To activate the carboxyl groups, the shortened MWCNTs were then resuspended in MES buffer pH=4.7 containing EDC (9.6 mg) and sulfo-NHS (5.43 mg). The mixture was incubated for 30 mins with gentle shaking followed by centrifugation at 10,000 rpm for 15mins to wash the carbon tubes. The washing step was repeated two additional times. Activated carboxyl-MWCNT was resuspended in PBS and CEA Ab A (37.5µg) was added to a final volume of 1mL. the mixture was incubated overnight at 4°C with gentle shaking. The MWCNT-CEA Ab A conjugates were washed by centrifuging at 5000 rpm for 5mins. The washing step was repeated 3 times. The prepared MWCNT-CEA Ab A conjugates were finally resuspended in eluent buffer (20 mM $Na_3PO_4 \cdot 12H_2O$, 5% BSA, 10% sucrose, and 0.25% Tween-20) and stored at 4°C until used.

5.2.4. Preparation of the MWCNT-Based LFSB for CEA Detection

The developed MWCNT-based LFSB was composed of 3 major components (conjugate pad, nitrocellulose membrane and absorption pad) all assembled on a sticky plastic backing layer (**Figure 5.1.**).

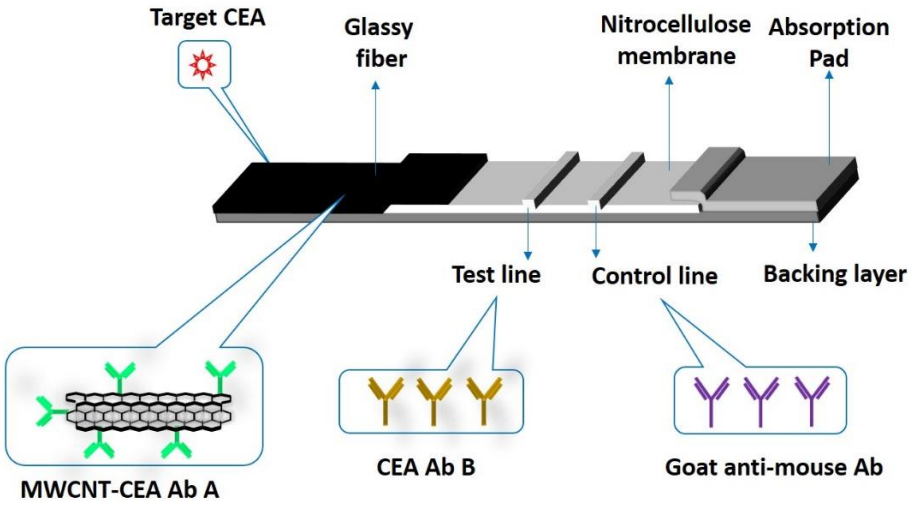

Figure 5.1. Setup of developed MWCNT-based LFSB for the detection of CEA.

The conjugate pad measured 21 x 300mm and was composed of porous glassy fiber that held MWCNT-CEA Ab A conjugates. The conjugate pad was spongy to ensure it held enough conjugate and was able to release conjugates upon wetting. The nitrocellulose membrane (25 ×300 mm) supported the test and control zones of the developed biosensor. CEA Ab B and goat anti-mouse IgG were dispensed on the nitrocellulose as the test and control lines respectively. After dispensing, the nitrocellulose membrane was dried at 37°C for 1 hour and stored at 4°C until used. The absorption pad was composed of cellulose fiber which absorbed assay fluids and drove the capillary movement of fluids during test runs. All three components were assembled on a non-pervious plastic backing layer. The components overlapped by at least 2mm to ensure continuous fluid flow. The assembled biosensor was then cut into 3mm wide strips with the guillotine cutter and stored at 4°C until used.

5.2.5. Assay Procedure

MWCNT-CEA Ab A conjugates (6uL) were dispensed onto the conjugate pad using a micropipette and allowed to air-dry for 5 mins. Sample CEA prepared in running buffer (PBS + 10% BSA) with total volume of 100 µL was applied to the LFSB. The sample moved through the biosensor towards the absorption pad by capillary action. After 20 mins, 100 µL of running buffer was added to wash the strip. The wash helped remove any nonspecifically adsorbed conjugates on the LFSB which led to the removal of background signals. For qualitative data, the test and control line signals could be observed with the naked eye after 20 mins. Quantitative data was obtained by reading the test and control line band intensities with a portable strip reader.

5.3. Results and Discussion

5.3.1. Principle of the Developed MWCNT-Based LFSB for CEA Detection

The working principle of the developed biosensor is as depicted in **Figure 5.2**. CEA Ab B and goat anti-mouse IgG were pre-immobilized on the nitrocellulose membrane as test and control lines respectively. CEA Ab A, coated onto MWCNTs to form the MWCNT-CEA Ab A conjugates served as the detection antibody. In the presence of sample, the solution moved along the biosensor by capillary action. Upon reaching the pre-dried conjugates, the conjugates were rehydrated, and target CEA underwent an immunoreaction with the CEA Ab A of the conjugate to form a MWCNT-CEA Ab A-CEA complex. The complex continued moving along the membrane and was captured on the test line by a second immunoreaction between the CEA component of the complex and the test line's pre-immobilized CEA Ab B (**Figure 5.2. a**).

CEA dependent accumulation of MWCNT on the test line resulted in a black band which was observable with the naked eye. Excess conjugates were captured on the control line by an immunoreaction between the CEA Ab A of the MWCNT-CEA Ab A conjugate and the goat anti-mouse IgG on the control line. This resulted in a second black band that served as verification that the assay was working properly (**Figure 5.2. a**). In the absence of target CEA, there was no observable black band on the test line (**Figure 5.2. b**). A single black band was observed on the control line. For qualitative data, the black bands on the strips were observed with the naked eye.

To get quantitative data, the test and control line black band intensities were measured with a portable strip reader (**Figure 5.2. c**). The reader captured images with an inbuilt camera and converted the pixel intensities of the test and control lines into gaussian curves which were displayed on the screen of a computer. The peak areas on the computer display correlated with the

amount of MWCNTs that were immobilized on the test line, which in turn correlated with the concentration of CEA in the test sample.

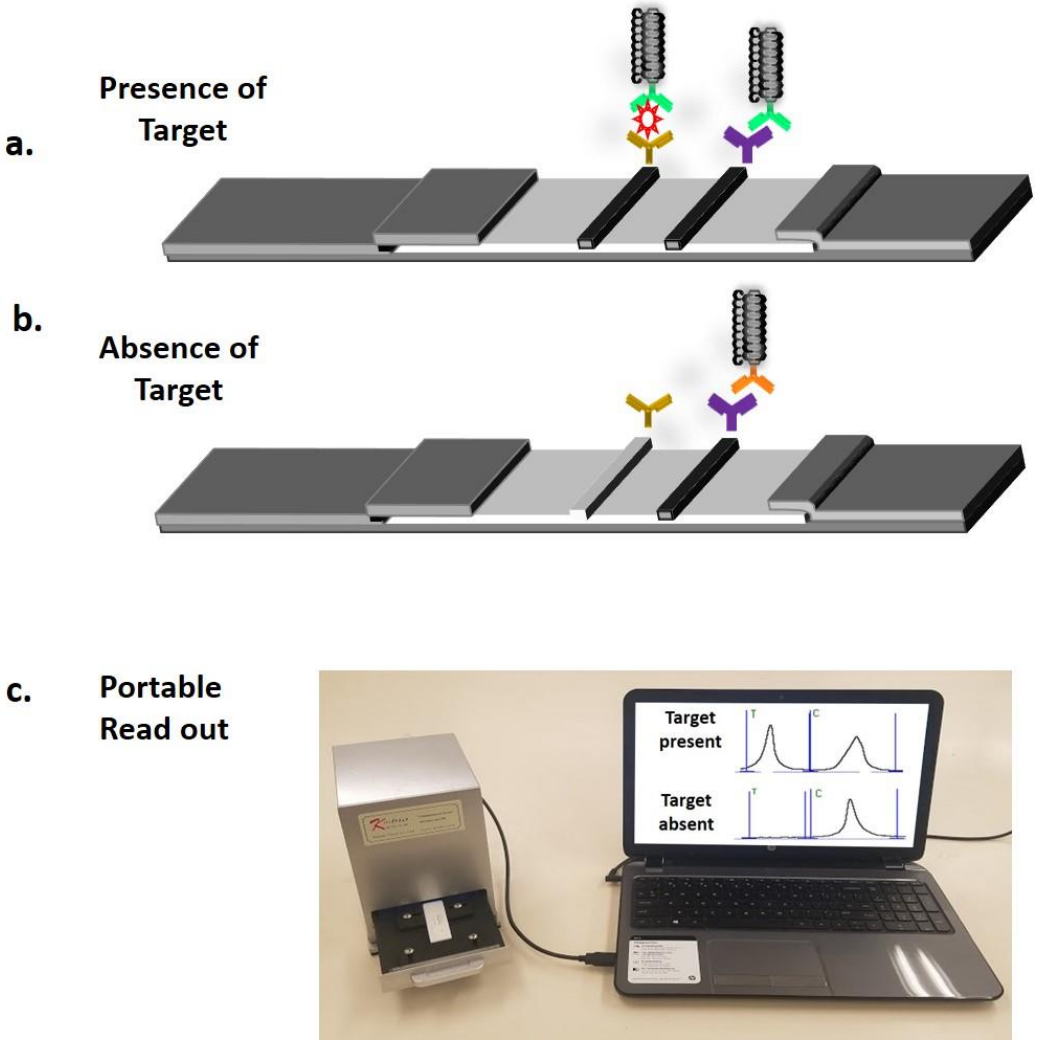

Figure 5.2. Principle of the MWCNT-based lateral flow strip biosensor for CEA detection (a) Capture of MWCNT on test and control lines in the presence of CEA (b) Capture of MWCNTs on the control line in the absence of CEA (c) Reading the test and control line intensities using a portable strip reader.

5.3.2. Optimization of Experimental Parameters

The performance of the assay depended on several factors like the membrane type used, dispense time of the test line, buffer composition, amount of antibodies for conjugate prep and the

volume of conjugates used). These assay conditions were optimized to obtain the best sensitivity and reproducibility with minimal nonspecific adsorption.

The time window for the immunoreactions that occurred on the test and control lines were dependent on the flow rate of the nitrocellulose membrane used. If the flow rate was very slow the time window for the immunoreactions was increased and there could be increased non-specific interactions. Conversely, if the flow rate was too rapid there could have been insufficient time for the target CEA to be efficiently captured on the test zone. Three membranes HF090MC100, HF180MC100 and HF240MC100 with flow rates 90, 180 and 240 seconds per 4cm respectively as reported by the manufacturer were tested for their performance on the LFSB (**Figure 5.3. a**). The 90 second membrane showed the highest S/N ratio. At slower flow rates (180 and 240 secs) the S/N ratio of the assay reduced. This reduction in S/N ratio was because of increased background signals due to non-specific adsorption. The 90 sec membrane was thus chosen for further development of the LFSB.

The dispense times of the test line also played a critical role in the performance of the assay. CEA Ab B at concentration of 1 mg mL^{-1} was dispensed 1, 2, 3 and 4 times on the nitrocellulose membrane and their performance compared (**Figure 5.3. b**). A 1-time dispense of the test line gave the best S/N ratio. The antibody concentration was optimal to allow efficient capture of target CEA on the test line. At higher dispense times (2, 3 and 4 times), there was increased background that led to a rapid reduction in the S/N ratios of the assay. For further development of the assay, 1-time dispense of the test line was chosen.

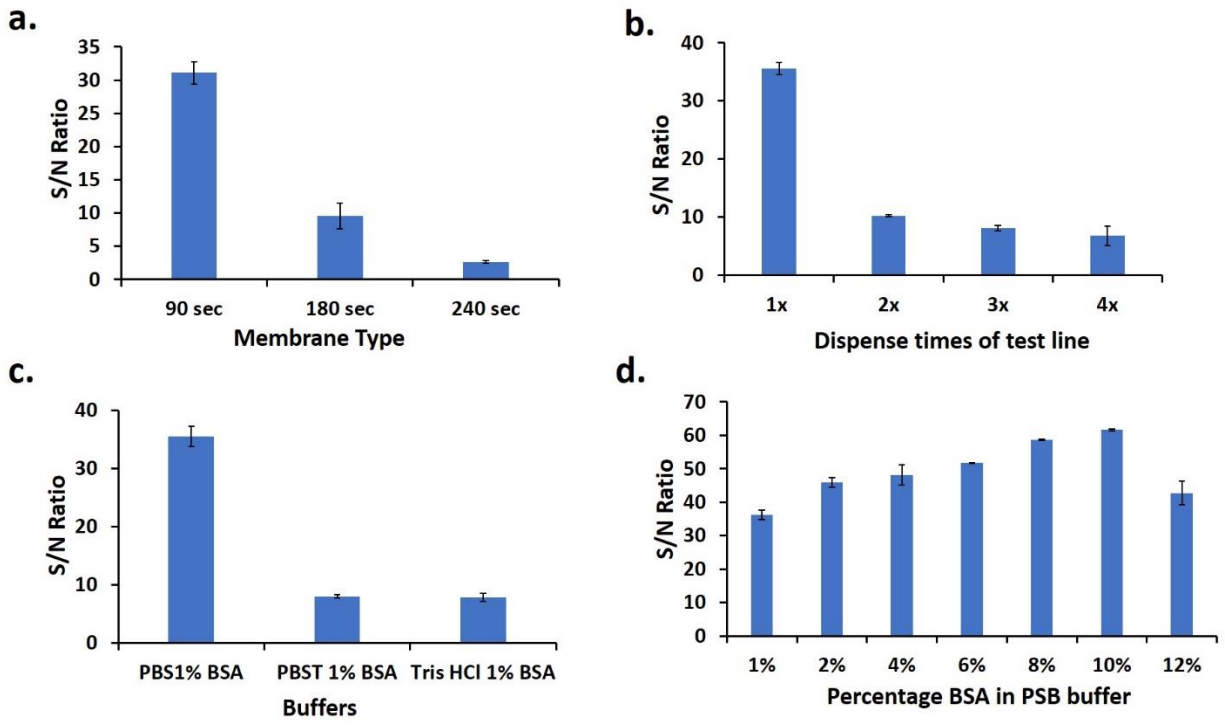

Figure 5.3. (a) Effect of different types of nitrocellulose membranes on the S/N ratio of the assay (b) Effect of the dispensing times of Anti-CEA Ab B on the S/N ratio of the assay. (c): Effect of buffer type on the S/N ratio of the assay (d) Effect of BSA percentage in buffer on the S/N ratio of the assay.

The next line of optimization was variation of buffer conditions to determine the best buffer for the developed assay. Three buffers (PBS + 1% BSA, PBST+ 1% BSA, Tris-HCl + 1% BSA) were tested for their performance on the lateral flow biosensor (**Figure 5.3. c**). PBS + 1% BSA showed the highest S/N ratio, however, some non-specific background signals were observed. The amount of BSA in the running buffer was further optimized to decrease non-specific interactions and thus increase the S/N ratio of the assay. BSA at varying concentrations (1, 2, 4, 6, 8, 10, 12 % w/v in PBS) were tested for their performance on the developed biosensor (**Figure 5.3. d**). The BSA successfully decreased the background signals and increased the S/N ratio up to a concentration 10% BSA. Beyond 10% the signal intensity of the test line was reduced. PBS + 10% BSA was thus chosen as running buffer for further development of the biosensor.

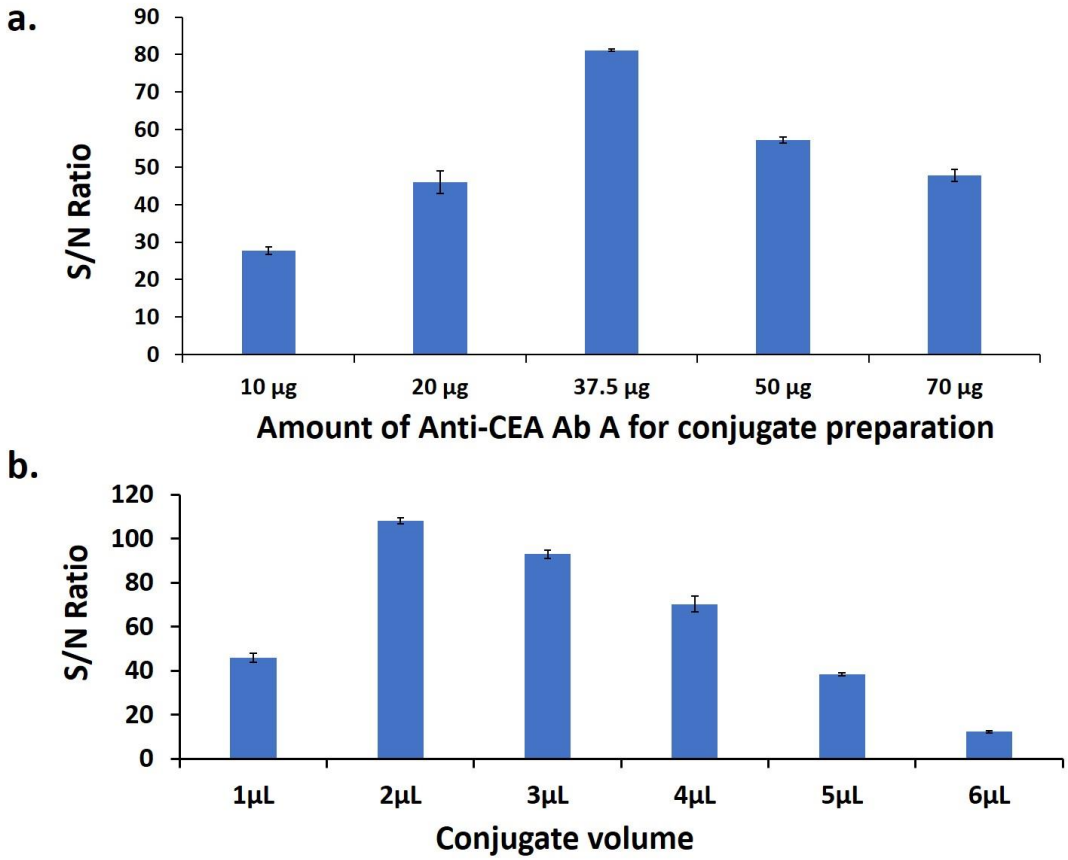

Figure 5.4. (a) Effect of the amount of anti-CEA Ab A used for conjugate preparation on the S/N ratio of the assay. (b) Effect of the volume of conjugate used on the S/N ratio of the assay.

The amount CEA Ab A used for the conjugate preparation was the next parameter to be optimized. Here, varying amounts of CEA Ab A (10, 20 37.5, 50 and 70 µg) were used for the preparation of conjugates and their performance compared on the LFSB (**Figure 5.4. a**). At low concentrations (10 and 20ug) of CEA Ab A, the S/N ratios was low, and this was attributed to the conjugate not having enough antibodies to enable efficient capturing of target CEA onto the test line. Conversely, at higher concentrations the observed decline in the S/N ratio of the assay was resultant of overcrowding of the antibodies on the MWCNT surface which led to stearic hindrance and thus reduced efficiency of the immunoreactions during the test run. The best performance was

observed when 37.5 µg of anti CEA Ab A was used for the conjugate preparation. For further development of the assay 37.5µg of CEA Ab A was used for conjugate preparation.

Finally, the conjugate volume used per assay run also significantly affected the performance of the assay. The assay was performed using varied volumes (1, 2, 3, 4 ,5 ,6 µL) of conjugates and their S/N ratios compared (**Figure 5.4. b**). At low conjugate volume (1µL), there was lowered S/N ratio which was attributed to insufficient conjugates presence to facilitate the efficient capture of target CEA. The highest S/N ratio was observed at 2 µL conjugate volume. At higher volumes beyond 2µL, the observed reduction in S/N ratios was attributed to increased non-specific interactions that led to elevated background signals. A conjugate volume of 2 µL was used for further development of the MWCNT-based LFSB.

5.3.3. Analytical Performance

Under optimized assay conditions (90-second nitrocellulose membrane, 1-time dispense of test line, PBS + 10% BSA running buffer, 37.5µg CEA Ab A for conjugate preparation and 2µL conjugate volume), the developed MWCNT-based LFSB was tested in the presence of varying amounts of CEA standards prepared in running buffer. All tests were run in triplicates.

Typical images of the assay in the presence of increasing CEA concentrations (0.1 to 25ng mL^{-1}) were as displayed in **Figure 5.5. a**. The test line intensities increased with increasing concentration of target CEA. The test strips showed no test line bands in the absence of target CEA which indicated that there was negligible non-specific adsorption. The visual LOD using the naked eye was 0.1ng mL^{-1} of CEA which was 50 times lower than previous report of 5ng mL using GNPs as labels.[90] The test line intensities were read with a portable strip reader for quantitative data. The measured test line intensities were plotted against the CEA concentration to obtain a calibration curve (**Figure 5.5. b**). The assay showed good linearity (R^2= 0.9955), with dynamic range of 0.1

ng mL^{-1} to 25 ng mL^{-1}. The equation of the calibration curve was y = 67.33x + 48.739; where y and x were the test line intensities and the CEA concentrations respectively. The assay showed good reproducibility. Six replicate tests were each performed at CEA concentrations 0, 1 and 15 ng mL^{-1} and the relative standard deviations were 4.2%, 3.1% and 5.3% respectively (data not shown).

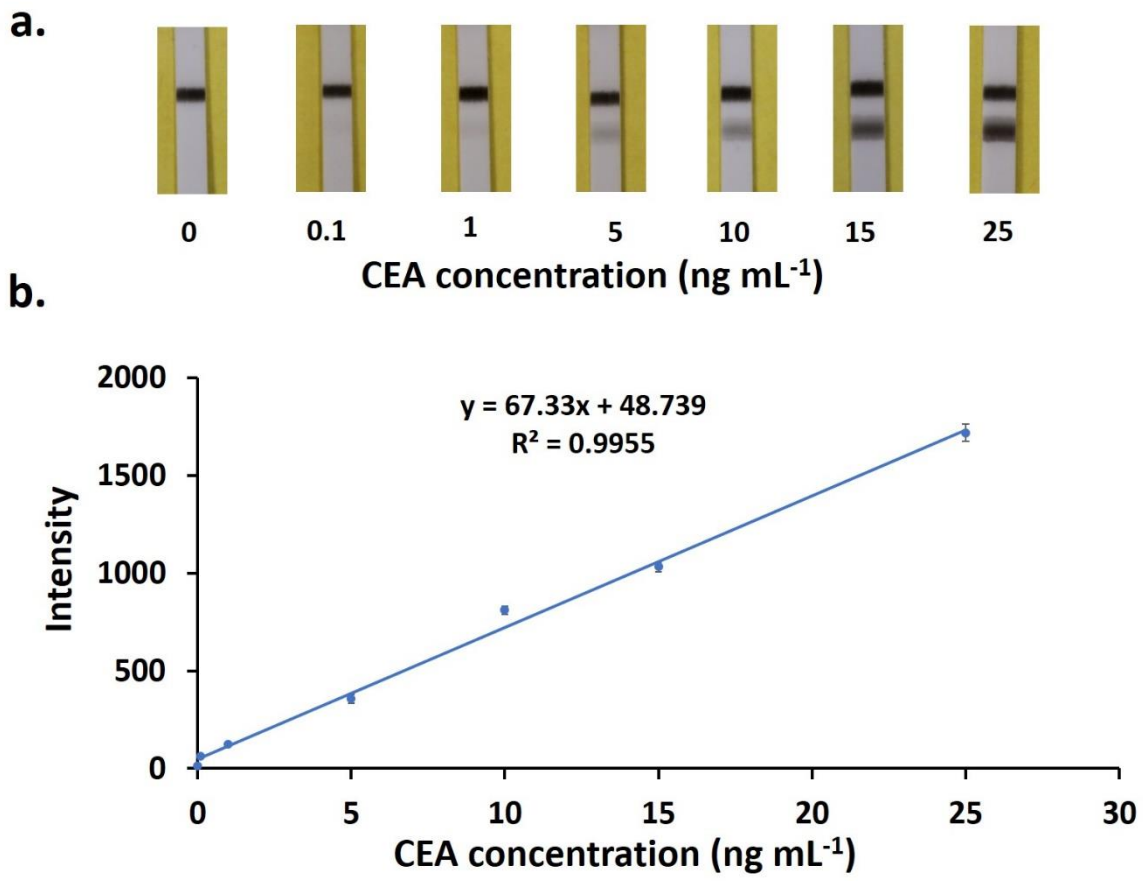

Figure 5.5. (a) Photo images of CNT-based LFSB in the presence of varying concentrations of CEA (b) Calibration curve of CEA detected on developed MWCNT-based lateral flow strip biosensor. Each data point represents the average value obtained from three different measurements.

The selectivity of the developed assay was assessed by testing the assay in the presence of some probable interfering proteins (C4B-alpha, Human IgG, Mammaglobin, and Thrombin at concentrations of 100ng/mL^{-1}; CA 19-9 at concentration of 100 U mL^{-1}) that may be present in

human plasma samples (**Figure 5.6.**). As shown in the graph, the signal for the CEA at concentration of 5ng mL^{-1} was very high compared to the signal for the other molecules (which were similar to the signal of the blank). This confirmed the excellent selectivity of the developed MWCNT-based LFSB for the detection of CEA.

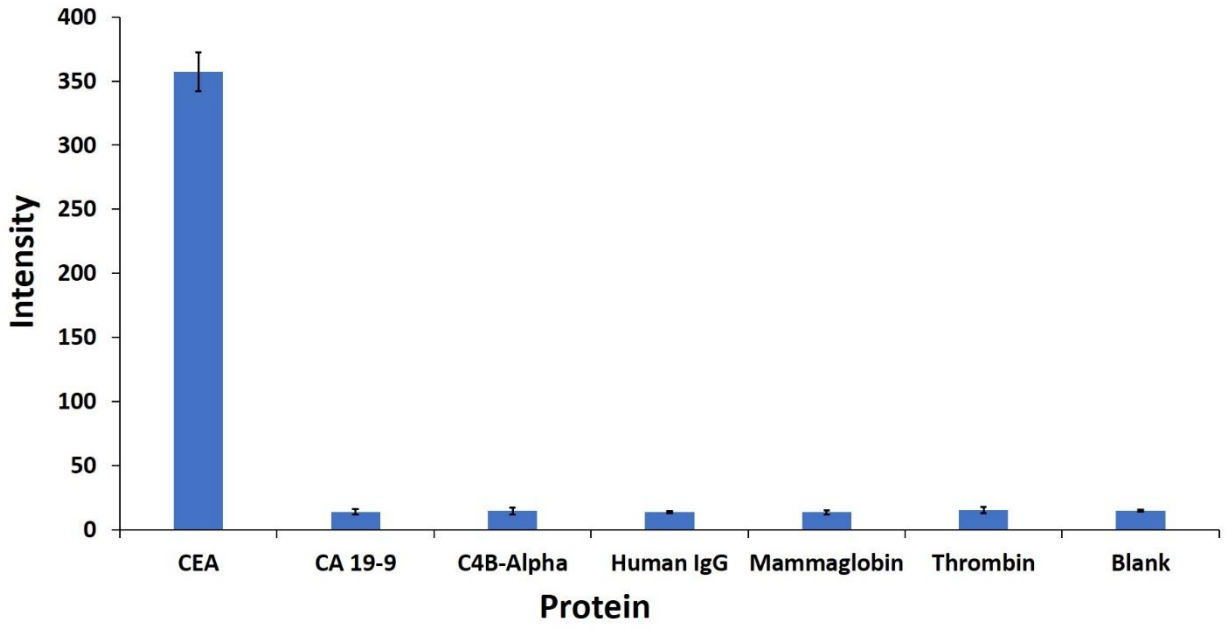

Figure **5.6.** Selectivity of the developed MWCNT-based LFSB (concentration of CEA was 5ng mL^{-1}, CA 19-9 was 100 U mL^{-1}, C4B-aplha, Human IgG, Mammaglobin, Thrombin were 100 ng mL^{-1}).

5.4. Conclusion

A MWCNT-based LFSB was successfully developed for the quantitative detection of CEA. Under optimized assay conditions the developed biosensor had a detection limit of 0.1ng mL^{-1} CEA which was about 20-fold improvement in detection limit over the GNP-based LFSB for CEA (Chapter 3). The developed assay showed a good linear dynamic range of 0.1 ng mL^{-1} to 25 ng mL^{-1}. Further work will aim to apply the developed assay for the screening of CEA in clinical samples. The assay shows great promise for application for CEA detection in medical diagnostics and screening, particularly in low resourced settings.

6. MULTI-WALLED CARBON NANOTUBE-BASED LATERAL FLOW STRIP BIOSENSOR FOR THE QUANTITATIVE DETECTION OF CARBOHYDRATE ANTIGEN (CA 19-9)

6.1. Introduction

Over the past few years pancreatic cancer has risen to be the third leading cause of cancer related deaths even though it is the thirteenth leading cause of cancer in the United States.[158] Over the years there has been little improvement in the survival rates of pancreatic cancer patients. Pancreatectomy remains the most effective way of treating pancreatic cancer. However, only about 5-25% of pancreatic cancer patients are prospects for curative pancreatectomy at diagnosis.[163] Pancreatic cancer has been diagnosed with imaging techniques such as computer tomography, angiography, magnetic resonance imaging, endoscopic ultrasound etc. as reviewed.[164] Tissue biopsies may also be examined by histochemical methods. These methods are expensive, require hospital visitation and have the need for skilled technical expertise. As such, they are not suitable for routine disease screening and monitoring purposes.

The screening of biomarkers present in blood presents an alternate avenue for the screening and monitoring of pancreatic cancer. Various biomarkers have been reported for the screening of pancreatic cancer.[98,165] However, carbohydrate antigen (CA 19-9) remains the only USFDA approved biomarker for pancreatic cancer. CA 19-9 was first isolated from colorectal carcinoma and later pancreatic carcinoma.[74] Since then CA 19-9 has been reported in other cancers of the gastrointestinal system [166] and other cancers like those of the breast [167] and lungs [168]. Still, CA 19-9 remains the best single biomarker for the management of pancreatic cancer. Accordingly, developing sensitive biosensors for the detection of CA 19-9 could help better manage and monitor pancreatic cancer cases.

CA 19-9 has been detected by various methods such as radioimmunoassay, ELISAs, western blotting and some electrophoretic methods.[169,170] Clinically, ELISAs are the gold standard for CA 19-9 detection and many commercial ELISA assays are available for CA19-9 detection.[169] Though ELISAs provide acceptable sensitivity, they have the disadvantages of having long assay times, multiple washing steps, and the requirement for skilled labor and expensive plate readers.

Lateral flow strip biosensors provide a simple, rapid and inexpensive alternative detection technique. In Chapter 2, a lateral flow assay was developed using GNPs as transducers for the detection of CA 19-9. Though this assay showed acceptable sensitivity, there is the need to develop more sensitive assays to enable more efficient monitoring of CA 19-9 levels. Based on the signal enhancement observed in the MWCNT-LFSB developed for the detection of proteins in human plasma (Chapter 4), a MWCNT-based LFSB for the detection of CA 19-9 is discussed in this chapter. Anti-CA 19-9 was covalently linked to the surface of MWCNT and used to detect CA 19-9 in a sandwich type immunoassay. The large surface area and the intense black color of the MWCNTs led to improved sensitivity over the GNP-based LFSB for the detection of CA 19-9.

6.2. Experimental Section

6.2.1. Apparatus

The Airjet AJQ 3000 dispenser, Biojet BJQ 3000 dispenser, Clamshell Laminator, and Guillotine Cutting module CM 4000 were purchased from Biodot LTD (Irvine, CA, USA). Quantitative data was collected using a portable test strip reader (DT2032) purchased from Shanghai Goldbio Tech. Co., LTD (Shanghai, China).

6.2.2. Reagents and Materials

Carboxylated multi-walled carbon nanotubes (carboxyl-MWCNT) (purity > 95 wt%) was purchased from Sun NanoTech (Nanchang, Jiangxi Province, China). Native CA 19-9 (30-AC14),

native CEA protein (30-1819), and mouse anti-CA 19-9 antibodies with catalogue numbers of 10-CA19A and 10-CA19 B was purchased from Fitzgerald Industries International (Acton, MA, USA). The anti-CA 19-9 antibodies were designated anti-CA 19-9 AbA and anti-CA 19-9 AbB respectively. Human mammaglobin was purchased from Creative BioMart (Shirley, NY, USA). Goat anti-Mouse IgG (GaM IgG) and thrombin were obtained from Thermo Fisher Scientific, Inc. (Rockford, IL, USA).

N-(3-Dimethylaminopropyl)-N'-ethylcarbodiimide hydrochloride (EDC), N- hydroxyl-sulfo succinimide (sulfo-NHS), 2-(4-Morpholino) ethanesulfonic acid (MES), tween 20, triton X-100, bovine serum albumin (BSA), sucrose, polyvinylpyrrolidone (PVP), hexadecyltrimethy-lammonium bromide (CTAB) phosphate buffer saline (0.01 M PBS, pH 7.4) and trizma hydro-chloride buffer solution (Tris-HCl, 1.0 M, pH 8.0) were purchased from Sigma–Aldrich (St. Louis, MO, USA) and were used without further purification. Glass fibers (GFCP000800), cellulose fiber sample pads (CFSP001700), nitrocellulose membranes (HFC090MC100, HFC180MC100, HFC240MC100) were purchased from Millipore (Billerica, MA). All the chemicals used in this study were analytical reagent grade. Solutions used were prepared with ultrapure (≥18M Ω) water from Millipore Milli-Q water purification system (Billerica, MA, USA).

6.2.3. Preparation of MWCNT-Anti-CA 19-9 AbA Conjugate

MWCNTS with activated carboxyl groups were prepared as previously described (Section 5.2.3). The prepared MWCNTs suspended in PBS at a concentration of 0.5 mg MWCNT per milliliter of buffer. CA 19-9 AbA (80 µg) was then added, and the mixture was incubated overnight with gentle shaking at 4°C. The prepared MWCNT-anti-CA 19-9 AbA was washed with PBS by centrifugation at 5000 rpm for 5 mins. The washing step was repeated 3 times. The supernatant was monitored by UV absorbance (280 nm) measurements to ensure no protein absorption was

present in the supernatant. The prepared MWCNT-anti CA 19-9 Ab A conjugates were resuspended in Eluent buffer (20 mM $Na_3PO_4 \cdot 12H_2O$, 5% BSA, 10% sucrose, and 0.25% Tween-20) and stored at 4°C until used.

6.2.4. Preparation of the MWCNT-Based LFSB for CA 19-9 Detection

The setup for the developed MWCNT-based LFSB for the detection of CA 19-9 was as shown in **Figure 6.1.** The biosensor was composed of three major components (conjugate pad, nitrocellulose membrane and absorption pad). The three components were assembled on a sticky plastic backing layer.

The conjugate pad was a glassy fiber that measured 21 x 300mm. The glassy fiber was porous to ensure the pad could hold a large volume of conjugate. The pad was also able to release the dried conjugates upon wetting. The nitrocellulose membrane supported the test line and control line antibodies. Anti-CA 19-9 AbB and goat anti-mouse IgG were dispensed as the test and control lines respectively. The absorption pad was the final component, and this absorbed excess reagents and created capillary force to drive fluid movement during the assay run. The components were assembled onto the sticky backing layer and were allowed to overlap by at least 2mm to ensure continuous movement of the solvent. The assemblies were then cut into 3mm width strips and stored at 4°C until used.

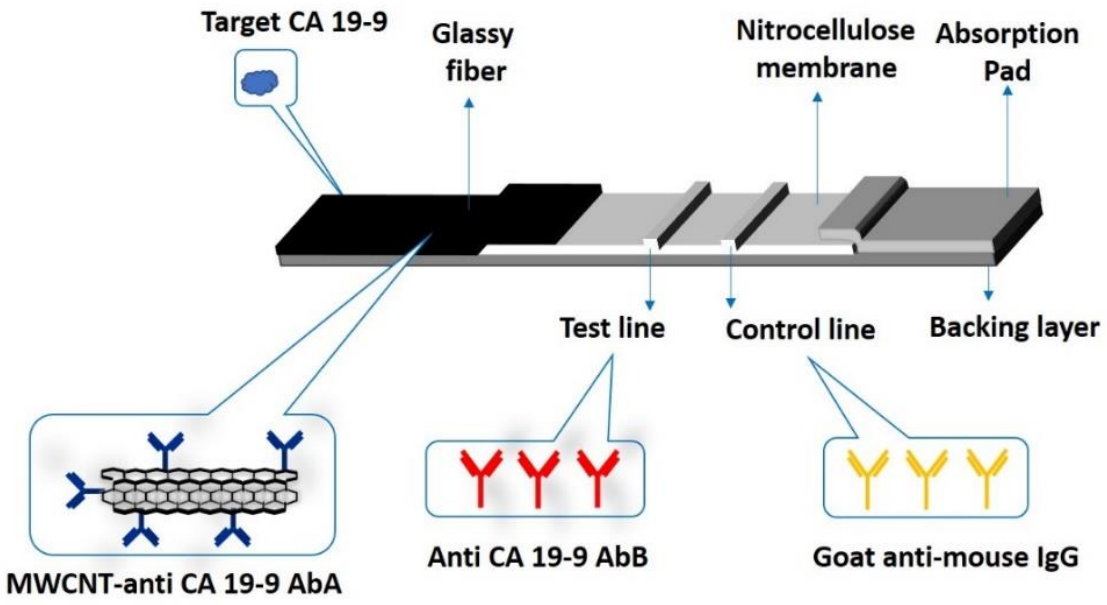

Figure 6.1 Scheme of developed MWCNT-based LFSB for the detection of CA 19-9.

6.2.5. Assay Procedure

MWCNT-anti-CA 19-9 AbA conjugates were pipetted onto the conjugate pad and allowed to dry for 5mins. Native CA 19-9 prepared in running buffer (PBS + 1%BSA + 1.5mM CTAB) with volume 100µLwas applied to the LFSB. The solution moved across the test strip by capillary action. After 20 mins, the strip was washed with 100 µL of running buffer. The washing step served to remove any nonspecifically adsorbed conjugates which reduce background signals. The test line could be visually examined with the naked eye for qualitative data. For quantitative data, the test and control line intensities were measured with a portable strip reader.

6.3. Results and Discussion

6.3.1. Principle of the Developed MWCNT-Based LFSB for CA 19-9 Detection

The developed assay relied on the CA 19-9 dependent accumulation of MWCNT on the test line to enable visual detection of CA 19-9 (**Figure 6.2. a**). The nitrocellulose membrane of the LFSB supported pre-immobilized anti-CA 19-9 AbB and goat anti-mouse IgG that served as the test and control lines respectively. Anti-CA 19-9 AbA component of the MWCNT- anti-CA 19-9

AbA conjugate served as the detection antibody. In the presence of sample containing target CA 19-9, there was an immunoreaction between the CA 19-9 and the anti-CA 19-9 AbA component of the MWCNT-anti-CA 19-9 AbA conjugate to form a MWCNT-anti-CA 19-9 AbA-CA 19-9 complex. The complex moved along the strip and upon encountering the test line, were captured by an immunoreaction between the CA 19-9 component of the complex and the test line anti-CA 19-9 AbB (**Figure 6.2. a**). The CA 19-9 dependent accumulation of MWCNT on the test line resulted in a black colored band that was visible to the naked eye. Excess conjugates moved further along the test strip and were captured by the control line goat anti-mouse IgG which resulted in a second black band (**Figure 6.2. a**). In the absence of target CA 19-9, there was no accumulation of MWCNTS on the test line, however, there was capture of the MWCNT-anti-CA 19-9 AbA conjugate at the control line which verified the assay was working well (**Figure 6.2. b**). To get quantitative data, the test and control line intensities of the test strips were read with a portable reader connected to a laptop. The strip reader captured images of the test and control lines and used their pixel intensities to construct gaussian curves which was read on the laptop screen (**Figure 6.2. c**). The area under the curve gave information about the amount MWCNTs that were immobilized on the test line, which in turn correlated with the concentration of CA 19-9 in the test sample.

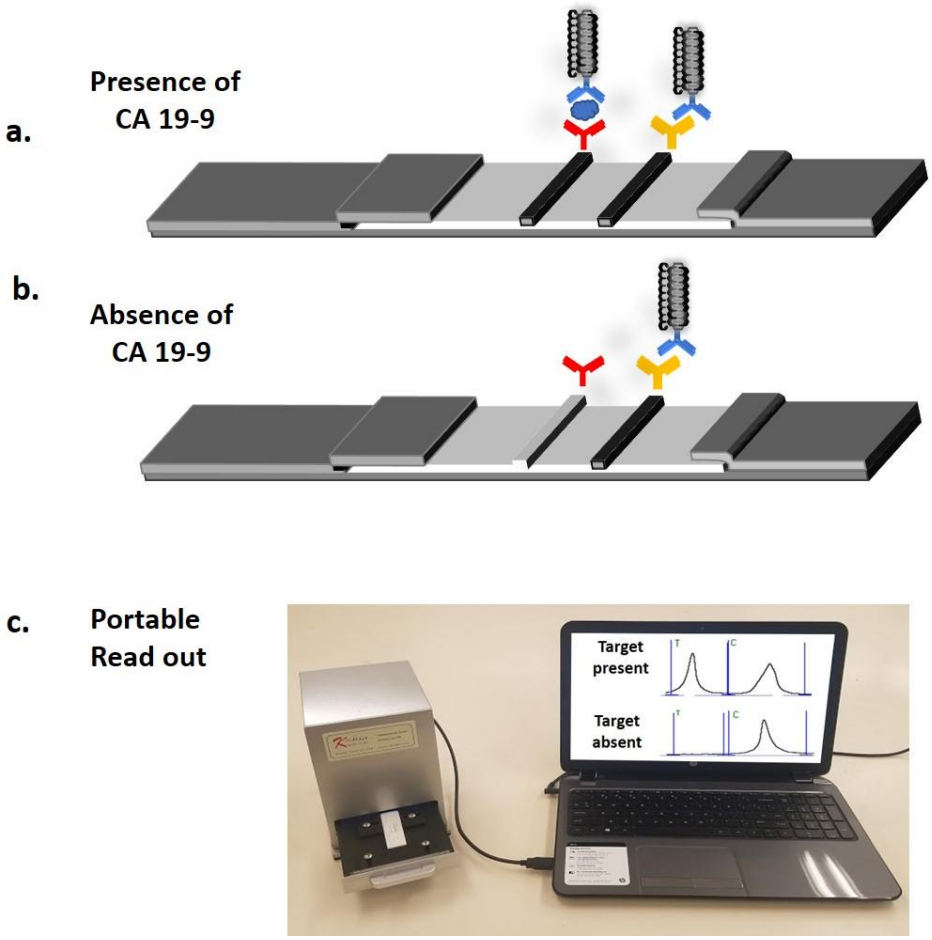

Figure 6.2. Working principle of the MWCNT-based lateral flow strip biosensor for CA 19-9 detection (a) Capture of MWCNT on test and control lines in the presence of CA 19-9 (b) Capture of MWCNTs on the control line in the absence of CA 19-9 (c) Reading the test and control line intensities using a portable strip reader.

6.3.2. Optimization of Experimental Parameters

The performance of the assay depended on parameters like the nitrocellulose membrane type used, dispense times of the test line, the composition of the running buffer, amount of antibodies used for conjugate preparation and the volume of conjugates used per test. These parameters had to be optimized to ensure the highest sensitivity while keeping background signal at a minimum.

The flow rate of the membrane that supported the test and control lines dictated the time window within which the immunoreactions at the test line would occur. Three membranes

(HFC090MC100, HFC180MC100, HFC240MC100) with flow rates of 90 secs, 3 mins and 4 mins per 4cm of membrane respectively were tested for their performance on the developed LFSB (**Figure 6.3. a**). From the chart, it is observed that the 90-sec membrane gave the best S/N ratio. There was a marked reduction in performance when the 3-min and 4-min membranes were used. The reduction in S/N ratios was because of increased background signals. The 90- sec membrane was therefore chosen for further development of the assay.

The anti-CEA AbB dispense times for the test line preparation was also optimized. Anti-CA 19-9 AbB at concentration of 1 mg mL^{-1} was dispensed varying times (1, 2, 3, 4 ,5x) and their S/N ration compared (**Figure 6.3. b**). At lower dispense times (1,2 and 3x) lowered S/N ratios were observed which was attributed to inadequate antibody concentration on the test lines. There were therefore lowered test line intensities that led to the observed reduction in S/N ratios. The highest S/N ratio was observed at 4x dispense cycles of the test line. Beyond 4x dispense there was a reduction in the S/N ratio as a result of increased background signals resulting from increased nonspecific adsorption. For further development of the assay, the test line anti-CA 19-9 AbB was dispensed 4 times.

The buffer composition also affected the assay performance. Target CA 19-9 was prepared in different buffers (PBS + 1% BSA, PBS + 1% BSA + 1.5Mm CTAB, PBST + 1% BSA, PBST + 1% BSA + 1.5Mm CTAB, Tris-HCl +1% BSA, Tris-HCl +1% BSA + 1.5mM CTAB) and their S/N ratios compared (**Figure 6.3. c**). Tris-HCl +1% BSA + 1.5mM CTAB showed the best performance and was thus chosen for further development of the assay.

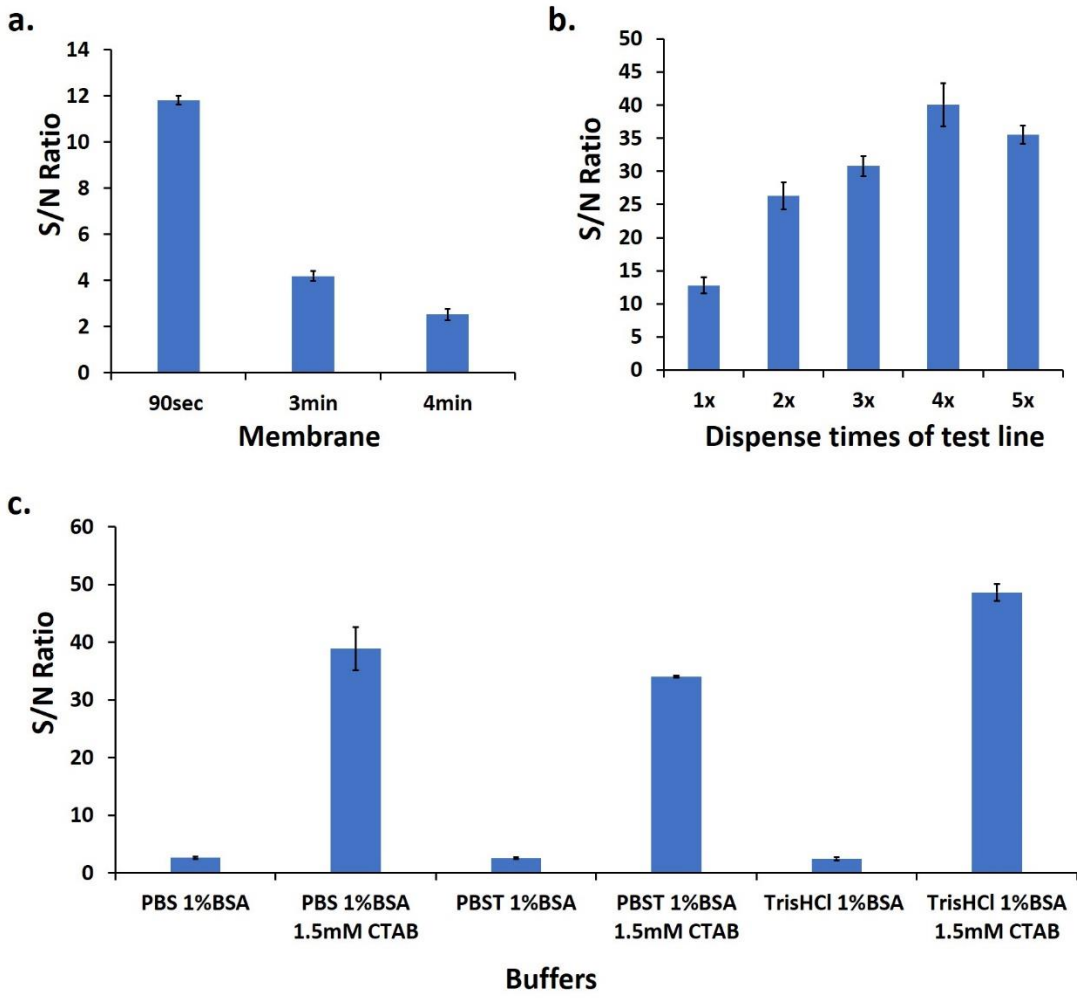

Figure 6.3. (a) Effect of different types of nitrocellulose membranes on the S/N ratio of the assay. (b) Effect of the dispensing times of Anti-CA 19-9 AbB on the S/N ratio of the assay. (c) Effect of buffer type on the S/N ratio of the assay.

The amount of anti-CA 19-9 AbA used for the preparation of the conjugate was the next line of optimizations performed. Varying amounts (20, 40, 60, 80, 100, 120, 160 µg) of anti-CA 19-9 AbA was used for the preparation of MWCNT-anti-CA 19-9 AbA and the S/N ratios compared (**Figure 6.4. a**). The S/N ratio peaked at 80 µg. Beyond 80 µg of antibody the S/N ratios dropped as the test line intensities reduced. At the higher concentrations, there was overcrowding of the antibodies on the MWCNT surface which resulted in stearic hindrance and thus reduced

efficiency of the immunoreactions during the test run. 80 µg of anti-CA 19-9 was therefore chosen for further development of the assay.

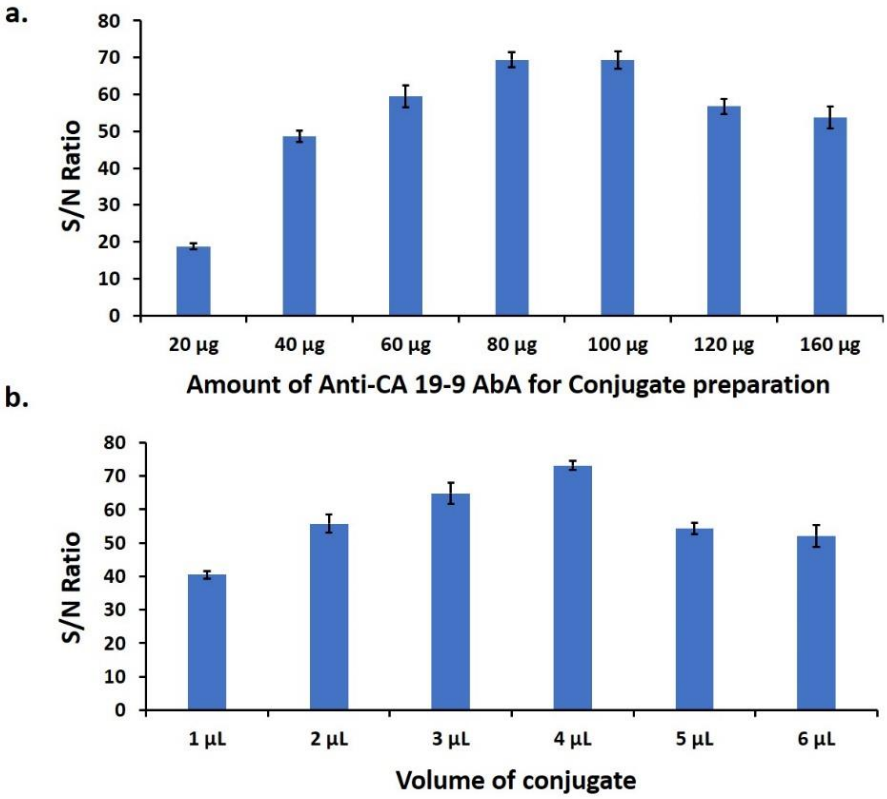

Figure 6.4. (a) Effect of the amount of anti-CA 19-9 AbA used for conjugate preparation on the S/N ratio of the assay (b) Effect of the volume of conjugate used on the S/N ratio of the assay.

The amount of conjugate dispensed onto the conjugate pad per assay ran also had a huge influence on the performance of the assay. Varying volumes of conjugates were tested on the developed LFSB and their S/N ratios compared (**Figure 6.4. b**). The highest S/N ratio was observed when 4 µL of conjugate was used. Lower volumes of conjugate gave inadequate sensitivity, and higher volumes showed increased background signals. 4 µL of MWCNT-anti CA 19-9 AbA conjugate was thus chosen for further testing.

6.3.3. Analytical Performance

Under optimized conditions (90-sec membrane, 4x dispense cycles of the test line, Tris-HCl + 1%BSA + 1.5mM CTAB running buffer, 80µg anti-CA 19-9 AbA for conjugate preparation, 4 µL of conjugate per assay run) the developed MWCNT-based LFSB was used to detect varying concentrations of CA 19-9 prepared in running buffer. Typical photo images of the biosensor's response to the varying CA 19-9 concentrations were are as shown in **Figure 6.5. a**. As expected, the intensity of the test line black bands increased with increasing concentration of target CA 19-9. In the absence of target, there was no observable black band on the test line which indicated that the optimization process successfully eliminated non-specific adsorption of the conjugate onto the test zone. The visual detection limit was 1 U mL^{-1} which was a five-fold reduction compared to the GNP-based LFSB for CA 19-9 detection.

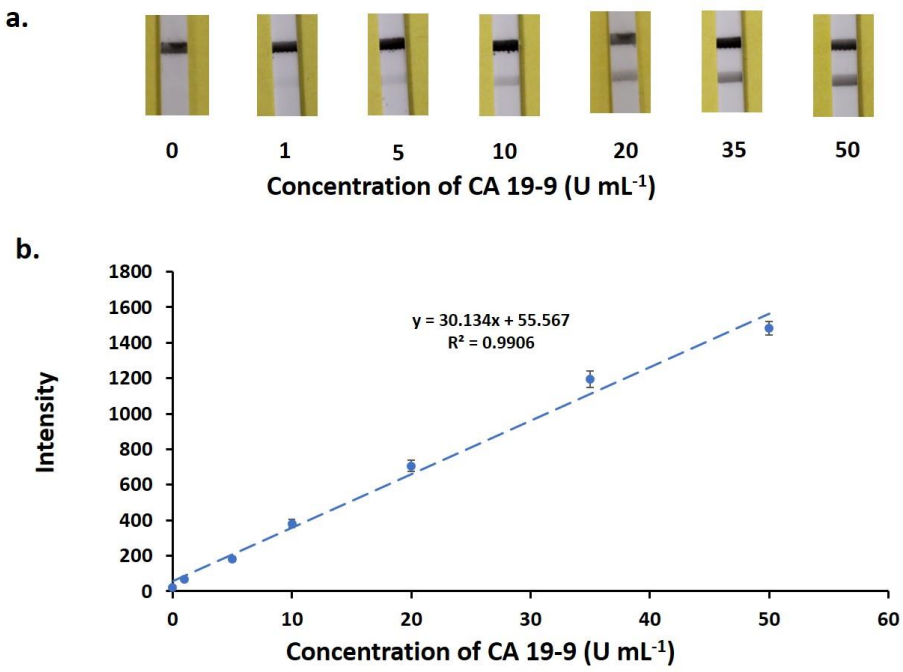

Figure 6.5. (a) Photo images of MWCNT-based LFSB in the presence of varying concentrations of CA 19-9 (b) Calibration curve of CA 19-9 detected on developed MWCNT-based lateral flow strip biosensor. Each data point represents the average value obtained from three different measurements.

For qualitative data (yes/no) the strips were observed with the naked eye. To get quantitative data, the test line intensities were read with a portable strip reader. The intensities of the test lines were plotted against the concentrations of CA 19-9 to obtain a calibration curve as displayed in **Figure 6.5. b**. The calibration curve showed good linearity (R^2= 0.9906) with a linear dynamic range from 1 U mL^{-1} to 50 U mL^{-1}. The equation of the curve was y = 30.134x + 55.567; where y and x were the test line intensities and the CA 19-9 concentrations respectively. The detection limit was calculated to be 0.14 U mL-1 (S/N ratio =3) which was an improvement over the GNP-based LFSB for CA 19-9 (5U mL^{-1}). The assay showed good reproducibility. Six parallel tests were each performed at CA 19-9 concentrations of 1 and 35 U mL^{-1} and the relative standard deviations were 7.2% and 5.1% respectively (data not shown).

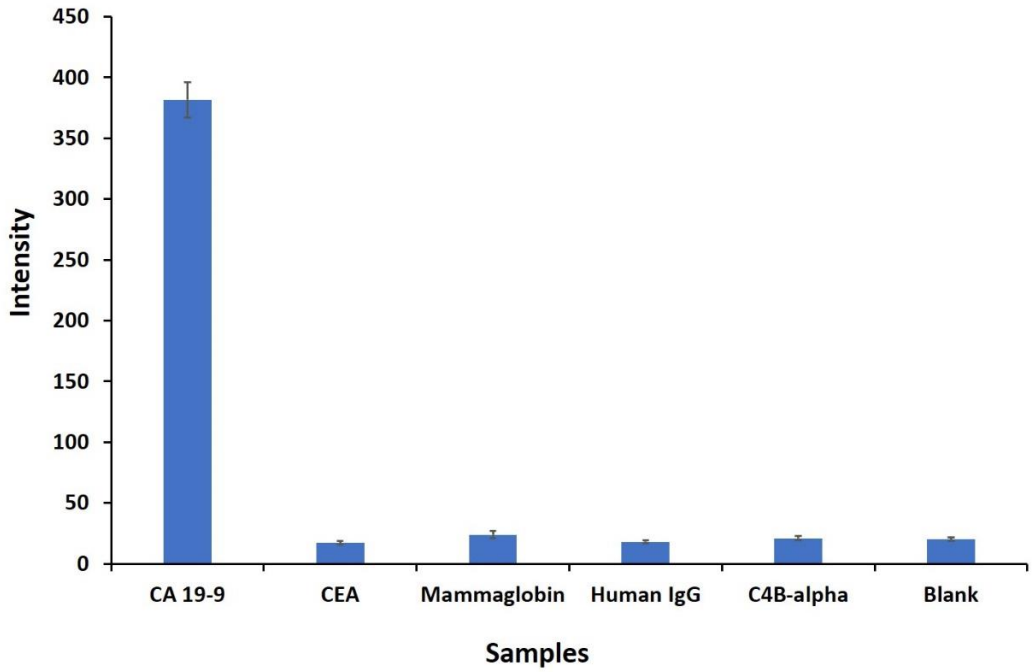

Figure 6.6. Selectivity of the developed MWCNT-based LFSB (concentration of CA 19-9 was 10 U mL^{-1}; CEA, Mammaglobin, Human IgG, C4B-aplha and Thrombin were at 100 ng mL^{-1}).

The assay also showed excellent selectivity as shown in **Figure 6.6**. The signal for CA 19-9 at concentration of 10 U mL^{-1} was much higher than the signal intensity for the other proteins

that were present at over 10-fold higher concentrations. The signal for the other proteins were like the signal for the blank.

6.4. Conclusion

A quantitative MWCNT-based LFSB was successfully developed for the detection of CA 19-9. The assay successfully detected varying concentrations of CA 19-9 in buffered solution and had an improved detection limit of 0.14 U mL^{-1} (S/N ratio = 3) which was about 35-fold more sensitive than the GNP-based LFSB for CA 19-9. The assay was capable of detecting CA 19-9 in under 30minutes and shows great potential for application as a point-of-care screening tool.

7. GOLD NANOPARTICLE-BASED LATERAL FLOW STRIP APTASENSOR FOR THE DETECTION OF EXOSOMES FROM HUMAN PLASMA

7.1. Introduction

Exosomes are small membrane bound biomolecular vesicles that are released from both healthy and cancerous cells. Various cargo like DNA, miRNA, lipids and proteins can be carried inside the exosome vesicles. The composition of the exosomal cargo and surface proteins is a reflection of the physiological and functional condition of the parent cell.[171] Exosomes influence diverse pathological and physiological functions of the parent cells of origin and destination cells.[172] In cancer, one of the fundamental determinants of cancer cell growth promotion and suppression is the tumor microenvironment. The tumor microenvironment is composed of fibroblasts, immune cells and extracellular matrix containing vesicles such as exosomes.[173] Exosomes in the tumor microenvironment help in localized cancer cell communication as well as communication with distant cells and tissues. Cancer cells are able to sort out oncoproteins and cancer related nucleic acids into exosomes which are then incorporated in adjacent healthy cells to drive neoplastic transition.[174] Exosomes have also been reported to play a pivotal role in angiogenesis, transformation of extracellular matrix, immune evasion and resistance to chemotherapeutic drugs. [175–178]

In cancer patients, tumors and cancer cells may have up-regulated extracellular vesicle shedding, and higher levels of exosomes has been measured patient serum, however, more studies are required in this area. Exosomes are found in various bodily fluids such as blood and urine. Exosomes are therefore good candidates for diagnosis and prognosis of diseases, and for the monitoring of patient response to therapy. The use of exosomes for diagnostics is an emerging field of study that has gained traction. Ultracentrifugation has been predominantly used to separate

and purify exosomes from bodily fluids.[179] More recent methods including nanomembrane concentrators, size exclusion chromatography (SEC), exosome precipitation, immunoaffinity capture and microfluidic based isolation techniques have been reviewed.[180]

For diagnostic purposes, it is important to quantify exosomes upon isolation and purification. Enzyme linked immunosorbent assays (ELISA) has been used for the quantitation of exosomes. [181,182] ELISAs for exosome detection generally have the exosomes directly immobilized at the bottom of well plates. Upon blocking with agents such as bovine serum albumin (BSA), primary antibodies are introduced to bind to pre-immobilized exosomes. Enzyme labelled secondary antibodies are then added and in the presence of substrate a colored complex whose intensity reflects the number of exosomes is observed. Oliviera-Radríguez and coworkers developed an in-house ELISA suing antibodies for CD9, CD81 and CD63 cell surface proteins to detect exosomes from cell culture media.[72] There are also commercially available kits such as ExoELISA™ and ExoQuant™ ELISA kits by Systems Biosciences and BioVision Inc. respectively which are used to quantify exosomes. Though the ELISA-based methods provide acceptable sensitivity, they suffer draw backs such as, multiple washing cycles leading to long assay times, requirement for refrigeration, and the need for skilled labor. Flow cytometric methods have also been used for exosome analysis.[183] They have the advantage of being high throughput, and may provide information about individual exosomes. However, flow cytometric analysis of extracellular vesicles suffer setbacks such as data variation between different platforms, variation in analysis of data from laboratory to laboratory, and high background noise from light scattering as reviewed.[184] Other methods of exosome analysis including electrochemical methods and fluorescent nanoparticle tracking analysis (NTA) have also been reviewed.[185] NTA analysis allows for the characterization of individual exosome sizes and can also give information about bulk

exosome concentrations. These detection techniques offer unique advantages, however, high cost, poor miniaturization for in-field usage, and the need for skilled technical labor limit their application for routine screening.

Lateral flow strip biosensors (LFSB) offer a rapid, low cost but sensitive and selective method of analysis. LFSBs traditionally rely on sandwich type immunoassay setup where a target is captured between an antibody immobilized on a solid support and a detection antibody linked to a nanoparticle transducer. Target dependent accumulation of the nanoparticles is measured to get quantitative data. Various nanoparticles including gold nanoparticles (GNP)[15,18,72,119], carbon nanotubes[25], fluorescent nanoparticles[23,120,121], GNP-coated silica nanorods[24,45] amongst others[26,28,116] have been applied on lateral flow for the detection of a variety of targets. The intense red color of GNPs resultant of their surface plasmon properties makes GNPs the gold standard in LFSB transducers. GNP based LFSI have been used for the detection of proteins, cells and some small molecules.

The class of LFSBs that rely on antibodies as biorecognition elements are termed lateral flow strip immunosensors (LFSI). Immunosensors have shortfalls such as high cost of production, batch to batch variation and long-term instability. As a result, LFSIs can suffer some inconsistencies in results and cause a divide between the current performance of LFSB and their expected low price and reliability.[186]

Aptamers are a class of nucleic acids that can replace antibodies as biorecognition elements. Aptamers fold into unique primary, secondary and tertiary structures that enhance their binding and specificity. Aptamers are developed by a process termed Systematic Evolution of Ligands by Exponential Enrichment (SELEX). Aptamers have the advantages of being cheap and simple to chemically synthesize or modify. They are also redox insensitive and heat stable, and

therefore require no form of refrigeration. Aptamers have been developed for targets such as proteins, cells, heavy metals and some other small molecules.[187] Aptamer based lateral flow assays are termed lateral flow strip aptasensors (LFSA). LFSAs have been developed for proteins and some small molecules.[14,17,188] Also, Mao and coworkers successfully demonstrated the detection of ramos cells using a GNP-based lateral aptasensor.[15]

Exosome detection has seen little attention on lateral flow strip biosensors. Oliveira-Rodríguez and coworkers developed a LFSI utilizing anti-CD-9 and anti-CD81 antibodies for the detection of exosomes from culture media and bodily fluids.[72] The assay though applied successfully, suffered a high LOD which limits its application. There remains the need for the development of more sensitive and selective point-of-care assays for exosome.

Considering the unique advantages afforded by replacing antibodies with aptamers, a GNP-based LFSA that utilizes an aptamer previously developed[189] for cell surface protein (EpCAM) is proposed for the detection of exosomes. EpCAM, a cell surface membrane protein that has been reported to be associated with various cancers including pancreatic cancer was chosen as a model target. Exosomes surface membranes can carry similar proteins as those expressed on the originating cells. In this work, exosomes were captured in a sandwich assay between the immobilized EpCAM aptamers on a solid support and aptamer labelled GNP. Under optimized conditions, the exosome dependent accumulation of GNP on the test zone resulted in a low detection limit of 1.3×10^3 exosomes/μL which was a significant improvement over previous report.[72] The GNP-based LFSA shows promise for the low cost and rapid detection of exosomes isolated from clinical samples.

7.2. Experimental Section

7.2.1. Apparatus

The Biojet BJQ 3000 dispenser, Clamshell Laminator and Guillotine cutting module CM 4000 used for the assembling of the LFSB were bought from Biodot LTD (Irvine, CA, USA). Strips were quantitatively read with a portable strip reader (DT2032) acquired from Shanghai Goldbio Tech. Co., LTD (Shanghai, China). Exosomes were isolated from human plasma by ultracentrifugation using Optima XE-90 ultracentrifuge purchased from Beckman Coulter, Inc (Indianapolis, IN, USA). Exosome were also isolated using qEVoriginal size exclusion columns purchased from Izon Science LTD (Medford, MA, United States). Strip images were captured with an S7 smart phone by Samsung Electronics (Seoul, South Korea).

7.2.2. Reagents and Materials

Gold (III) chloride ($HAuCl_2$), phosphate buffered saline (0.01 M PBS, pH 7.4), Dulbecco's phosphate-buffered saline (DPBS), trizma hydrochloride buffer solution (Tris-HCl, 1.0 M, pH 8.0), tween 20, triton X-100, bovine serum albumin (BSA), sucrose, sodium chloride (NaCl), magnesium chloride ($MgCl_2$) and sodium phosphate tribasic deodecahydrate ($Na_3PO_4.12H_2O$) were purchased from Sigma–Aldrich (St. Louis, MO, USA) and were used without further purification. Glass fibers (GFCP000800), cellulose fiber (CFSP001700), and nitrocellulose membranes (HFC090MC100, HFC135MC100, HFC180MC100) were purchased from Sigma–Aldrich (St. Louis, MO, USA) for the fabrication of the LFSB platform. Streptavidin was purchased from Prospec-Tany Technogene Ltd (Ness-Ziona, Israel). Deoxyadenosine triphosphate (dATP) and goat anti-mouse IgG were purchased from Thermofisher Scientific (Waltham, MA, United States). Anti-EpCAM antibodies with catalogue numbers ABIN1684521 and ABIN4949645 were purchased from Antibodies-online Inc. (Atlanta, GA, United States). All

DNA sequences were purchased from Integrated DNA Technologies, Inc. (Coralville, CA, United States). The DNA sequences used in the assay are as follows:

Biotinylated EpCAM capture probe: 5'-/Biosg/-CACTACAGAGGTTGCGTCTGTCCCACGT TGTCATGGGGGGTTGGCCTG-3'

Thiolated EpCAM detection Probe: 5'-ThioMC6-D/CACTACAGAGGTTGCGTCTGTCCCAC GTTGTCATGGGGGGTTGGCCTG-3'

Biotinylated control line Probe: 5'-/Biosg/ATATATATATATATATATA-3'

Thiolated control probe: 5'-ThioMC6-D/TATATATATATATATATAT-3'

All reagents were analytical grade. All solutions used in the study were prepared in ultrapure (≥18M Ω) water from Millipore Milli-Q water purification system (Billerica, MA, USA).

7.2.3. Preparation of GNPs

GNPs with diameters 13nm ± 3.5 were prepared as previously described.[119,190] All glass-ware used for the preparation of the GNPs were washed with detergent and further cleaned by soaking in *aqua regia* (3:1; HCl:HNO_3). The glassware was then washed with copious amounts of distilled water and dried out. $HAuCl_4$ stock solution (50% w/v) was prepared in ultrapure water. Fifty microliters (50µL) of stock $HAuCl_4$ was mixed with 250mL of ultrapure water in a glass vessel. The mixture was heated with vigorous stirring until it boiled. Sodium citrate was then added, and the mixture was boiled until the color changed to the characteristic red color of GNPs. The mixture was then boiled for an additional 10 mins. The GNP solution was cooled down to room temperature (RT) with gentle stirring. The volume was then topped up to 250 mL with ultrapure water. The prepared GNP solution was stored at 4°C until used.

7.2.4. Preparation of GNP-Aptamer Conjugates

GNP solution was spun down at 12,000 rpm and concentrated 5-fold in ultra-pure water. To 1mL of 5-fold concentrated GNPs, dATP was added to a final concentration of 7.05μM and incubated at RT for 20 mins with gentle shaking. 1% SDS (15uL) was added slowly and mixture was incubated with shaking for 10 mins. Fifty microliters (50μL) of 2M NaCl was added at a rate of 3 μL every 3 mins to age the gold nanoparticles. Thiolated EpCAM detection probe and thiolated control probe were added to the mixture and transferred to a water bath at 60°C for a 3 hr-incubation period. Prepared GNP-aptamer conjugates were washed with BSA solution (1% w/v) by centrifuging at 12,000 rpm. The wash step was repeated three times. The prepared conjugates were resuspended in 1mL of eluent buffer (20 mM Na3PO4·12H2O, 5% BSA, 10% sucrose, and 0.25% Tween-20). The GNP-aptamer conjugates were then stored at 4°C until used.

7.2.5. Preparation of GNP-Antibody Conjugates

GNP solution was spun down at 12,000 rpm. The pellets were collected and resuspended at 5-fold concentration in water with pH adjusted to 9. Twenty micrograms (20ug) of anti-EpCAM antibody (catalogue number ABIN4949645) was added to 1mL of 5-fold GNPs and incubated at 4°C overnight with gentle shaking. 20% BSA solution was added to a final concentration of 1% BSA. The mixture was further incubated for 1hr at RT. The mixture was then spun down and washed 3 times with PBS 1% BSA solution. The prepared GNP-anti EpCAM conjugates were then resuspended in 1mL of eluent buffer and stored at 4°C until used.

7.2.6. Preparation of Streptavidin-Biotinylated DNA Probe Conjugate

Fifty nanomoles (50nmols) of biotinylated DNA (EpCAM capture probe or control line probe) was mixed with 200 μL of a 2.5 mg mL^{-1} solution of streptavidin and incubated at RT for 1hr with gentle shaking. The mixture was then diluted in 15mL of PBS and transferred into a

centrifugal filter tube (30kDa molecular cutoff). The tube was spun at 6000 rpm for 20 mins at 4°C. The eluent was then discarded and washing step repeated two more times. Finally, the streptavidin-biotinylated DNA probe conjugate left on the filter was collected, diluted to 600 µL with PBS and dispensed immediately.

7.2.7. Preparation of the LFSA for Exosome Detection

The setup for the developed GNP-based LFSA for the detection of exosomes was as shown in **Figure 7.1**. The sensor was composed of three major sections (conjugate pad, nitrocellulose membrane and absorption pad) immobilized on a sticky backing layer made of impermeable plastic. The conjugate pad was a glass fiber sheet (21mm x 300m) on which the GNP conjugates were pre-dispensed before the assay was performed. The glassy fiber was spongy to enhance the adsorption of suitable volumes of conjugate. The glassy fiber material also ensured that the adsorbed conjugates were released upon wetting during assay runs. The conjugate pad also served as the point of sample application. The nitrocellulose membrane (25 mm × 300 mm) supported the test and control lines DNA probes. Biotinylated EpCAM capture probe or control line probes were dispensed 3mm apart on the nitrocellulose membrane as the test and control lines respectively. Post-dispensing, the nitrocellulose membrane was dried at 37°C for 1hr and stored at 4°C until used. The final section of the LFSB, the absorption pad, was composed of a 17 mm × 300 mm cellulose fiber pad. The absorption pad wicked the assay fluids to create capillary pull during test performance. All three components were finally assembled on a sticky backing layer card (60 mm × 300 mm). The components overlapped by at least 2mm to ensure continuous fluid flow by capillary action. The assembled unit was then cut into strips 3mm in width using the Guillotine cutting module CM 4000. The cut LBSBs were kept at 4°C until used.

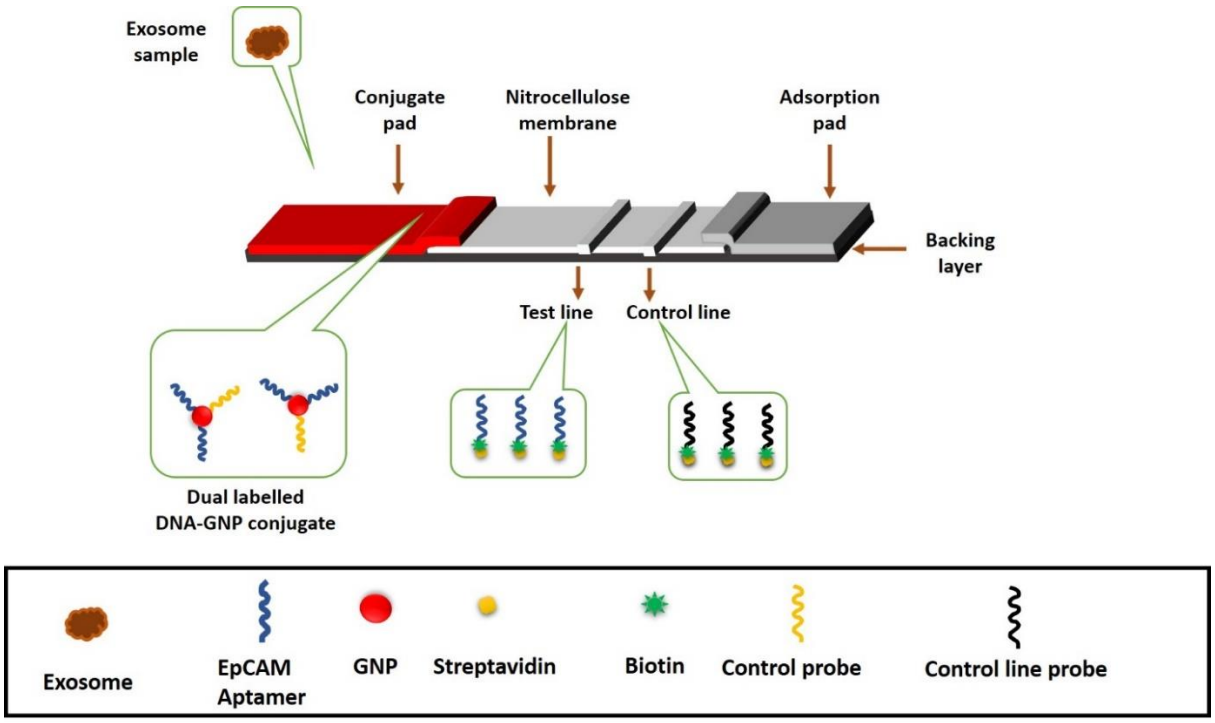

Figure 7.1. Scheme of developed GNP-based lateral flow strip aptasensor for exosome detection.

7.2.8. Preparation of Antibody-Based LFSB for Exosome Detection

The setup of the antibody-based LFSB was similar to that of the GNP-based LFSA, however, for the immunosensor, the test and control line DNA sequences were replaced with antibodies. Anti-EpCAM antibody (catalogue number: ABIN1684521) and goat-anti mouse IgG at concentrations of 1 mg mL^{-1} were dispensed 3 mm apart on nitrocellulose membrane as test and control lines respectively. The nitrocellulose membrane was dried at 37°C for 1hour. Glass fiber conjugate pad, the nitrocellulose membrane and absorption pads were assembled on a sticky plastic card and cut into 3mm wide strips. The prepared immunosensors were stored at 4°C until used.

7.2.9. Isolation of Exosomes from Human Plasma

Plasma samples were provided by Dr. Brand from the University of Pittsburg. Exosomes were purified by ultracentrifugation in Dr. Thomas Schmittgen's laboratory at the University of Florida using a modified protocol as reported by Ostenfeld.[191] Plasma samples were thawed on ice

and diluted 1:10 with cold DPBS (pH 7.4). The samples were then subjected to centrifugation at 2,000 x g for 15 min to remove cellular debris, and at 16,000 x g for 120 min to remove large membrane vesicles and apoptotic bodies. The supernatant was passed through a 0.22 µm filter, transferred into an ultracentrifuge tube and subjected to ultracentrifugation at 100,000 x g for 2 hours to pellet the exosomes. The exosomes were resuspended in 75 µL of DPBS and quantified by nanoparticle tracking analysis. Purified exosomes were frozen at -80°C until they were shipped on dry ice to North Dakota State University. Upon receipt, exosomes were stored at -80°C until used.

7.2.10. Assay Procedure

Exosomes solutions were prepared in running buffer (20mM Tris HCl + 20mM $MgCl_2$ + 1%BSA). One hundred microliters (100µL) of the exosome solution was applied to the conjugate pad that had pre-dispensed GNP conjugates. The sample could migrate through the LFSB in 20 mins. An additional 100 µL of running buffer was added to wash the strip. Washing the strip removed any nonspecifically adsorbed conjugates which reduced background signals. After 10 mins, distinct red colored test and control line bands were observed with the naked eye on the nitrocellulose membrane. For quantitative data, the test line intensities were read with the portable strip reader.

7.3. Results and Discussion

7.3.1. Working Principle of the Developed LFSA for Exosomes Detection

The GNP-based LFSA followed a classic sandwich assay format as depicted in **Figure 7.2**. EpCAM aptamer which served as the test line capture probe was pre-dispensed on the nitrocellulose membrane. The nitrocellulose membrane also supported the control line DNA probe which also pre-immobilized prior to running the assay. Onto the conjugate pad, GNP-aptamer

conjugate was dropped and air dried for 5 mins before assay was performed. Exosome samples prepared in running buffer was applied to the conjugate pad. The exosomes then interacted with the detection probe of the conjugate to form a GNP-aptamer-exosome complex. The complex moved along the LFSA onto the nitrocellulose membrane by capillary action. Upon reaching the test line the exosome component of the GNP-aptamer-exosome complex interacted with the test line EpCAM aptamer probe and was thus captured on the test line. The accumulation of GNPs on the test line gave a characteristic red band which was visible to the naked eye (**Figure 7.2. a**). Excess uncaptured GNP-aptamer conjugate moved on to the control zone where it was captured by the hybridization between the control probe on the conjugate and the control line capture probe. This resulted in a second red colored band which served as validation of assay performance. In the absence of target exosomes, no band was observed in the test zone, however the red band on the control line was observed and served as validation that assay was working properly (**Figure 7.2. b**). The amount of GNP captured on the test line was directly proportional to the concentration of exosomes in the test sample. The intensity of the test and control line bands were read with a portable strip reader for quantitative data. The strip reader took images of the strips and converted the pixel intensity of the bands into peaks. The peak areas were proportional to the number of GNPs captured on the test and control lines, and hence the amount of exosomes in the test sample.

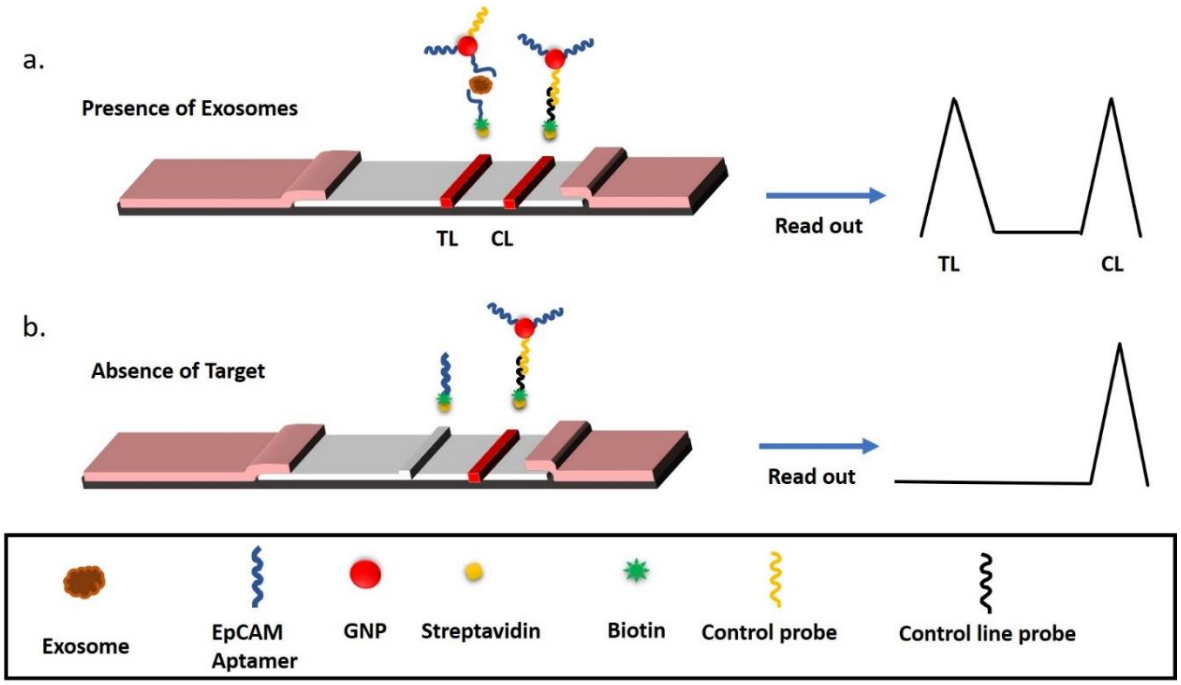

Figure 7.2. Working principle of the developed GNP-based LFSA (a) Capture of exosomes between test line and conjugate EpCAM aptamer and the capture of excess conjugate on the control line (b) Assay in the absence of exosomes.

To confirm the increased sensitivity of the GNP-based LFSA over the antibody based LFSB, the two setups were tested in the presence and absence of exosomes. **Figure 7.3** shows photo images of the strips after assay were ran. It is observed, that the GNP-based LFSA showed an intense test line band in the presence of 0.75×10^{6} exosomes μL^{-1} compared to the immunoassay which showed a very weak response in the presence of a much higher concentration of exosomes (2.0×10^{-7} exosomes μL^{-1}). The low dissociation constants (22.8±6.0 nM) [189] of the reported EpCAM aptamer resulted in more efficient binding to target exosomes which increased the sensitivity of the aptasensor.

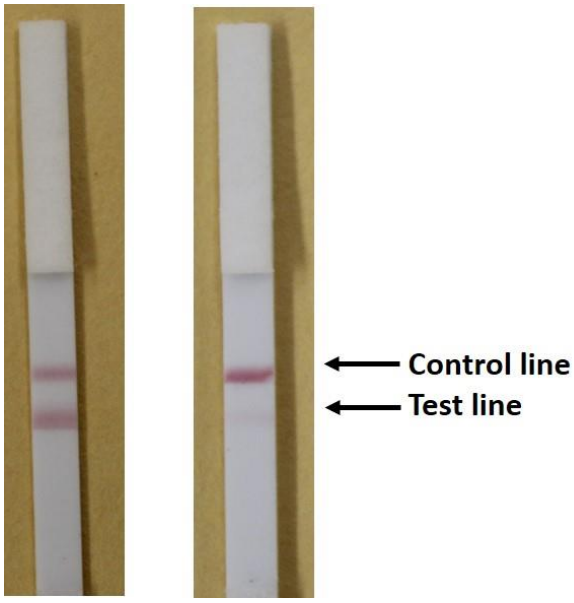

Figure 7.3. Photo images of the developed aptamer LFS (left) and the lateral flow immunosensor (right) with exosome concentrations 0.75 x 10^6 exosomes/µL and 20 x10^6 exosomes/µL respectively.

7.3.2. Optimization of Assay Parameters

To attain the optimal sensitivity of the developed assay various experimental parameters like the membrane flow rate, test line dispense cycles, buffer composition, quantity of aptamers coated on the GNP and the volume of conjugates per test were optimized. The overall sensitivity of the developed assay relied on an interplay of these parameters.

Firstly, the type of nitrocellulose membrane used had to be optimized. Three nitrocellulose membranes HF090MC100, HF135MC100 and HF180MC100 with capillary flow rate of 90 sec, 180 sec and 3 min per 4cm of membrane as reported by the manufacturer were assessed for their performance on the LFSA (**Figure 7.4 a**). The flow rate of analyte and conjugates on the LFSA dictated the time frame allowed for the target and aptamers to interact. As shown in **Figure 7.4. a**, the 90-sec membrane showed the lowest signal to noise (S/N) ratio. This was the membrane with the fastest flow rate, and hence, the least amount of time for aptamer-target interactions. This led to lowered test line intensities. In the case of the 3-min membrane, the slow flow rate resulted in a

longer time frame for the interaction between the target exosomes and aptamers on the test line and conjugates. This resulted in increased background signals, thus reducing the S/N ratio. As observed in **Figure 7.4. a**, the 135sec membrane showed the best S/N ratio and was thus chosen for further development of the aptasensor.

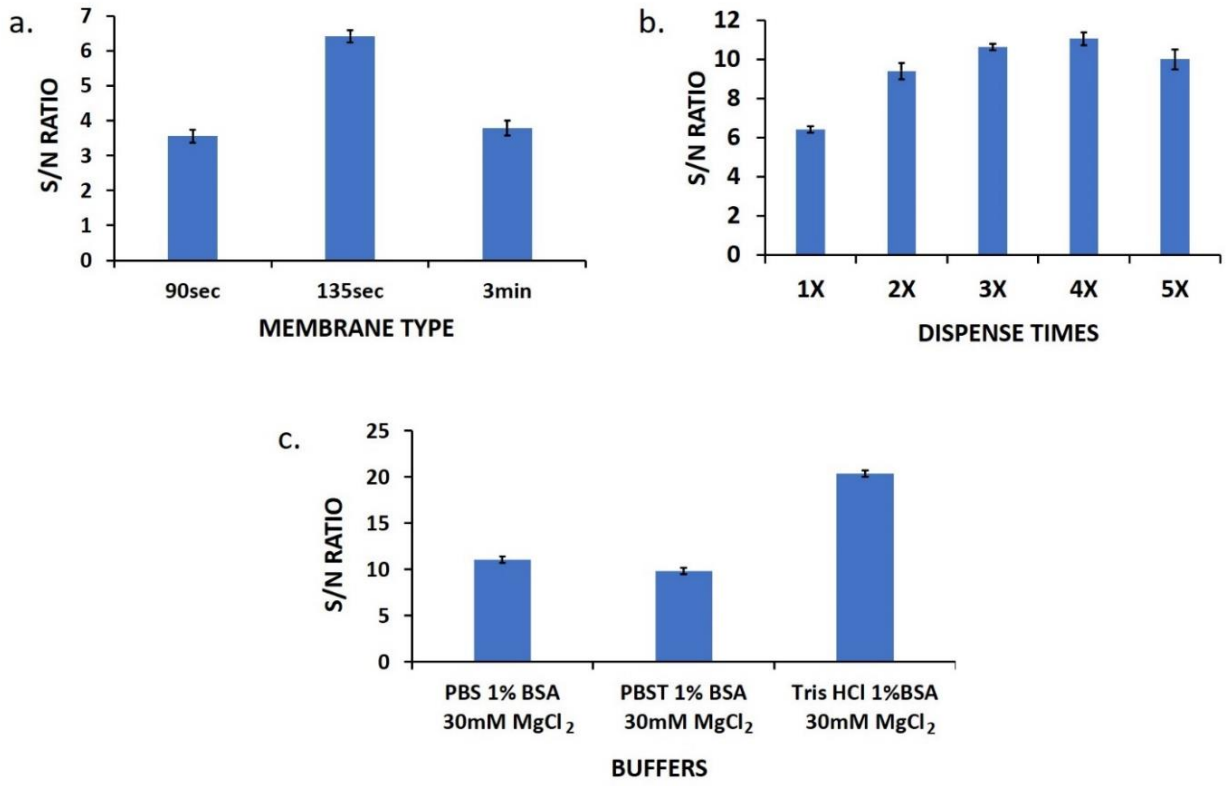

Figure 7.4. Optimization of assay parameters (a) Effect of membrane type on the S/N ratio of the assay (b) Effect of dispense times of the test line aptamer on the performance of the assay (c) Effect of running buffer composition on the S/N ratio of the assay.

The next line of optimizations was the dispense times of the test line. The amount of aptamers immobilized on the test line had a significant effect on the performance of the LFSA. A streptavidin-biotinylated aptamer complex in solution was dispensed a varying number of times (1, 2 ,3 4, 5) and their S/N ratios for exosome detection compared (**Figure 7.4. b**). At low dispense cycles (1,2 and 3) it is observed that the S/N ratios were lowered. This was attributed to the test line not having enough aptamer probes to efficiently capture the target exosomes. Beyond 4 times

dispense of the test line, there was lowering of the S/N ratio. Overcrowding of aptamers on the test line led to steric hinderance that limited access of targets to aptamer binding sites. Four times dispense of the test line had the optimal concentration of aptamers on the test line and resulted in the highest S/N ratio.

The aptamers and the targets interacted in buffers, and the composition of these buffers could either enhance or reduce the magnitude of these interactions. PBS (1% BSA, 30mM $MgCl_2$), PBST (1% BSA, 30mM $MgCl_2$) and 20mM Tris-HCl (1% BSA, 30mM $MgCl_2$) were tested as running buffer and their S/N ration were compared (**Figure 7.4. c**). The added $MgCl_2$ shielded the negative charge of the DNA oligomer backbones and thus stabilized binding to target exosomes and control line probes. The Tris-HCl (1% BSA, 30mM $MgCl_2$) gave the best S/N ratio and was thus used for all subsequent test runs.

The amount of detection probe on the GNP-aptamer conjugate was also optimized. The aptamers on the GNP were the first to interact with the sample exosomes. This reaction had to be efficient to ensure effectual exosome dependent localization of the GNP conjugates on the test line as test progressed. To a fixed volume of GNP, varied amounts (0.1, 0.2, 0.3, 0.4, 0.5 optical densities (OD)) of thiolated EpCAM detection probe were conjugated. The resultant GNP-aptamer conjugates were tested for their performance on the developed aptasensor (**Figure 7.5. a**). At 0.1 OD it was rationalized that insufficient detection probe immobilization on the GNP surface led to the lowered S/N ratio recorded. The highest S/N ratio was observed when0.2 OD detection probe was used for conjugate preparation. Beyond 0.2OD the S/N ratio declined. The decline in S/N ratio may have been because of overcrowding of aptamers on the GNP surface which hindered the access of exosomes to the detection probe. 0.2 OD detection probe was subsequently used for further conjugate preparation and testing.

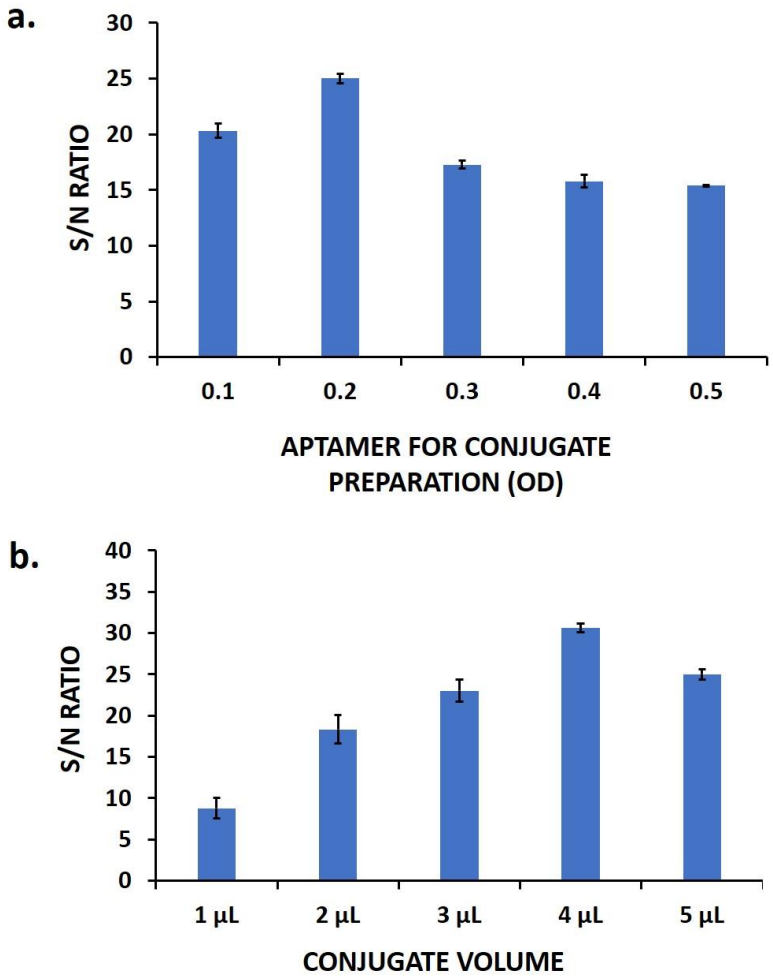

Figure 7.5. (a) Effect of the amount of EpCAM aptamer used for conjugate preparation on the performance of the GNP-based LFSA (b) Effect of conjugate volume on the S/N ratio of the assay.

The final optimization performed was the volume of GNP-aptamer conjugates dispensed on the conjugate pad prior to running the assay. **Figure 7.5. b** shows a series of volumes (1, 2, 3 ,4, 5 and 6 µL) of GNP-aptamer conjugates were tested and their S/N ratios compared. At low volumes (1, 2 and 3 µL) the amount of GNP-aptamer conjugates present was low, and this resulted in lowered test line intensities and thus the observed lower S/N ratios. Beyond 4 µL, there was a decline in the S/N ratio due to increased background signals resultant of increased nonspecific adsorption. The highest S/N ratio was observed when 4 µL GNP-aptamer conjugate was used per test-run. 4 µL conjugate volume was used for further development of the assay.

7.3.3. Analytical Performance

Under optimized conditions [nitrocellulose membrane (135sec membrane), dispense cycles of test line (4 times), running buffer (Tris-HCl + 1% BSA + 30mM $MgCl_2$), detection probe for conjugate preparation (0.2 OD) and conjugate volume (4µL)], the developed GNP-based LFSA was used to analyze exosome solutions ranging from 0.0 to 1.0 x 10^6 exosomes μL^{-1} of running buffer. All tests were run in triplicate with test line intensities read and averaged for each concentration. **Figure 7.6. a** shows typical images for the detection assay and as expected the test line intensities increased with increasing concentration of exosomes. The blank sample had no observable test line band. It was thus concluded that the optimization process did not result in any significant non-specific adsorption.

The test line intensities were read with a portable strip reader and their intensities had a good linear relationship ($R^2 = 0.9921$) with the exosome concentration (**Figure 7.6. b**). The GNP-based LFSA had a wide dynamic range of 5.0 x10^4 to 1.0 x 10^6 exosomes μL^{-1} of solution. The calibration equation was $y = 776.62x + 36.59$, where y and x represent the test line intensities and concentrations of exosomes respectively.

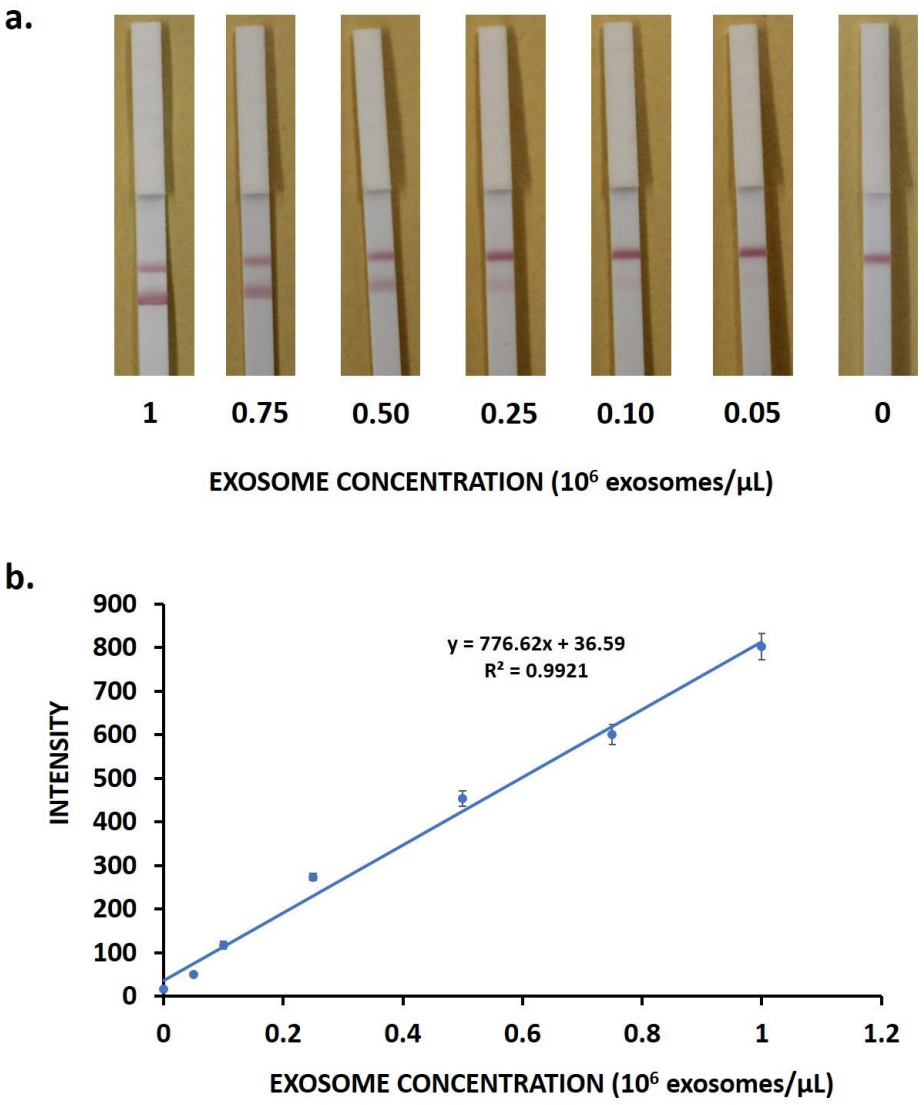

Figure 7.6. (a) Typical images of GNP-based LFSA in the presence of varying concentration of exosomes (b) Calibration curve for developed aptasensor.

The detection limit of the assay was 1.3 x 10^{-4} exosomes μL^{-1} (S/N ratio =3). The developed assay showed over 60-fold lower detection limit than previous report using antibodies to detect exosomes on a LFSB. [72] Aside the low detection limit achieved, the GNP-based LFSA showed very good reproducibility. The reproducibility of the assay was evaluated by running the assay in the absence and the presence of 1.0 x10^5 and 5x 10^5 exosome μL^{-1}. For each concentration, six replicate tests were performed. The test line intensities were measured with the portable reader and

their intensities averaged. The relative standard deviation at 0, 1.0 x10^5 and 5x 10^5 exosomes μL^{-1} were calculated to be 5.3%, 6.6% and 7.2% respectively (data not shown).

7.4. Conclusion

In this work, a quantitative GNP-based lateral flow strip aptasensor was successfully developed for the rapid and sensitive detection of exosomes. The aptasensor achieved a detection limit of 1.3 x 10^4 exosome μL^{-1}which was about 60-fold lower than previous reports of exosomes on an antibody- based LFSB.[72] The assay had a linear dynamic range from 5.0 x 10^4 to 1.0 x 10^6 exosomes µL. The developed GNP-based LFSA offers an inexpensive, quick and sensitive method for the detection of exosomes by utilizing their EpCAM expression profiles. Upon further development and validation, the developed assay may find clinical application in cancer screening and monitoring.

8. SUMMARY AND CONCLUSIONS

In clinical practice, cancer diagnosis has been done using complex and expensive instrumental methods such as computer tomography scans, angiography and magnetic resonance imaging. Other methods like laparoscopy and needle biopsies have also been used to diagnose cancer. These methods are not ideal for routine disease diagnosis and disease monitoring. This dissertation aimed to develop lateral flow strip biosensors for the detection of cancer biomarkers in human plasma to help in the routine screening of cancer. The LFSB platform was chosen because they are inexpensive and hence do not require expensive equipment and skilled labor for operation. The developed LFSBs have the added advantages of being rapid, sensitive and required small volumes of sample. GNP- based LFSB was each developed for the screening of CA 19-9, CEA and exosomes in clinical samples. Further, based on previous work that showed improvement in sensitivity of DNA detection when MWCNT replaced traditional GNPs as transducers on the LFSB, MWCNT-based LFSBs were developed for the detection of CA 19-9 and CEA.

The following lateral flow biosensors are reported in this dissertation:

- GNPs were used as labels for the detection of CA 19-9. The GNPs efficiently loaded anti-CA 19-9 antibodies to enable the sensitive detection of CA 19-9. After systematic optimizations a visual detection limit of 5 U mL^{-1} was achieved which was below the reference value of 37 U mL^{-1}. The developed GNP-based LFSB was successfully applied for the screening of CA-19-9 in human plasma. The assay showed good performance with results confirmed by commercial ELISA.
- A GNP-based LFSB was developed for the detection of CEA in pancreatic cyst fluid. The assay showed good sensitivity with a detection limit of 2 ng mL^{-1} (S/N=3). This detection limit was much lower than the CEA reference value of 192

ng mL^{-1} in pancreatic cyst fluid. The developed biosensor was successfully used to distinguished mucinous from non-mucinous pancreatic cyst fluid.

- As proof of concept, a quantitative MWCNT-based LFSB was developed for the detection of proteins in human plasma. Rabbit IgG was used as a model target. Goat anti-Rabbit IgG was covalently loaded onto MWCNT and used to detect rabbit IgG. The enhanced loading of antibodies along with the intense black color of the MWCNTs enabled the attainment of an ultra-low detection limit of 1.32 pg mL^{-1} rabbit IgG. This was an over 1500-fold improvement over the GNP-based LFSB. The assay was successfully applied for the detection of Rabbit IgG spiked into human plasma. Based on the good performance of the MWCNT-based LFSB for protein detection, MWCNT based LFSBs were developed for the detection of CEA and CA 19-9. These biosensors also showed improvement over the GNP-based LFSBs. The MWCNT-based LFSB for the detection of CA 19-9 showed a detection limit of 0.14 U mL^{-1} which was about 35-fold lower than that of the GNP-based system. The MWCNT-based LFSB for CEA detection, showed a detection limit of 0.1ng mL^{-1} which was a 20-fold improvement over the corresponding GNP-based assay for CEA detection.
- Exosomes were detected by aptamers previously developed for EpCAM, a cell surface protein that has been reported to be elevated in pancreatic cancer patients. The EpCAM aptamer was successfully coated onto the surface of GNPs and applied for the detection of exosomes isolated from human plasma. The developed GNP-based lateral flow aptasensor had a detection limit of 1.3×10^4 exosome μL^{-1}which

was about 60-fold lower than previous report of exosome detection on lateral flow strip immunosensor.[72]

The developed sensors show good sensitivity, however future work must be performed to further validate the assays using larger sample sizes. Also, to increase future prospects for the commercialization of the developed assays, batch-to-batch variability of the LFSBs has to be examined. In the future, the developed MWCNT-based LFSBs for the detection of CA 19-9 and CEA will have to be assessed for their performance at screening clinical samples. Overall, the work presented in this dissertation successfully developed lateral flow strip biosensors for the rapid, inexpensive and sensitive detection of cancer biomarkers. The assays show great promise for application in routine cancer screening, particularly in limited resource settings.

REFERENCES

(1) Strimbu, K.; Tavel, J. A. What Are Biomarkers? *Curr. Opin. HIV AIDS* **2010**, *5* (6), 463–466. https://doi.org/10.1097/COH.0b013e32833ed177.

(2) Ludwig, J. A.; Weinstein, J. N. Biomarkers in Cancer Staging, Prognosis and Treatment Selection. *Nat. Rev. Cancer* **2005**, *5* (11), 845–856. https://doi.org/10.1038/nrc1739.

(3) Xi, X.; Li, T.; Huang, Y.; Sun, J.; Zhu, Y.; Yang, Y.; Lu, Z. RNA Biomarkers: Frontier of Precision Medicine for Cancer. *Non-Coding RNA* **2017**, *3* (1), 9. https://doi.org/10.3390/ncrna3010009.

(4) Ludwig, J. A.; Weinstein, J. N.; Rifai, N.; Gillette, M. A.; Carr, S. A. Protein Biomarker Discovery and Validation: The Long and Uncertain Path to Clinical Utility. *Nat. Biotechnol.* **2006**, *24* (11), 971. https://doi.org/10.1038/nrc1739.

(5) Henry, N. L.; Hayes, D. F. Cancer Biomarkers. *Mol. Oncol.* **2012**, *6* (2), 140–146. https://doi.org/10.1016/J.MOLONC.2012.01.010.

(6) Lowry, O. H.; Rosebrough, N. J.; Farr, A. L.; Randall, R. J. Protein Measurement with the Folin Phenol Reagent. *J. Biol. Chem.* **1951**, *193*, 265–275.

(7) Baryeh, K.; Takalkar, S.; Lund, M.; Liu, G. Introduction to Medical Biosensors for Point of Care Applications. In *Medical Biosensors for Point of Care (POC) Applications*; Woodhead Publishing, 2016; pp 3–25. https://doi.org/10.1016/B978-0-08-100072-4.00001-0.

(8) Gubala, V.; Harris, L. F.; Ricco, A. J.; Tan, M. X.; Williams, D. E. Point of Care Diagnostics: Status and Future. *Anal. Chem.* **2012**, *84* (2), 487–515. https://doi.org/10.1021/ac2030199.

(9) Gervais, L.; de Rooij, N.; Delamarche, E. Microfluidic Chips for Point-of-Care Immunodiagnostics. *Adv. Mater.* **2011**, *23* (24), H151–H176. https://doi.org/10.1002/adma.201100464.

(10) Patel, S.; Nanda, R.; Sahoo, S.; Mohapatra, E. Biosensors in Health Care: The Milestones Achieved in Their Development towards Lab-on-Chip-Analysis. *Biochem. Res. Int.* **2016**, *2016*, 1–12. https://doi.org/10.1155/2016/3130469.

(11) Sajid, M.; Kawde, A.-N.; Daud, M. Designs, Formats and Applications of Lateral Flow Assay: A Literature Review. *J. Saudi Chem. Soc.* **2015**, *19* (6), 689–705. https://doi.org/10.1016/J.JSCS.2014.09.001.

(12) Tuerk, C.; Gold, L. Systematic Evolution of Ligands by Exponential Enrichment: Chemi-SELEX. *Science (80-.).* **1990**, *249*, 505–510. https://doi.org/10.1038/346818a0.

(13) Ellington, A. D.; Szostak, J. W. In Vitro Selection of RNA Molecules That Bind Specific Ligands. *Nature* **1990**, *346*, 818–822. https://doi.org/10.1016/0021-9797(80)90501-9.

(14) Ahmad Raston, N. H.; Nguyen, V.-T.; Gu, M. B. A New Lateral Flow Strip Assay (LFSA) Using a Pair of Aptamers for the Detection of Vaspin. *Biosens. Bioelectron.* **2017**, *93*, 21–25. https://doi.org/10.1016/J.BIOS.2016.11.061.

(15) Mao, X.; Phillips, J. A.; Xu, H.; Tan, W.; Zeng, L.; Liu, G. Aptamer-Nanoparticle Strip Biosensor for Rapid and Sensitive Detection of Cancer Cells. *Anal. Chem.* **2009**, *81* (24), 10013–10018. https://doi.org/10.1021/ac901889s.

(16) Bruno, J. Application of DNA Aptamers and Quantum Dots to Lateral Flow Test Strips for Detection of Foodborne Pathogens with Improved Sensitivity versus Colloidal Gold. *Pathogens* **2014**, *3* (2), 341–355. https://doi.org/10.3390/pathogens3020341.

(17) Kaiser, L.; Weisser, J.; Kohl, M.; Deigner, H.-P. Small Molecule Detection with Aptamer Based Lateral Flow Assays: Applying Aptamer-C-Reactive Protein Cross-Recognition for Ampicillin Detection. *Sci. Rep.* **2018**, *8* (1), 5628. https://doi.org/10.1038/s41598-018-23963-6.

(18) Kawde, A.; Mao, X.; Xu, H.; Zeng, Q.; He, Y.; Liu, G. Moving Enzyme-Linked Immuno-Sorbent Assay to the Point-of-Care Dry- Reagent Strip Biosensors. *Am. J. Biomed. Sci.* **2010**, *2* (1), 23–32. https://doi.org/10.5099/aj100100023.

(19) Mao, X.; Ma, Y.; Zhang, A.; Zhang, L.; Zeng, L.; Liu, G. Disposable Nucleic Acid Biosensors Based on Gold Nanoparticle Probes and Lateral Flow Strip. *Anal. Chem.* **2009**, *81* (4), 1660–1668. https://doi.org/10.1021/ac8024653.

(20) Kalogianni, D. P.; Bravou, V.; Christopoulos, T. K.; Ioannou, P. C.; Zoumbos, N. C. Dry-Reagent Disposable Dipstick Test for Visual Screening of Seven Leukemia-Related Chromosomal Translocations. *Nucleic Acids Res.* **2007**, *35* (4), e23–e23.

(21) López-Marzo, A. M.; Pons, J.; Blake, D. A.; Merkoçi, A. High Sensitive Gold-Nanoparticle Based Lateral Flow Immunodevice for Cd2+ Detection in Drinking Waters. *Biosens. Bioelectron.* **2013**, *47*, 190–198. https://doi.org/10.1016/j.bios.2013.02.031.

(22) Guo, Y. R.; Liu, S. Y.; Gui, W. J.; Zhu, G. N. Gold Immunochromatographic Assay for Simultaneous Detection of Carbofuran and Triazophos in Water Samples. *Anal. Biochem.* **2009**, *389* (1), 32–39. https://doi.org/10.1016/j.ab.2009.03.020.

(23) Takalkar, S.; Baryeh, K.; Liu, G. Fluorescent Carbon Nanoparticle-Based Lateral Flow Biosensor for Ultrasensitive Detection of DNA. *Biosens. Bioelectron.* **2017**, *98* (June), 147–154. https://doi.org/10.1016/j.bios.2017.06.045.

(24) Xu, H.; Chen, J.; Birrenkott, J.; Zhao, J. X.; Takalkar, S.; Baryeh, K.; Liu, G. Gold-Nanoparticle-Decorated Silica Nanorods for Sensitive Visual Detection of Proteins. *Anal. Chem.* **2014**, *86* (15), 7351–7359. https://doi.org/10.1021/ac502249f.

(25) Qiu, W.; Xu, H.; Takalkar, S.; Gurung, A. S.; Liu, B.; Zheng, Y.; Guo, Z.; Baloda, M.; Baryeh, K.; Liu, G. Carbon Nanotube-Based Lateral Flow Biosensor for Sensitive and Rapid Detection of DNA Sequence. *Biosens. Bioelectron.* **2015**, *64*, 367–372. https://doi.org/10.1016/j.bios.2014.09.028.

(26) Huang, Y.; Wen, Y.; Baryeh, K.; Takalkar, S.; Lund, M.; Zhang, X.; Liu, G. Magnetized Carbon Nanotubes for Visual Detection of Proteins Directly in Whole Blood. *Anal. Chim. Acta* **2017**, *993*, 79–86. https://doi.org/10.1016/j.aca.2017.09.025.

(27) Huang, Y.; Wen, Y.; Baryeh, K.; Takalkar, S.; Lund, M.; Zhang, X.; Liu, G. Lateral Flow Assay for Carbohydrate Antigen 19-9 in Whole Blood by Using Magnetized Carbon Nanotubes. *Mikrochim. Acta* **2017**, *184* (11), 4287–4294. https://doi.org/10.1007/s00604-017-2464-0.

(28) Edwards, K. A.; Baeumner, A. J. Optimization of DNA-Tagged Dye-Encapsulating Liposomes for Lateral-Flow Assays Based on Sandwich Hybridization. *Anal. Bioanal. Chem.* **2006**, *386* (5), 1335–1343. https://doi.org/10.1007/s00216-006-0705-x.

(29) Baeumner, A. J.; Jones, C.; Wong, C. Y.; Price, A. A Generic Sandwich-Type Biosensor with Nanomolar Detection Limits. *Anal. Bioanal. Chem.* **2004**, *378* (6), 1587–1593.

(30) Ho, J. A. A.; Wauchope, R. D. A Strip Liposome Immunoassay for Aflatoxin B1. *Anal. Chem.* **2002**, *74* (7), 1493–1496. https://doi.org/10.1021/ac010903q.

(31) Lönnberg, M.; Drevin, M.; Carlsson, J. Ultra-Sensitive Immunochromatographic Assay for Quantitative Determination of Erythropoietin. *J. Immunol. Methods* **2008**, *339* (2), 236–244. https://doi.org/10.1016/j.jim.2008.09.022.

(32) Bahadır, E. B.; Sezgintürk, M. K. Lateral Flow Assays: Principles, Designs and Labels. *TrAC - Trends Anal. Chem.* **2016**, *82*, 286–306. https://doi.org/10.1016/j.trac.2016.06.006.

(33) Chan, C. P. Y.; Sum, K. W.; Cheung, K. Y.; Glatz, J. F. C.; Sanderson, J. E.; Hempel, A.; Lehmann, M.; Renneberg, I.; Renneberg, R. Development of a Quantitative Lateral-Flow Assay for Rapid Detection of Fatty Acid-Binding Protein. *J. Immunol. Methods* **2003**, *279* (1), 91–100. https://doi.org/https://doi.org/10.1016/S0022-1759(03)00243-6.

(34) Heeschen, C.; Goldmann, B. U.; Moeller, R. H.; Hamm, C. W. *Analytical Performance and Clinical Application of a New Rapid Bedside Assay for the Detection of Serum Cardiac Troponin I.*

(35) Müller-Bardorff, M.; Rauscher, T.; Kampmann, M.; Schoolmann, S.; Laufenberg, F.; Mangold, D.; Zerback, R.; Remppis, A.; Katus, H. A. Quantitative Bedside Assay for Cardiac Troponin T: A Complementary Method to Centralized Laboratory Testing. *Clin. Chem.* **1999**, *45* (7), 1002 LP-1008.

(36) Barbosa, A. I.; Gehlot, P.; Sidapra, K.; Edwards, A. D.; Reis, N. M. Portable Smartphone Quantitation of Prostate Specific Antigen (PSA) in a Fluoropolymer Microfluidic Device. *Biosens. Bioelectron.* **2015**, *70*, 5–14. https://doi.org/https://doi.org/10.1016/j.bios.2015.03.006.

(37) Lu, W.; Wang, K.; Xiao, K.; Qin, W.; Hou, Y.; Xu, H.; Yan, X.; Chen, Y.; Cui, D.; He, J. Dual Immunomagnetic Nanobeads-Based Lateral Flow Test Strip for Simultaneous Quantitative Detection of Carcinoembryonic Antigen and Neuron Specific Enolase. *Sci. Rep.* **2017**, *7*, 42414.

(38) Choi, S.; Choi, E. Y.; Kim, D. J.; Kim, J. H.; Kim, T. S.; Oh, S. W. A Rapid, Simple Measurement of Human Albumin in Whole Blood Using a Fluorescence Immunoassay (I). *Clin. Chim. Acta* **2004**, *339* (1–2), 147–156. https://doi.org/10.1016/J.CCCN.2003.10.002.

(39) Ahn, J. S.; Choi, S.; Jang, S. H.; Chang, H. J.; Kim, J. H.; Nahm, K. B.; Oh, S. W.; Choi, E. Y. Development of a Point-of-Care Assay System for High-Sensitivity C-Reactive Protein in Whole Blood. *Clin. Chim. Acta.* **2003**, *332* (1–2), 51–59. https://doi.org/10.1016/S0009-8981(03)00113-X.

(40) Gupta, R. K.; Periyakaruppan, A.; Meyyappan, M.; Koehne, J. E. Label-Free Detection of C-Reactive Protein Using a Carbon Nanofiber Based Biosensor. *Biosens. Bioelectron.* **2014**, *59*, 112–119. https://doi.org/10.1016/j.bios.2014.03.027.

(41) Lou, S. C.; Patel, C.; Ching, S.; Gordon, J. One-Step Competitive Immunochromatographic Assay for Semiquantitative Determination of Lipoprotein(a) in Plasma. *Clin. Chem.* **1993**, *39* (4).

(42) Schubert-Ullrich, P.; Rudolf, J.; Ansari, P.; Galler, B.; Führer, M.; Molinelli, A.; Baumgartner, S. Commercialized Rapid Immunoanalytical Tests for Determination of Allergenic Food Proteins: An Overview. *Anal. Bioanal. Chem.* **2009**, *395* (1), 69–81. https://doi.org/10.1007/s00216-009-2715-y.

(43) Piepenburg, O.; Williams, C. H.; Stemple, D. L.; Armes, N. A. DNA Detection Using Recombination Proteins. *PLoS Biol.* **2006**, *4* (7), 1115–1121. https://doi.org/10.1371/journal.pbio.0040204.

(44) Baeumner, A. J.; Pretz, J.; Fang, S. A Universal Nucleic Acid Sequence Biosensor with Nanomolar Detection Limits. **2004**. https://doi.org/10.1021/ac034945l.

(45) Takalkar, S.; Xu, H.; Chen, J.; Baryeh, K.; Qiu, W.; Zhao, J. X.; Liu, G. Gold Nanoparticle Coated Silica Nanorods for Sensitive Visual Detection of MicroRNA on a Lateral Flow Strip Biosensor. *Anal. Sci.* **2016**, *32* (6), 617–622. https://doi.org/10.2116/analsci.32.617.

(46) Wang, C.; Zhang, L.; Shen, X. Development of a Nucleic Acid Lateral Flow Strip for Detection of Hepatitis C Virus (HCV) Core Antigen. *Nucleosides, Nucleotides and Nucleic Acids* **2013**, *32* (2), 59–68. https://doi.org/10.1080/15257770.2013.763976.

(47) Jauset-Rubio, M.; Svobodová, M.; Mairal, T.; McNeil, C.; Keegan, N.; Saeed, A.; Abbas, M. N.; El-Shahawi, M. S.; Bashammakh, A. S.; Alyoubi, A. O.; et al. Ultrasensitive, Rapid and Inexpensive Detection of DNA Using Paper Based Lateral Flow Assay. *Sci. Rep.* **2016**, *6* (November), 1–10. https://doi.org/10.1038/srep37732.

(48) Chen, M. H.; Kuo, S. T.; Renault, T.; Chang, P. H. The Development of a Loop-Mediated Isothermal Amplification Assay for Rapid and Sensitive Detection of Abalone Herpesvirus DNA. *J. Virol. Methods* **2014**, *196*, 199–203. https://doi.org/10.1016/j.jviromet.2013.11.011.

(49) Chowdry, V. K.; Luo, Y.; Widén, F.; Qiu, H. J.; Shan, H.; Belák, S.; Liu, L. Development of a Loop-Mediated Isothermal Amplification Assay Combined with a Lateral Flow Dipstick for Rapid and Simple Detection of Classical Swine Fever Virus in the Field. *J. Virol. Methods* **2014**, *197*, 14–18. https://doi.org/10.1016/j.jviromet.2013.11.013.

(50) Cordray, R.-K. S.; Malar, J. A Paper and Plastic Device for the Combined Isothermal Amplification and Lateral Flow Detection of Plasmodium DNA. *Malar. J.* **2015**, *14*, 472. https://doi.org/10.1186/s12936-015-0995-6.

(51) Zheng, W.; Yao, L.; Teng, J.; Yan, C.; Qin, P.; Liu, G.; Chen, W. Lateral Flow Test for Visual Detection of Multiple MicroRNAs. *Sensors Actuators B Chem.* **2018**, *264*, 320–326. https://doi.org/10.1016/J.SNB.2018.02.159.

(52) Wang, X.; Teng, D.; Guan, Q.; Tian, F.; Wang, J. Detection of Roundup Ready Soybean by Loop-Mediated Isothermal Amplification Combined with a Lateral-Flow Dipstick. *Food Control* **2013**, *29* (1), 213–220. https://doi.org/10.1016/j.foodcont.2012.06.007.

(53) Kolm, C.; Mach, R. L.; Krska, R.; Brunner, K. A Rapid DNA Lateral Flow Test for the Detection of Transgenic Maize by Isothermal Amplification of the 35S Promoter. *Anal. Methods* **2015**, *7* (1), 129–134. https://doi.org/10.1039/c4ay01997k.

(54) Litos, I. K.; Ioannou, P. C.; Christopoulos, T. K.; Traeger-Synodinos, J.; Kanavakis, E. Multianalyte, Dipstick-Type, Nanoparticle-Based DNA Biosensor for Visual Genotyping of Single-Nucleotide Polymorphisms. *Biosens. Bioelectron.* **2009**, *24* (10), 3135–3139. https://doi.org/10.1016/j.bios.2009.03.010.

(55) Sivasubramaniyan, K.; Harichandan, A.; Schilbach, K.; Mack, A. F.; Bedke, J.; Stenzl, A.; Kanz, L.; Niederfellner, G.; Bühring, H. J. Expression of Stage-Specific Embryonic Antigen-4 (SSEA-4) Defines Spontaneous Loss of Epithelial Phenotype in Human Solid Tumor Cells. *Glycobiology* **2015**, *25* (8), 902–917. https://doi.org/10.1093/glycob/cwv032.

(56) Wang, J.; Chen, W.; Hu, K.; Li, W. Development of a Gold-Immunochromatography Test for Rapid Detecting E. Coli O157. *J. Hyg. Res.* **2006**, *35* (4), 439—441.

(57) Seo, K. H.; Holt, P. S.; Stone, H. D.; Gast, R. K. Simple and Rapid Methods for Detecting Salmonella Enteritidis in Raw Eggs. *Int. J. Food Microbiol.* **2003**, *87* (1–2), 139–144. https://doi.org/10.1016/S0168-1605(03)00053-9.

(58) Yan, Z.; Zhou, L.; Zhao, Y.; Wang, J.; Huang, L.; Hu, K.; Liu, H.; Wang, H.; Guo, Z.; Song, Y.; et al. Rapid Quantitative Detection of Yersinia Pestis by Lateral-Flow Immunoassay and up-Converting Phosphor Technology-Based Biosensor. *Sensors Actuators, B Chem.* **2006**, *119* (2), 656–663. https://doi.org/10.1016/j.snb.2006.01.029.

(59) Li, C. Z.; Vandenberg, K.; Prabhulkar, S.; Zhu, X.; Schneper, L.; Methee, K.; Rosser, C. J.; Almeide, E. Paper Based Point-of-Care Testing Disc for Multiplex Whole Cell Bacteria Analysis. *Biosens. Bioelectron.* **2011**, *26* (11), 4342–4348. https://doi.org/10.1016/j.bios.2011.04.035.

(60) Mazumdar, D.; Liu, J.; Lu, G.; Zhou, J.; Lu, Y. Easy-to-Use Dipstick Tests for Detection of Lead in Paints Using Non-Cross-Linked Gold Nanoparticle-DNAzyme Conjugates. *Chem. Commun.* **2010**, *46* (9), 1416–1418. https://doi.org/10.1039/b917772h.

(61) Fang, Z.; Huang, J.; Lie, P.; Xiao, Z.; Ouyang, C.; Wu, Q.; Wu, Y.; Liu, G.; Zeng, L. Lateral Flow Nucleic Acid Biosensor for Cu2+detection in Aqueous Solution with High Sensitivity and Selectivity. *Chem. Commun.* **2010**, *46* (47), 9043–9045. https://doi.org/10.1039/c0cc02782k.

(62) He, Y.; Zhang, X.; Zeng, K.; Zhang, S.; Baloda, M.; Gurung, A. S.; Liu, G. Visual Detection of Hg 2+ in Aqueous Solution Using Gold Nanoparticles and Thymine-Rich Hairpin DNA Probes. *Biosens. Bioelectron.* **2011**, *26* (11), 4464–4470. https://doi.org/10.1016/j.bios.2011.05.003.

(63) Zhu, C.; Zhang, G.; Huang, Y.; Yang, S.; Ren, S.; Gao, Z.; Chen, A. Dual-Competitive Lateral Flow Aptasensor for Detection of Aflatoxin B1in Food and Feedstuffs. *J. Hazard. Mater.* **2018**, *344*, 249–257. https://doi.org/10.1016/j.jhazmat.2017.10.026.

(64) Santos, V. O.; Pelegrini, P. B.; Mulinari, F.; Lacerda, A. F.; Moura, R. S.; Cardoso, L. P. V.; Bührer-Sékula, S.; Miller, R. N. G.; Grossi-De-Sa, M. F. Development and Validation of a Novel Lateral Flow Immunoassay Device for Detection of Aflatoxins in Soy-Based Foods. *Anal. Methods* **2017**, *9* (18), 2715–2722. https://doi.org/10.1039/c7ay00601b.

(65) Anfossi, L.; Giovannoli, C.; Giraudi, G.; Biagioli, F.; Passini, C.; Baggiani, C. A Lateral Flow Immunoassay for the Rapid Detection of Ochratoxin a in Wine and Grape Must. *J. Agric. Food Chem.* **2012**, *60* (46), 11491–11497. https://doi.org/10.1021/jf3031666.

(66) Zhang, G. P.; Wang, X. N.; Yang, J. F.; Yang, Y. Y.; Xing, G. X.; Li, Q. M.; Zhao, D.; Chai, S. J.; Guo, J. Q. Development Ofan Immunochromatographic Lateral Flow Test Strip for Detection of β-Adrenergic Agonist Clenbuterol Residues. *J. Immunol. Methods* **2006**, *312*, 27–32. https://doi.org/10.1016/j.jim.2006.02.017.

(67) Tang, Y.; Xu, X.; Liu, X.; Huang, X.; Chen, Y.; Wang, W.; Xiang, J. Development of a Lateral Flow Immunoassay (LFA) Strip for the Rapid Detection of 1-Aminohydantoin in Meat Samples. *J. Food Sci.* **2011**, *76* (6), 138–143. https://doi.org/10.1111/j.1750-3841.2011.02217.x.

(68) Molinelli, A.; Grossalber, K.; Führer, M.; Baumgartner, S.; Sulyok, M.; Krska, R. Development of Qualitative and Semiquantitative Immunoassay-Based Rapid Strip Tests for the Detection of T-2 Toxin in Wheat and Oat. *J. Agric. Food Chem.* **2008**, *56* (8), 2589–2594. https://doi.org/10.1021/jf800393j.

(69) Zakir Hossain, S. M.; Luckham, R. E.; McFadden, M. J.; Brennan, J. D. Reagentless Bidirectional Lateral Flow Bioactive Paper Sensors for Detection of Pesticides in Beverage and Food Samples. *Proc. Natl. Acad. Sci. U.S.A* **2004**, *2* (1), 9055–9064. https://doi.org/10.1021/ac901714h.

(70) Zhang, C.; Zhang, Y.; Wang, S. Development of Multianalyte Flow-through and Lateral-Flow Assays Using Gold Particles and Horseradish Peroxidase as Tracers for the Rapid Determination of Carbaryl and Endosulfan in Agricultural Products. *J. Agric. Food Chem.* **2006**, *54* (7), 2502–2507. https://doi.org/10.1021/jf0531407.

(71) Wang, L.; Lu, D.; Wang, J.; Du, D.; Zou, Z.; Wang, H.; Smith, J. N.; Timchalk, C.; Liu, F.; Lin, Y. A Novel Immunochromatographic Electrochemical Biosensor for Highly Sensitive and Selective Detection of Trichloropyridinol, a Biomarker of Exposure to Chlorpyrifos. *Biosens. Bioelectron.* **2011**, *26* (6), 2835–2840. https://doi.org/10.1016/j.bios.2010.11.008.

(72) Oliveira-Rodríguez, M.; Ló Pez-Cobo, S.; Reyburn, H. T.; Costa-García, A.; Ló Pez-Martín, S.; Yá N ˜ Ez-Mó, M.; Cernuda-Morolló, E.; Paschen, A.; Valé S-Gó Mez, M.; Blanco-Ló Pez, M. C.; et al. Development of a Rapid Lateral Flow Immunoassay Test for Detection of Exosomes Previously Enriched from Cell Culture Medium and Body Fluids. *# Cit. J. Extracell. Vesicles* **2016**, No. 5, 31803. https://doi.org/10.3402/jev.v5.31803.

(73) Kondo, N.; Murakami, Y.; Uemura, K.; Hayashidani, Y.; Sudo, T.; Hashimoto, Y.; Nakashima, A.; Sakabe, R.; Shigemoto, N.; Kato, Y.; et al. Prognostic Impact of Perioperative Serum CA 19-9 Levels in Patients with Resectable Pancreatic Cancer. *Ann. Surg. Oncol.* **2010**, *17* (9), 2321–2329. https://doi.org/10.1245/s10434-010-1033-0.

(74) Koprowski, H.; Herlyn, M.; Steplewski, Z.; Sears, H. F. Specific Antigen in Serum of Patients with Colon Carcinoma. *Science* **1981**, *212* (4490), 53–55.

(75) Koprowski, H.; Steplewski, Z.; Mitchell, K.; Herlyn, M.; Herlyn, D.; Fuhrer, P. Colorectal Carcinoma Antigens Detected by Hybridoma Antibodies. *Somatic Cell Genet.* **1979**, *5* (6), 957–971.

(76) Magnani, J. L.; Nilsson, B.; Brockhaus, M.; Zopf, D.; Steplewski, Z.; Koprowski, H.; Ginsburg, V. A Monoclonal Antibody-Defined Antigen Associated with Gastrointestinal Cancer Is a Ganglioside Containing Sialylated Lacto-N-Fucopentaose II. *J. Biol. Chem.* **1982**, *257* (23), 14365–14369.

(77) Magnani, J. L.; Steplewski, Z.; Koprowski, H.; Ginsburg, V. *Identification of the Gastrointestinal and Pancreatic Cancer-Associated Antigen Detected by Monoclonal Antibody 19-9 in the Sera of Patients as a Mucin1*; 1983; Vol. 43.

(78) Kannagi, R.; Kitahara, A.; Itai, S.; Zenita, K.; Shigeta, K.; Tachikawa, T.; Nuda, A.; Hirano, H.; Abe, M.; Shin, S.; et al. *Quantitative and Qualitative Characterization of Human Cancer-Associated Serum Glycoprotein Antigens Expressing Epitopes Consisting of Sialyl or Sialyl-Fucosyl Type 1 Chain1*; 1988; Vol. 48.

(79) Chung, Y. S.; Ho, J. J.; Kim, Y. S.; Tanaka, H.; Nakata, B.; Hiura, A.; Motoyoshi, H.; Satake, K.; Umeyama, K. The Detection of Human Pancreatic Cancer-Associated Antigen in the Serum of Cancer Patients. *Cancer* **1987**, *60* (7), 1636–1643.

(80) Passerini, R.; Cassatella, M. C.; Boveri, S.; Salvatici, M.; Radice, D.; Zorzino, L.; Galli, C.; Sandri, M. T. The Pitfalls of CA19-9: Routine Testing and Comparison of Two Automated Immunoassays in a Reference Oncology Center. *Am. J. Clin. Pathol.* **2012**, *138* (2), 281–287. https://doi.org/10.1309/AJCPOPNPLLCYR07H.

(81) Duffy, M. J. CA 19-9 as a Marker for Gastrointestinal Cancers: A Review. *Ann. Clin. Biochem. An Int. J. Biochem. Lab. Med.* **1998**, *35* (3), 364–370. https://doi.org/10.1177/000456329803500304.

(82) Duffy, M. J.; Sturgeon, C.; Lamerz, R.; Haglund, C.; Holubec, V. L.; Klapdor, R.; Nicolini, A.; Topolcan, O.; Heinemann, V. Tumor Markers in Pancreatic Cancer: A European Group on Tumor Markers (EGTM) Status Report. *Ann. Oncol.* **2010**, *21* (3), 441–447. https://doi.org/10.1093/annonc/mdp332.

(83) *American Cancer Society. Cancer Facts & Figures 2017. American Cancer Society;* 2017.

(84) Del Villano, B. C.; Brennan, S.; Brock, P.; Bucher, C.; Llu, V.; Mcclure, M.; Rake, B.; Space, S.; Westrick, B.; Schoemaker, H.; et al. *Radloimmunometric Assay for a Monoclonal Antibody-Defined Tumor Marker, CA 19-9*; 1983; Vol. 29.

(85) Alubaidi, G. H.; Ali, Z. A.; Mahmood, A. R. *Detection of Carbohydrate Antigen CA19-9 Levels in Sera and Tissues' Homogenate of Breast and Thyroid Benign Cases*; Vol. 19.

(86) Gu, B.; Xu, C.; Yang, C.; Liu, S.; Wang, M. ZnO Quantum Dot Labeled Immunosensor for Carbohydrate Antigen 19-9. *Biosens. Bioelectron.* **2011**, *26* (5), 2720–2723. https://doi.org/10.1016/J.BIOS.2010.09.031.

(87) Zhu, H.; Fan, G.-C.; Abdel-Halim, E. S.; Zhang, J.-R.; Zhu, J.-J. Ultrasensitive Photoelectrochemical Immunoassay for CA19-9 Detection Based on CdSe@ZnS Quantum Dots Sensitized TiO2NWs/Au Hybrid Structure Amplified by Quenching Effect of Ab2@V2+ Conjugates. *Biosens. Bioelectron.* **2016**, *77*, 339–346. https://doi.org/10.1016/J.BIOS.2015.09.051.

(88) Chung, J. W.; Bernhardt, R.; Pyun, J. C. Additive Assay of Cancer Marker CA 19-9 by SPR Biosensor. *Sensors Actuators B Chem.* **2006**, *118* (1–2), 28–32. https://doi.org/10.1016/J.SNB.2006.04.015.

(89) Granger, J. H.; Granger, M. C.; Firpo, M. A.; Mulvihill, S. J.; Porter, M. D. Toward Development of a Surface-Enhanced Raman Scattering (SERS)-Based Cancer Diagnostic Immunoassay Panel. *Analyst* **2013**, *138* (2), 410–416. https://doi.org/10.1039/C2AN36128K.

(90) Zeng, Q.; Mao, X.; Xu, H.; Wang, S.; Liu, G. Quantitative Immunochromatographic Strip Biosensor for the Detection of Carcinoembryonic Antigen Tumor Biomarker in Human Plasma. *Am. J. Biomed. Sci.* **2009**, *1* (1), 70–79. https://doi.org/10.5099/aj090100070.

(91) Yang, Y.; Ozsoz, M.; Liu, G. Gold Nanocage-Based Lateral Flow Immunoassay for Immunoglobulin G. *Microchim. Acta* **2017**, *184* (7), 2023–2029. https://doi.org/10.1007/s00604-017-2176-5.

(92) Li, D.; Wei, S.; Yang, H.; Li, Y.; Deng, A. A Sensitive Immunochromatographic Assay Using Colloidal Gold–antibody Probe for Rapid Detection of Pharmaceutical Indomethacin in Water Samples. *Biosens. Bioelectron.* **2009**, *24* (7), 2277–2280. https://doi.org/10.1016/J.BIOS.2008.11.004.

(93) Tang, Y.; Zhai, Y.-F.; Xiang, J.-J.; Wang, H.; Liu, B.; Guo, C.-W. Colloidal Gold Probe-Based Immunochromatographic Assay for the Rapid Detection of Lead Ions in Water Samples. *Environ. Pollut.* **2010**, *158* (6), 2074–2077. https://doi.org/10.1016/J.ENVPOL.2010.03.001.

(94) Song, Y.; Song, S.; Liu, L.; Kuang, H.; Guo, L.; Xu, C. Simultaneous Detection of Tylosin and Tilmicosin in Honey Using a Novel Immunoassay and Immunochromatographic Strip Based on an Innovative Hapten. *Food Agric. Immunol.* **2016**, *27* (3), 314–328. https://doi.org/10.1080/09540105.2015.1089843.

(95) Wang, Z.; Zou, S.; Xing, C.; Song, S.; Liu, L.; Xu, C. Preparation of a Monoclonal Antibody against Testosterone and Its Use in Development of an Immunochromatographic Assay. *Food Agric. Immunol.* **2016**, *27* (4), 547–558. https://doi.org/10.1080/09540105.2015.1137276.

(96) Yu, L.; Liu, L.; Song, S.; Kuang, H.; Xu, C. Development of an Immunochromatographic Test Strip and Ic-ELISA for Tetrabromobisphenol : A Detection in Lake Water and Rice Pudding Samples. *FOOD Agric. Immunol.* **2016**, *27* (4), 460–470. https://doi.org/10.1080/09540105.2015.1126234.

(97) Grabar, K. C.; Freeman, R. G.; Hommer, M. B.; Natan, M. J. Preparation and Characterization of Au Colloid Monolayers. *Anal. Chem.* **1995**, *67* (4), 735–743. https://doi.org/10.1021/ac00100a008.

(98) Lee, K. J.; Yi, S. W.; Chung, M. J.; Park, S. W.; Song, S. Y.; Chung, J. B.; Park, J. Y. Serum CA 19-9 and CEA Levels as a Prognostic Factor in Pancreatic Adenocarcinoma. *Yonsei Med. J.* **2013**, *54* (3), 643–649. https://doi.org/10.3349/ymj.2013.54.3.643.

(99) McAllister, F.; Montiel, M. F.; Uberoi, G. S.; Uberoi, A. S.; Maitra, A.; Bhutani, M. S. Current Status and Future Directions for Screening Patients at High Risk for Pancreatic Cancer. *Gastroenterol. Hepatol.* **2017**, *13* (5), 268–275.

(100) Baryeh, K.; Takalkar, S.; Lund, M.; Liu, G. *1 - Introduction to Medical Biosensors for Point of Care Applications*; Elsevier Ltd, 2017. https://doi.org/10.1016/B978-0-08-100072-4.00001-0.

(101) Thévenot, D. R.; Toth, K.; Durst, R. A.; Wilson, G. S. Electrochemical Biosensors: Recommended Definitions and Classification. *Biosens. Bioelectron.* **2001**, *16* (1–2), 121–131. https://doi.org/10.1016/S0956-5663(01)00115-4.

(102) Brugge, W. R.; Lewandrowski, K.; Lee-Lewandrowski, E.; Centeno, B. A.; Szydlo, T.; Regan, S.; del Castillo, C. F.; Warshaw, A. L. Diagnosis of Pancreatic Cystic Neoplasms: A Report of the Cooperative Pancreatic Cyst Study. *Gastroenterology* **2004**, *126* (5), 1330–1336. https://doi.org/10.1053/j.gastro.2004.02.013.

(103) Ngamruengphong, S.; Lennon, A. M. Analysis of Pancreatic Cyst Fluid. *Surg. Pathol. Clin.* **2016**, *9* (4), 677–684. https://doi.org/10.1016/j.path.2016.05.010.

(104) Park, W. G. Screening for Pancreatic Cancer: What Can Cyst Fluid Analysis Tell Us? *F1000 Med. Rep.* **2011**, *3* (3). https://doi.org/10.3410/M3-3.

(105) Lai, S.; Wang, S.; Luo, J.; Lee, L. J.; Yang, S.-T.; Madou, M. J. Design of a Compact Disk-like Microfluidic Platform for Enzyme-Linked Immunosorbent Assay. **2004**. https://doi.org/10.1021/ac0348322.

(106) Gu, X.; She, Z.; Ma, T.; Tian, S.; Kraatz, H.-B. Electrochemical Detection of Carcinoembryonic Antigen. *Biosens. Bioelectron.* **2018**, *102*, 610–616. https://doi.org/10.1016/J.BIOS.2017.12.014.

(107) Wang, Y.; Zhao, G.; Zhang, Y.; Pang, X.; Cao, W.; Du, B.; Wei, Q. Sandwich-Type Electrochemical Immunosensor for CEA Detection Based on Ag/MoS2@Fe3O4 and an Analogous ELISA Method with Total Internal Reflection Microscopy. *Sensors Actuators B Chem.* **2018**, *266*, 561–569. https://doi.org/10.1016/J.SNB.2018.03.178.

(108) Wang, Y.; Wang, Y.; Wu, D.; Ma, H.; Zhang, Y.; Fan, D.; Pang, X.; Du, B.; Wei, Q. Label-Free Electrochemical Immunosensor Based on Flower-like Ag/MoS2/RGO Nanocomposites for Ultrasensitive Detection of Carcinoembryonic Antigen. *Sensors Actuators B Chem.* **2018**, *255*, 125–132. https://doi.org/10.1016/J.SNB.2017.07.129.

(109) Altintas, Z.; Uludag, Y.; Gurbuz, Y.; Tothill, I. E. Surface Plasmon Resonance Based Immunosensor for the Detection of the Cancer Biomarker Carcinoembryonic Antigen. *Talanta* **2011**, *86*, 377–383. https://doi.org/10.1016/J.TALANTA.2011.09.031.

(110) Špringer, T.; Homola, J. Biofunctionalized Gold Nanoparticles for SPR-Biosensor-Based Detection of CEA in Blood Plasma. *Anal. Bioanal. Chem.* **2012**, *404*, 2869–2875. https://doi.org/10.1007/s00216-012-6308-9.

(111) Li, R.; Feng, F.; Chen, Z.-Z.; Bai, Y.-F.; Guo, F.-F.; Wu, F.-Y.; Zhou, G. Sensitive Detection of Carcinoembryonic Antigen Using Surface Plasmon Resonance Biosensor with Gold Nanoparticles Signal Amplification. *Talanta* **2015**, *140*, 143–149. https://doi.org/10.1016/J.TALANTA.2015.03.041.

(112) Tang, D.-Q.; Zhang, D.-J.; Tang, D.-Y.; Ai, H. Amplification of the Antigen–antibody Interaction from Quartz Crystal Microbalance Immunosensors via Back-Filling Immobilization of Nanogold on Biorecognition Surface. *J. Immunol. Methods* **2006**, *316* (1–2), 144–152. https://doi.org/10.1016/J.JIM.2006.08.012.

(113) Chen Dian-Yong Tang, Z.-G. A. Antigen-Antibody Interaction from Quartz Crystal Microbalance Immunosensors Based on Magnetic CoFe 2 O 4 /SiO 2 Composite Nanoparticle-Functionalized Biomimetic Interface. https://doi.org/10.1007/s00449-007-0120-5.

(114) Chon, H.; Lee, S.; Wook Son, S.; Hwan Oh, C.; Choo, J. Highly Sensitive Immunoassay of Lung Cancer Marker Carcinoembryonic Antigen Using Surface-Enhanced Raman Scattering of Hollow Gold Nanospheres. *Z. Biosens. Bioelectron* **2004**, *76* (1), 3029–3034. https://doi.org/10.1021/ac802722c.

(115) Yang, L.-B.; Chen, G.-Y.; Wang, J.; Wang, T.-T.; Li, M.-Q.; Liu, J.-H. Sunlight-Induced Formation of Silver-Gold Bimetallic Nanostructures on DNA Template for Highly Active Surface Enhanced Raman Scattering Substrates and Application in TNT/Tumor Marker Detection †. *J. Mater. Chem.* **2009**, *19*, 6849–6856. https://doi.org/10.1039/b909600k.

(116) Wen, H.-W.; Borejsza-Wysocki, W.; DeCory, T. R.; Baeumner, A. J.; Durst, R. A. A Novel Extraction Method for Peanut Allergenic Proteins in Chocolate and Their Detection by a Liposome-Based Lateral Flow Assay. *Eur. Food Res. Technol.* **2005**, *221* (3–4), 564–569. https://doi.org/10.1007/s00217-005-1202-8.

(117) Tripathi, P.; Upadhyay, N.; Nara, S. Recent Advancements in Lateral Flow Immunoassays A Journey for Toxin Detection in Food. *Crit. Rev. Food Sci. Nutr.* **2018**, *58* (10), 1715–1734. https://doi.org/10.1080/10408398.2016.1276048.

(118) Lee, K. M.; Runyon, M.; Herrman, T. J.; Phillips, R.; Hsieh, J. Review of Salmonella Detection and Identification Methods: Aspects of Rapid Emergency Response and Food Safety. *Food Control* **2015**, *47*, 264–276. https://doi.org/10.1016/j.foodcont.2014.07.011.

(119) Baryeh, K.; Takalkar, S.; Lund, M.; Liu, G. Development of Quantitative Immunochromatographic Assay for Rapid and Sensitive Detection of Carbohydrate Antigen 19-9 (CA 19-9) in Human Plasma. *J. Pharm. Biomed. Anal.* **2017**, *146*, 285–291. https://doi.org/10.1016/j.jpba.2017.09.004.

(120) Savin, M.; Mihailescu, C. M.; Matei, I.; Stan, D.; Moldovan, C. A.; Ion, M.; Baciu, I. A Quantum Dot-Based Lateral Flow Immunoassay for the Sensitive Detection of Human Heart Fatty Acid Binding Protein (HFABP) in Human Serum. *Talanta* **2018**, *178* (July 2017), 910–915. https://doi.org/10.1016/j.talanta.2017.10.045.

(121) Qu, H.; Zhang, Y.; Qu, B.; Kong, H.; Qin, G.; Liu, S.; Cheng, J.; Wang, Q.; Zhao, Y. Rapid Lateral-Flow Immunoassay for the Quantum Dot-Based Detection of Puerarin. *Biosens. Bioelectron.* **2016**, *81*, 358–362. https://doi.org/10.1016/j.bios.2016.03.008.

(122) Bradford, M. M. A Rapid and Sensitive Method for the Quantitation of Microgram Quantities of Protein Utilizing the Principle of Protein-Dye Binding. *Anal. Biochem.* **1976**, *72* (1–2), 248–254. https://doi.org/10.1016/0003-2697(76)90527-3.

(123) GORNALL, A. G.; BARDAWILL, C. J.; DAVID, M. M. Determination of Serum Proteins by Means of the Biuret Reaction. *J. Biol. Chem.* **1949**, *177* (2), 751–766.

(124) Smith, P. K.; Krohn, R. I.; Hermanson, G. T.; Mallia, A. K.; Gartner, F. H.; Provenzano, M. D.; Fujimoto, E. K.; Goeke, N. M.; Olson, B. J.; Klenk, D. C. Measurement of Protein Using Bicinchoninic Acid. *Anal. Biochem.* **1985**, *150* (1), 76–85. https://doi.org/10.1016/0003-2697(85)90442-7.

(125) Leca-Bouvier, B.; Blum, L. J.; Loı¨c, L.; Blum, J. Analytical Letters Biosensors for Protein Detection: A Review Biosensors for Protein Detection: A Review. *Anal. Lett.* **2005**, *38*, 1491–1517. https://doi.org/10.1081/AL-200065780.

(126) Bass, J. J.; Wilkinson, D. J.; Rankin, D.; Phillips, B. E.; Szewczyk, N. J.; Smith, K.; Atherton, P. J. An Overview of Technical Considerations for Western Blotting Applications to Physiological Research. *Scand. J. Med. Sci. Sports* **2017**, *27* (1), 4–25. https://doi.org/10.1111/sms.12702.

(127) Azam, S.; Tanver Rahman, R.; Lou, Z.; Tang, Y.; Muhammed Raqib, S.; Sultana Jothi, J. Review: Advancements and Application of Immunosensors in the Analysis of Food Contaminants. *Nusant. Biosci.* **2014**, *6* (2), 186–195. https://doi.org/10.13057/nusbiosci/n060212.

(128) Staden, R.-I. S.-V.; Bokretsion, R. G.; Frederick Van Staden, J.; Aboul-Enein, H. Y.; Stefan-Van Staden, I.; Aboul, H. Y.; Girmai Bokretsion, R. Critical Reviews in Analytical Chemistry Immunosensors in Clinical and Environmental Analysis Immunosensors in Clinical and Environmental Analysis. *Crit. Rev. Anal. Chem.* **2015**, *45*, 1–2. https://doi.org/10.1080/10408347.2013.866035.

(129) Justino, C. I. L.; Duarte, A. C.; Rocha-Santos, T. A. P. Recent Progress in Biosensors for Environmental Monitoring: A Review. *Sensors (Switzerland)* **2017**, *17* (12). https://doi.org/10.3390/s17122918.

(130) Lequin, R. M. Enzyme Immunoassay (EIA)/Enzyme-Linked Immunosorbent Assay (ELISA). *Clin. Chem.* **2005**, *51* (12), 2415–2418. https://doi.org/10.1373/clinchem.2005.051532.

(131) Soper, S. A.; Brown, K.; Ellington, A.; Frazier, B.; Garcia-Manero, G.; Gau, V.; Gutman, S. I.; Hayes, D. F.; Korte, B.; Landers, J. L.; et al. Point-of-Care Biosensor Systems for Cancer Diagnostics/Prognostics. *Biosens. Bioelectron.* **2006**, *21* (10), 1932–1942. https://doi.org/10.1016/J.BIOS.2006.01.006.

(132) Moina, C.; Ybarr, G. Fundamentals and Applications of Immunosensors. In *Advances in Immunoassay Technology*; InTech, 2012. https://doi.org/10.5772/36947.

(133) Zhao, Z.; Jiang, H. Enzyme-Based Electrochemical Biosensors. In *Biosensors*; InTech, 2010. https://doi.org/10.5772/7200.

(134) Prodromidis, M. I. Impedimetric Immunosensors—A Review. *Electrochim. Acta* **2010**, *55* (14), 4227–4233. https://doi.org/10.1016/J.ELECTACTA.2009.01.081.

(135) Wu, Y.; Guo, W.; Peng, W.; Zhao, Q.; Piao, J.; Zhang, B.; Wu, X.; Wang, H.; Gong, X.; Chang, J. Enhanced Fluorescence ELISA Based on HAT Triggering Fluorescence "Turn-on" with Enzyme–Antibody Dual Labeled AuNP Probes for Ultrasensitive Detection of AFP and HBsAg. *ACS Appl. Mater. Interfaces* **2017**, *9* (11), 9369–9377. https://doi.org/10.1021/acsami.6b16236.

(136) Wu, Y.; Zeng, L.; Xiong, Y.; Leng, Y.; Wang, H.; Xiong, Y. Fluorescence ELISA Based on Glucose Oxidase-Mediated Fluorescence Quenching of Quantum Dots for Highly Sensitive Detection of Hepatitis B. *Talanta* **2018**, *181*, 258–264. https://doi.org/10.1016/J.TALANTA.2018.01.026.

(137) Wang, Z.; Yang, X.; Yang, J.; Jiang, Y.; He, N. Peroxidase-like Activity of Mesoporous Silica Encapsulated Pt Nanoparticle and Its Application in Colorimetric Immunoassay. *Anal. Chim. Acta* **2015**, *862*, 53–63. https://doi.org/10.1016/J.ACA.2014.12.046.

(138) Koczula, K. M.; Gallotta, A. Lateral Flow Assays. *Essays Biochem.* **2016**, *60*, 111–120. https://doi.org/10.1042/EBC20150012.

(139) Posthuma-Trumpie, G. A.; Korf, J.; van Amerongen, A. Lateral Flow (Immuno)Assay: Its Strengths, Weaknesses, Opportunities and Threats. A Literature Survey. *Anal. Bioanal. Chem.* **2009**, *393* (2), 569–582. https://doi.org/10.1007/s00216-008-2287-2.

(140) Choi, D. H.; Lee, S. K.; Oh, Y. K.; Bae, B. W.; Lee, S. D.; Kim, S.; Shin, Y.-B.; Kim, M.-G. A Dual Gold Nanoparticle Conjugate-Based Lateral Flow Assay (LFA) Method for the Analysis of Troponin I. *Biosens. Bioelectron.* **2010**, *25* (8), 1999–2002. https://doi.org/10.1016/J.BIOS.2010.01.019.

(141) Xu, Y.; Liu, Y.; Wu, Y.; Xia, X.; Liao, Y.; Li, Q. Fluorescent Probe-Based Lateral Flow Assay for Multiplex Nucleic Acid Detection. *Anal. Chem.* **2014**, *86* (12), 5611–5614. https://doi.org/10.1021/ac5010458.

(142) Wang, Y.; Nugen, S. R. Development of Fluorescent Nanoparticle-Labeled Lateral Flow Assay for the Detection of Nucleic Acids. *Biomed. Microdevices* **2013**, *15* (5), 751–758. https://doi.org/10.1007/s10544-013-9760-1.

(143) Suárez-Pantaleón, C.; Wichers, J.; Abad-Somovilla, A.; van Amerongen, A.; Abad-Fuentes, A. Development of an Immunochromatographic Assay Based on Carbon Nanoparticles for the Determination of the Phytoregulator Forchlorfenuron. *Biosens. Bioelectron.* **2013**, *42*, 170–176. https://doi.org/10.1016/J.BIOS.2012.11.001.

(144) Guo, Z.; Zheng, Y.; Xu, H.; Zheng, B.; Qiu, W.; Liu, G. Lateral Flow Test for Visual Detection of Silver(I) Based on Cytosine-Ag(I)-Cytosine Interaction in C-Rich Oligo-nucleotides. *Microchim. Acta* **2017**, *184* (11), 4243–4250. https://doi.org/10.1007/s00604-017-2460-4.

(145) Hou, S.-Y.; Hsiao, Y.-L.; Lin, M.-S.; Yen, C.-C.; Chang, C.-S. MicroRNA Detection Using Lateral Flow Nucleic Acid Strips with Gold Nanoparticles. *Talanta* **2012**, *99*, 375–379. https://doi.org/10.1016/J.TALANTA.2012.05.067.

(146) Loynachan, C. N.; Thomas, M. R.; Gray, E. R.; Richards, D. A.; Kim, J.; Miller, B. S.; Brookes, J. C.; Agarwal, S.; Chudasama, V.; McKendry, R. A.; et al. Platinum Nano-catalyst Amplification: Redefining the Gold Standard for Lateral Flow Immunoassays with Ultrabroad Dynamic Range. *ACS Nano* **2018**, *12* (1), 279–288. https://doi.org/10.1021/acsnano.7b06229.

(147) Shen, G.; Zhang, S.; Hu, X. Signal Enhancement in a Lateral Flow Immunoassay Based on Dual Gold Nanoparticle Conjugates. **2013**. https://doi.org/10.1016/j.clinbiochem.2013.08.010.

(148) Iijima, S. Helical Microtubules of Graphitic Carbon. *Nature* **1991**, *354* (6348), 56–58. https://doi.org/10.1038/354056a0.

(149) Baughman, R. H.; Zakhidov, A. A.; Heer, W. A. de. Carbon Nanotubes--the Route Toward Applications. *Science (80-.).* **2002**, *297* (5582), 787–792. https://doi.org/10.1126/SCIENCE.1060928.

(150) Javey, A.; Guo, J.; Wang, Q.; Lundstrom, M.; Dai, H. Ballistic Carbon Nanotube Field-Effect Transistors. *Nature* **2003**, *424* (6949), 654–657. https://doi.org/10.1038/nature01797.

(151) Qu, L.; Dai, L.; Stone, M.; Xia, Z.; Wang, Z. L. Carbon Nanotube Arrays with Strong Shear Binding-on and Easy Normal Lifting-Off. *Science* **2008**, *322* (5899), 238–242. https://doi.org/10.1126/science.1159503.

(152) Zhang, Q.; Zhao, B.; Yan, J.; Song, S.; Min, R.; Fan, C. Nanotube-Based Colorimetric Probe for Ultrasensitive Detection of Ataxia Telangiectasia Mutated Protein. *Anal. Chem* **2011**, *83*, 9191–9196. https://doi.org/10.1021/ac2023684.

(153) Abera, A.; Choi, J.-W. Quantitative Lateral Flow Immunosensor Using Carbon Nanotubes as Label. *Anal. Methods* **2010**, *2* (11), 1819. https://doi.org/10.1039/c0ay00412j.

(154) Meng, L.-L.; Song, T.-T.; Mao, X. Novel Immunochromatographic Assay on Cotton Thread Based on Carbon Nanotubes Reporter Probe. *Talanta* **2017**, *167*, 379–384. https://doi.org/10.1016/J.TALANTA.2017.02.023.

(155) Liu, Y.; Song, T.; Jia, X.; Meng, L.; Mao, X. Gold Nanoparticles Decorated Carbon Nanotube Probe Based Immunochromatographic Assay on Cotton Thread. *Sensors Actuators B Chem.* **2017**, *251*, 1112–1118. https://doi.org/10.1016/J.SNB.2017.04.144.

(156) Hou, P.-X.; Liu, C.; Cheng, H.-M. Purification of Carbon Nanotubes. *Carbon N. Y.* **2008**, *46* (15), 2003–2025. https://doi.org/10.1016/J.CARBON.2008.09.009.

(157) Sun, W.; Hu, X.; Liu, J.; Zhang, Y.; Lu, J.; Zeng, L. A Novel Multi-Walled Carbon Nanotube-Based Antibody Conjugate for Quantitative and Semi-Quantitative Lateral Flow Assays. *Biosci. Biotechnol. Biochem.* **2017**, *81* (10), 1874–1882. https://doi.org/10.1080/09168451.2017.1365590.

(158) *American Cancer Society. Cancer Facts & Figures 2019. Atlanta: American Cancer Society*; 2019.

(159) Shao, Y.; Sun, X.; He, Y.; Liu, C.; Liu, H. Elevated Levels of Serum Tumor Markers CEA and CA15-3 Are Prognostic Parameters for Different Molecular Subtypes of Breast Cancer. *PLoS One* **2015**, *10* (7), e0133830. https://doi.org/10.1371/journal.pone.0133830.

(160) Grunnet, M.; Sorensen, J. B. Carcinoembryonic Antigen (CEA) as Tumor Marker in Lung Cancer. *Lung Cancer* **2012**, *76* (2), 138–143. https://doi.org/10.1016/j.lungcan.2011.11.012.

(161) Chen, F.; Shen, J.; Wang, J.; Cai, P.; Huang, Y. Clinical Analysis of Four Serum Tumor Markers in 458 Patients with Ovarian Tumors: Diagnostic Value of the Combined Use of HE4, CA125, CA19-9, and CEA in Ovarian Tumors. *Cancer Manag. Res.* **2018**, *Volume 10*, 1313–1318. https://doi.org/10.2147/CMAR.S155693.

(162) Meng, Q.; Shi, S.; Liang, C.; Liang, D.; Xu, W.; Ji, S.; Zhang, B.; Ni, Q.; Xu, J.; Yu, X. Diagnostic and Prognostic Value of Carcinoembryonic Antigen in Pancreatic Cancer: A Systematic Review and Meta-Analysis. *Onco. Targets. Ther.* **2017**, *10*, 4591–4598. https://doi.org/10.2147/OTT.S145708.

(163) Winek, T.; Hamre, D.; Mozell, E.; Vetto, R. M. Prognostic Factors for Survival after Pancreaticoduodenectomy for Malignant Disease. *Am J Surg* **1990**, *159*, 454–546.

(164) Lee, E. S.; Lee, J. M. Imaging Diagnosis of Pancreatic Cancer: A State-of-the-Art Review. *World J. Gastroenterol.* **2014**, *20* (24), 7864–7877. https://doi.org/10.3748/wjg.v20.i24.7864.

(165) Li, X.; Gao, P.; Wang, Y.; Wang, X. Blood-Derived MicroRNAs for Pancreatic Cancer Diagnosis: A Narrative Review and Meta-Analysis. *Front. Physiol.* **2018**, *9*, 685. https://doi.org/10.3389/fphys.2018.00685.

(166) Zhang, J.; Huang, T.; Zhang, F.; Xu, J.; Chen, G.; Wang, X.; Huang, L.; Peng, Z. Prognostic Role of Serum Carbohydrate Antigen 19-9 Levels in Patients with Resectable Hepatocellular Carcinoma. *Tumor Biol.* **2015**, *36* (4), 2257–2261. https://doi.org/10.1007/s13277-014-2435-6.

(167) Papantoniou, V.; Tsiouris, S.; Koutsikos, J.; Ptohis, N.; Lazaris, D.; Zerva, C. Increased Serum Carbohydrate Antigen 19-9 in Relapsed Ductal Breast Carcinoma. *Hell. J. Nucl. Med.* **2006**, *9* (1), 36–38.

(168) Prieto De Paula, J. M.; Toranzo, E. M.; Borge, L. G.; Hidalgo, S. F. Small-Cell Lung Cancer and Elevated CA 19.9 Tumor Marker Levels. *Arch. Bronconeumol. (English Ed.* **2012**, *48* (10), 385–386. https://doi.org/10.1016/j.arbr.2012.07.009.

(169) Huang, Y.; Wen, Y.; Baryeh, K.; Takalkar, S.; Lund, M.; Zhang, X.; Liu, G. Lateral Flow Assay for Carbohydrate Antigen 19–9 in Whole Blood by Using Magnetized Carbon Nanotubes. *Microchim. Acta* **2017**, *184* (11), 4287–4294. https://doi.org/10.1007/s00604-017-2464-0.

(170) Huang, Z.; Jiang, Z.; Zhao, C.; Han, W.; Lin, L.; Liu, A.; Weng, S.; Lin, X. Simple and Effective Label-Free Electrochemical Immunoassay for Carbohydrate Antigen 19-9 Based on Polythionine-Au Composites as Enhanced Sensing Signals for Detecting Different Clinical Samples. *Int. J. Nanomedicine* **2017**, *12*, 3049–3058. https://doi.org/10.2147/IJN.S131805.

(171) Seigneuric, J.; Cordonnie, M.; Gobbo, J.; Marcion, G.; Garrido, C. Tumor Exosomes: Potential Biomarkers and Targets in Cancer. *J. Clin. Cell. Immunol.* **2016**, *07* (06), 1–2. https://doi.org/10.4172/2155-9899.1000472.

(172) Samanta, S.; Rajasingh, S.; Drosos, N.; Zhou, Z.; Dawn, B.; Rajasingh, J. Exosomes: New Molecular Targets of Diseases. *Acta Pharmacol. Sin.* **2018**, *39* (4), 501–513. https://doi.org/10.1038/aps.2017.162.

(173) Munson, P.; Shukla, A. Exosomes: Potential in Cancer Diagnosis and Therapy. *Medicines* **2015**, *2* (4), 310–327. https://doi.org/10.3390/medicines2040310.

(174) Rajagopal, C.; Harikumar, K. B. The Origin and Functions of Exosomes in Cancer. *Front. Oncol.* **2018**, *8*, 66. https://doi.org/10.3389/fonc.2018.00066.

(175) EL Andaloussi, S.; Mäger, I.; Breakefield, X. O.; Wood, M. J. A. A. Extracellular Vesicles: Biology and Emerging Therapeutic Opportunities. *Nat. Rev. Drug Discov.* **2013**, *12* (5), 347–357. https://doi.org/10.1038/nrd3978.

(176) Keng, P.; Yan, Y.; Keng, S. Exosomes in the Ascites of Ovarian Cancer Patients: Origin and Effects on Anti-Tumor Immunity. *Oncol. Rep.* **2011**, *25* (3), 749–762. https://doi.org/10.3892/or.2010.1119.

(177) Chen, W.; Liu, X.; Lv, M.; Chen, L.; Zhao, J.; Zhong, S.; Ji, M.; Hu, Q.; Luo, Z.; Wu, J.; et al. Exosomes from Drug-Resistant Breast Cancer Cells Transmit Chemoresistance by a Horizontal Transfer of MicroRNAs. *PLoS One* **2014**, *9* (4), e95240. https://doi.org/10.1371/journal.pone.0095240.

(178) Zhao, L.; Liu, W.; Xiao, J.; Cao, B. The Role of Exosomes and "Exosomal Shuttle MicroRNA" in Tumorigenesis and Drug Resistance. **2014**. https://doi.org/10.1016/j.canlet.2014.10.027.

(179) Zarovni, N.; Corrado, A.; Guazzi, P.; Zocco, D.; Lari, E.; Radano, G.; Muhhina, J.; Fondelli, C.; Gavrilova, J.; Chiesi, A. Integrated Isolation and Quantitative Analysis of Exosome Shuttled Proteins and Nucleic Acids Using Immunocapture Approaches. *Methods* **2015**, *87*, 46–58. https://doi.org/10.1016/j.ymeth.2015.05.028.

(180) Li, P.; Kaslan, M.; Lee, S. H.; Yao, J.; Gao, Z. Progress in Exosome Isolation Techniques. *Theranostics* **2017**, *7* (3), 789–804. https://doi.org/10.7150/thno.18133.

(181) Properzi, F.; Logozzi, M.; Fais, S. Exosomes: The Future of Biomarkers in Medicine. *Biomark. Med.* **2013**, *7* (5), 769–778. https://doi.org/10.2217/bmm.13.63.

(182) Hartman, Z. C.; Wei, J.; Glass, O. K.; Guo, H.; Lei, G.; Yang, X.-Y.; Osada, T.; Hobeika, A.; Delcayre, A.; Le Pecq, J.-B.; et al. Increasing Vaccine Potency through Exosome Antigen Targeting. *Vaccine* **2011**, *29* (50), 9361–9367. https://doi.org/10.1016/J.VACCINE.2011.09.133.

(183) Dudani, J. S.; Gossett, D. R.; Tse, H. T. K.; Lamm, R. J.; Kulkarni, R. P.; Carlo, D. Di. Rapid Inertial Solution Exchange for Enrichment and Flow Cytometric Detection of Microvesicles. *Biomicrofluidics* **2015**, *9* (1), 014112. https://doi.org/10.1063/1.4907807.

(184) Erdbrugger, U.; Lannigan, J. Analytical Challenges of Extracellular Vesicle Detection: A Comparison of Different Techniques. *Cytom. Part A* **2016**, *89A*, 123–134. https://doi.org/10.1002/cyto.a.22795.

(185) Boriachek, K.; Islam, M. N.; Möller, A.; Salomon, C.; Nguyen, N.-T.; Hossain, M. S. A.; Yamauchi, Y.; Shiddiky, M. J. A. Biological Functions and Current Advances in Isolation and Detection Strategies for Exosome Nanovesicles. *Small* **2018**, *14* (6), 1702153. https://doi.org/10.1002/smll.201702153.

(186) Chen, A.; Yang, S. Replacing Antibodies with Aptamers in Lateral Flow Immunoassay. *Biosens. Bioelectron.* **2015**, *71*, 230–242. https://doi.org/10.1016/j.bios.2015.04.041.

(187) Stoltenburg, R.; Reinemann, C.; Strehlitz, B. SELEX-A (r)Evolutionary Method to Generate High-Affinity Nucleic Acid Ligands. *Biomol. Eng.* **2007**, *24*, 381–403. https://doi.org/10.1016/j.bioeng.2007.06.001.

(188) Wu, Z.; He, D.; Xu, E.; Jiao, A.; Chughtai, M. F. J.; Jin, Z. Rapid Detection of β-Conglutin with a Novel Lateral Flow Aptasensor Assisted by Immunomagnetic Enrichment and Enzyme Signal Amplification. *Food Chem.* **2018**, *269*, 375–379. https://doi.org/10.1016/J.FOODCHEM.2018.07.011.

(189) Song, Y.; Zhu, Z.; An, Y.; Zhang, W.; Zhang, H.; Liu, D.; Yu, C.; Duan, W.; Yang, C. J. Selection of DNA Aptamers against Epithelial Cell Adhesion Molecule for Cancer Cell Imaging and Circulating Tumor Cell Capture. *Anal. Chem.* **2013**. https://doi.org/10.1021/ac400366b.

(190) Grabar, K. C.; Griffith Freeman, R.; Hommer, M. B.; Natan, M. J.; Chem Phys Lett, N. P. *Kluwer Academic: The Netherlands*; UTC, 1995; Vol. 67.

(191) Stampe Ostenfeld, M.; Grann Jensen, S.; Kjølhede Jeppesen, D.; Christensen, L.-L.; Buch Thorsen, S.; Stenvang, J.; Hvam, M. L.; Thomsen, A.; Mouritzen, P.; Rasmussen, M. H.; et al. MiRNA Profiling of Circulating EpCAM+ Extracellular Vesicles: Promising Biomarkers of Colorectal Cancer. *J. Extracell. Vesicles* **2016**, *5*, 31488. https://doi.org/10.3402/jev.v5.31488.